

N72-28718

# CASE FILE COPY

ANNUAL REPORT

Prepared for

Goddard Space Flight Center

April 1, 1971 - March 31, 1972

## PHYSICS

The University of  
Western Ontario

ANNUAL REPORT  
PREPARED FOR  
GODDARD SPACE FLIGHT CENTER

Title: Elastic and Inelastic Scattering of Positrons in Gases and Solids

Contract: NGR-52-029-006

Report Period: April 1, 1971 - March 31, 1972

Principal Investigator: J. William McGowan, Chairman  
Department of Physics  
University of Western Ontario  
London 72, Ontario, Canada  
(519) 679-2282

Major Contributors: D. Bartell  
E.L. Chaney (presently U. of Colorado)  
W. Ketchabaw, Technician  
C.J. Keyser, Electronics  
J. Wm. McGowan  
P.H. Orth (presently U. of British Columbia)  
S. Pendyala  
I. Schmidt, Technical Officer  
H. Walter, Technician  
P.W. Zitzewitz

Theoretical Complement by: P.A. Fraser, D.F. Gallaher, J. Nuttall,  
B.Y. Tong

Partial Support: National Research Council, Canada and  
the University of Western Ontario

Abstract: Three apparatuses have been designed and built in conjunction with this grant. The first, which is now operative, was designed to study the details of positron thermalization in solids and the subsequent emission of the low energy positrons from moderating foils. The ejection of low energy positrons from the moderator surface has now been studied for the krylon covered  $\text{Co}^{58}$  source. The positrons emitted from this surface are primarily in a narrow peak  $\sim 0.2$  eV FWHM while positrons coming either from mica or gold or mica-gold combinations show considerable

structure. The narrow, single peak from the krylon moderator is excellent as a source of  $e^+$  for scattering experiments, while the identification of a rich spectrum of structure in the emitted positrons represents the beginning of a new solid state spectroscopy which reflects information from the bulk solid, the surface and most likely gases bound to surfaces.

The second apparatus now under test is a positron bottle similar in design to the electron trap used by Demelt and his associates. This apparatus was built to store positrons at a fixed energy and to look at the number of stored positrons (storage time) as a function of a scattering gas in the vacuum chamber. It is the eventual plan to scatter positrons from H atoms.

The third apparatus is a crossed beam apparatus where  $e^+$ , alkali scattering will be studied. Much of the apparatus is now under test with electrons. In fact, it is our intent to scatter positrons and electrons from the same target and to get the ratio of the two cross sections as a function of the electron or positron energy. In the alkali systems, the  $P_s$  formation channel is always open and in the case of ( $e^+$ , Cs) scattering  $P_s^*(n=2)$  is preferred. This system is to receive primary attention.

The experimental work is complemented by an extensive theoretical program supported entirely by NRC.

## 1. INTRODUCTION

For years theory has been generated describing positron scattering from atoms, however, until recently, very few reliable experimental results were available to test this theory. Perhaps the most exciting results to date reflect the good agreement between theory and recent experiments for the  $(e^+, He)$  system. The present state of agreement is reviewed in a recent paper by Costello et al<sup>1</sup> and recent experimental and theoretical reviews by McGowan<sup>2</sup> and Drachman.<sup>3</sup>

The future of positron scattering from atoms and molecules hinges largely upon the development of the low energy positron sources of sufficient strength to allow for scattering.<sup>4</sup> These are presently being developed in our laboratory. The program underway at the University of Western Ontario is a natural extension of work initiated at Gulf General Atomic but, instead of a LINAC as the source of high energy positrons, radio active sources have been effectively used.

In the first experiment, a study of the moderating process has been effectively undertaken and is reviewed in Section 2. Not only have we been able to produce a reasonably intense, highly resolved beam of positrons which is effective for positron scattering experiments at low energies, but we have been able to identify, for some materials, a rich

spectrum of structure in the emitted positrons which apparently reflects information from within the solid or from the surface of the moderating solids. We believe that we are now on the threshold of developing a rich, new spectroscopy of solids.

It is the primary purpose of our study to investigate elastic and inelastic scattering of positrons from atoms in an attempt to test in detail scattering theory. Already, with the completion of the first ( $e^+$ ,He) experiment, we have learned that virtual positronium and the polarization of positronium are sizeable effects in positron-atom scattering.

Theoretically, the most tractable positron scattering system is ( $e^+$ ,H), a system we plan to study in a few years' time. Towards that end, two apparatuses are being built. The first is a Penning electromagnetic trap similar to that used at the University of Washington by Dehmelt and his associates. It is the purpose of this experiment to bottle low energy positrons and subsequently scatter them from the trap, and to obtain, from a measurement of the loss of positrons, some information on the total scattering cross section. In time, it is hoped that hydrogen atoms can be used as the scattering medium.

With the completion of the test, most likely helium or  $H_2$  will receive first attention. (There are some theoretical

studies of these systems presently being carried out here.) The present state of the experiment associated with the first scattering apparatus is reviewed in Section 3.

In Section 4 we describe in detail the positron alkali atom crossed beam apparatus which is being completed. Experiments have been focussed on the alkalis since they are hydrogen-like and since, unlike hydrogen, the positronium formation channel is always open. The first experiments will be associated with positron cesium scattering. The choice of cesium reflects our ability to produce very dense atom beams of cesium in our apparatus. It is one of the prime interests in this experiment to identify the Lyman-alpha of positronium due to the charge transfer mechanism. This channel is energetically preferred.

In Section 5 we describe the theoretical studies which accompany the experiment supported by NASA. In Section 6 we roughly outline the plan for continuing study. In the Appendices we have included copies of the papers published and submitted for publication, as well as copies of abstracts which have been submitted for publication during the past contract period. Also, in the Appendices we have included short paragraphs describing other atomic physics experiments here which complement our work.

## 2. SOLID STATE STUDIES

### 2.1 Positron Sources

The need for sources of very low energy positrons with narrow energy distributions cannot be overemphasized. Some applications to atomic physics where are being examined in this laboratory include positron-atom scattering at low energies and studies of excited states of positronium by photon emission (these aspects are discussed in Section 4). The use of positrons in solid state spectroscopy, a totally new application, is clearly emerging from the present studies. This is discussed at length in Section 2.3.

Emission of slow positrons below 10 eV, using  $\text{Na}^{22}$  and a mica moderator coated with a film of chromium, was mentioned by Cherry<sup>5</sup> in his thesis. Their existence was subsequently confirmed by Groce et al<sup>4,6</sup> using bremsstrahlung from a LINAC to produce  $(e^-, e^+)$  pairs which were subsequently slowed to eV energies with the use of moderators. Similar results have been reported using radioactive sources by Madey<sup>7</sup> and Jaduszliwer et al.<sup>8</sup> In the present experiments the yield of low energy positrons from a radioactive positron source using different solid moderators is being investigated. Also included is a detailed study of the production mechanism, as well as the energy and angular distributions of the slow positrons. This is done in an attempt to optimize the pro-

duction of slow positrons by understanding the processes involved in their formation.

A 180° electrostatic analyzer, suitable for energies in the range of a few eV, similar to the one discussed by Kuyatt and Simpson,<sup>9</sup> has been built and is operating. A block diagram of the detection system is shown in Fig. 2.1. The geometry of the source and moderator is shown in Fig. 2.2. The source and moderator are separated by about 75 microns. Results have also been obtained with the moderator directly on top of the source in an attempt to measure any effects due to the solid angle of emission.

The studies to date have dealt with different thicknesses of mica, gold, aluminum or copper on mica, self-supporting gold films, and the problems of self-moderation by the source. The thickness of mica typically is 1 to  $10^4$  nm. Results obtained so far are discussed in Section 2.4.

## 2.2 Negative Work Function

An electron in a solid (usually a metal) can be removed only by supplying a positive external energy (or by thermal excitation) because of the binding of the electron to the solid. This external energy is referred to as the "work function" in the case of metals. However, a positron thermalized in a solid is thrown out with a non-zero kinetic energy



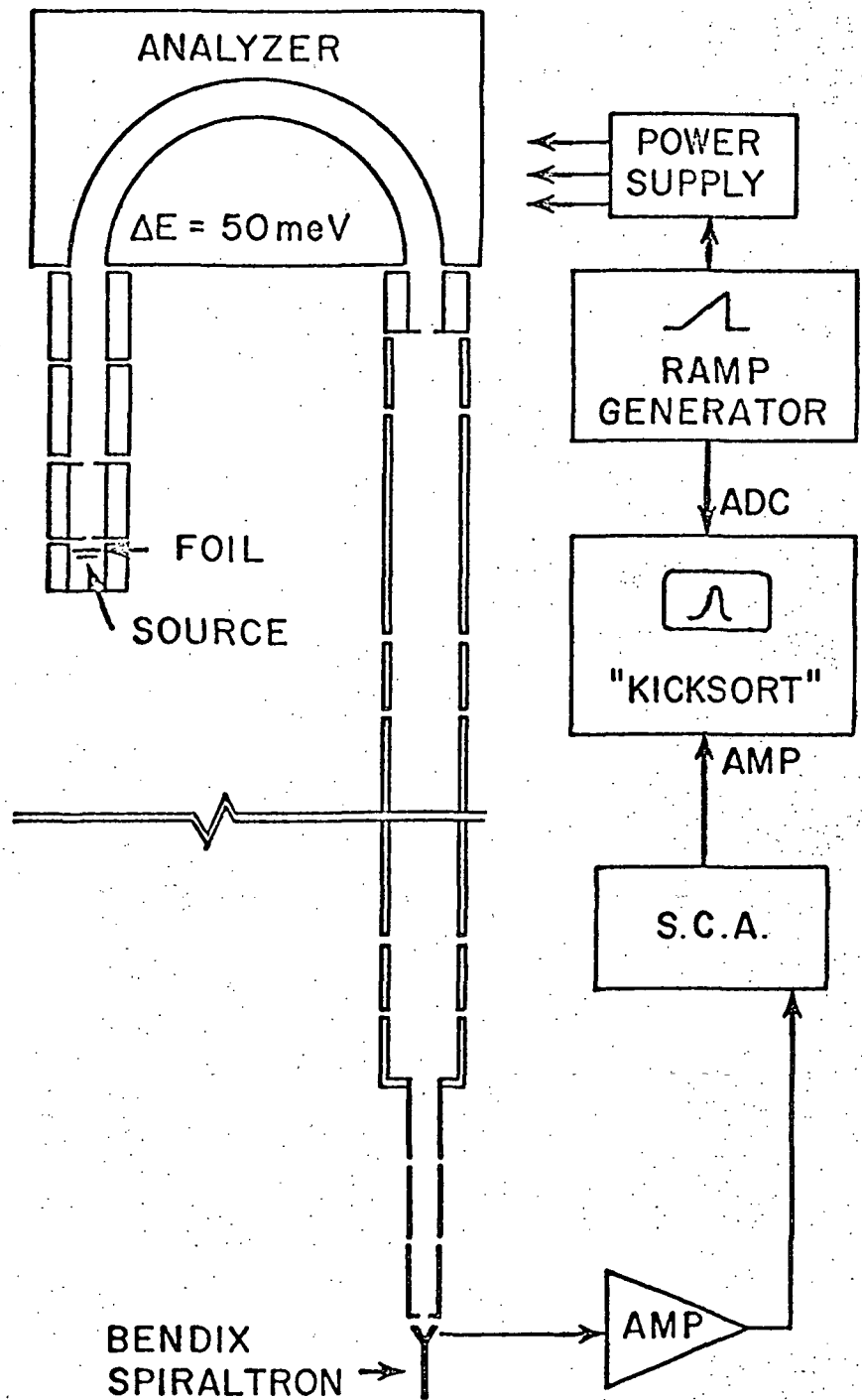
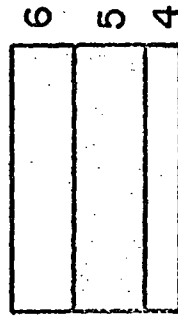


FIGURE 2.1

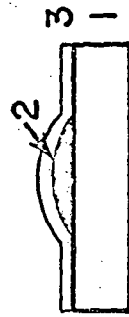
BLOCK DIAGRAM OF THE ANALYZER AND DETECTION SYSTEM

POSITRON SOURCE DETAIL



MODERATOR

- 6. Au, evaporated, 20 to 320nm
- 5. Mica,  $3.8 \times 10^{-3}$  cm
- 4. Au, evaporated, 20nm
- 3. Krylon spray
- 2.  $\text{Co}^{58}$  source, electroplated, carrier free,  $\sim 30$  mCi
- 1. Cu disc



SOURCE

FIGURE 2.2

SOURCE GEOMETRY

characteristic of the solid. No external energy is required. This kinetic energy has been named the "negative work function".

The work function of a particle with reference to a solid is the difference between the energy of the particle when it is in the solid and when it is removed to infinity. If this difference in energy is negative, the work function is positive. In this case, the particle (here a negative electron) cannot escape from the solid without the supply of external energy. However, if the difference in energy is positive, the work function is negative, and no external energy is needed for the particle (here a positive electron) to leave the solid (it should be noted, however, that most of the positrons which enter the solid usually annihilate there).

The work function,  $\phi$ , is given by the expression

$$\phi = \Delta\phi^P - \mu^P$$

where  $\Delta\phi^P$  is the lowering of the mean electrostatic potential across the solid surface and  $\mu^P$  is the chemical potential of the positrons. In the case of a thermalized positron, the chemical potential is the correlation energy of the positron with the electrons of the solid.

In the random phase approximation (RPA)

$$\mu^P \approx -2.68r_s^{-1/2} \text{ eV}$$

$\Delta\phi$  is approximately equal to  $-\Delta\phi^e$ . The values of  $\Delta\phi^e$  are estimated by Smith,<sup>10</sup> and Lang and Kohn.<sup>11</sup> These concepts

have been well discussed in two recent papers by Costello et al<sup>4</sup> and Tong.<sup>12</sup> The values of negative work function for various metals are given in Table I of the paper by Tong. (See appendices.)

### 2.3 Positrons and Solid State Spectroscopy

Use of positrons in the study of solids is traditionally confined to the investigation of Fermi surfaces in metals. The angular distribution of  $\gamma$ -rays due to free annihilation of thermalized positrons with core and conduction electrons is studied to obtain values of electron momenta. The life times of positrons and positronium in liquids and nonconductors are studied to obtain information on electron densities, clusters and various defects in solids.

In the present experiments, for the first time, fine structures have been observed in the energy spectra of the slow positrons coming from the moderating foils. The resolution of the analyser is 0.5%, i.e. about 0.05 eV at the median energy 11 eV. Energy spectra from various moderators are shown in Figs. 2.3, 2.4, and 2.5. The energy spectrum from the source with no moderator is shown in Fig. 2.3. In addition to the main peak, there is a real, very weak peak at the higher energy side of the main peak. The spectrum of mica with no gold film (position 6 in Fig. 2.2) has considerable structure, Fig. 2.4.

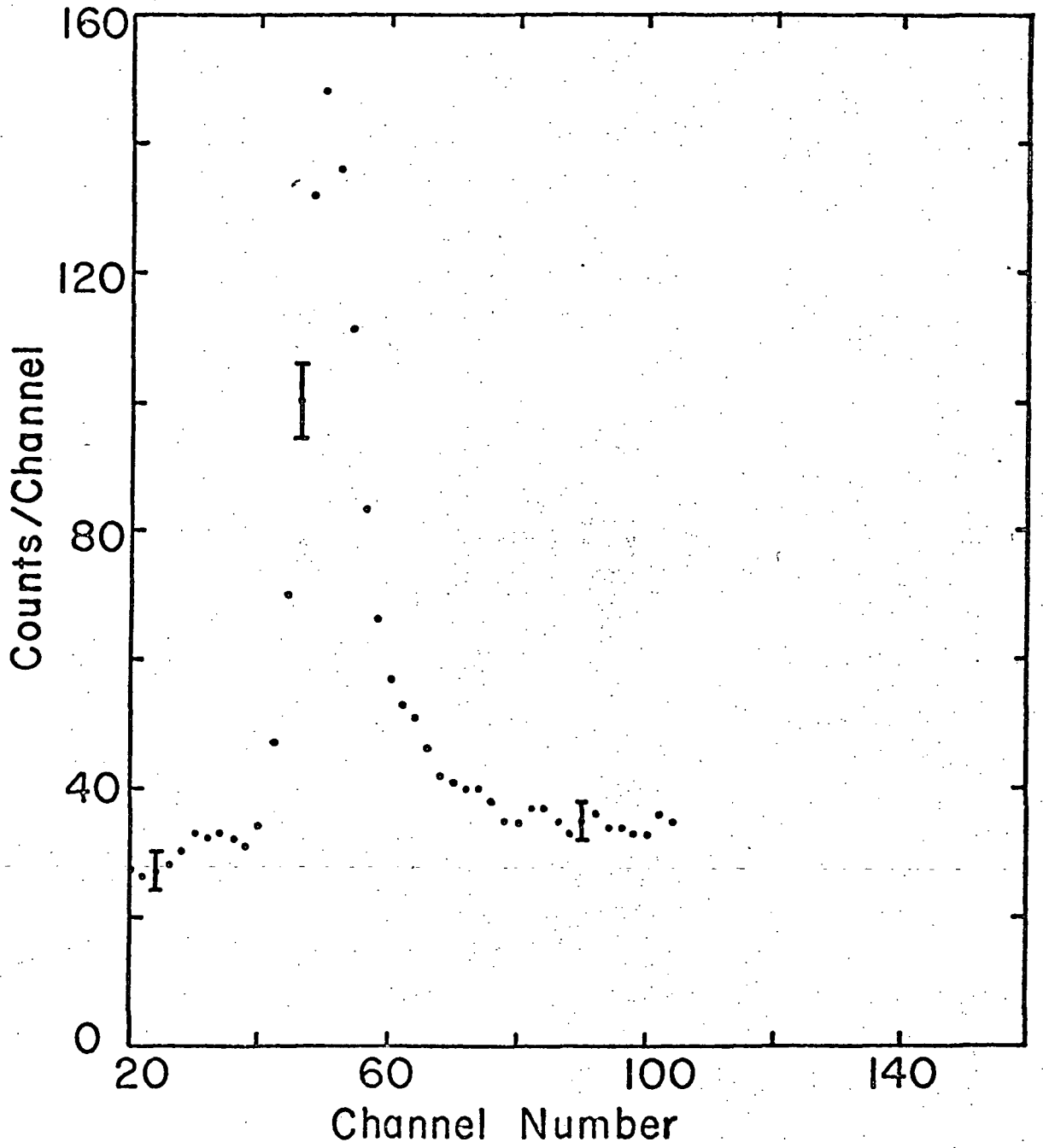


FIGURE 2.3

ENERGY SPECTRUM FROM SOURCE ALONE

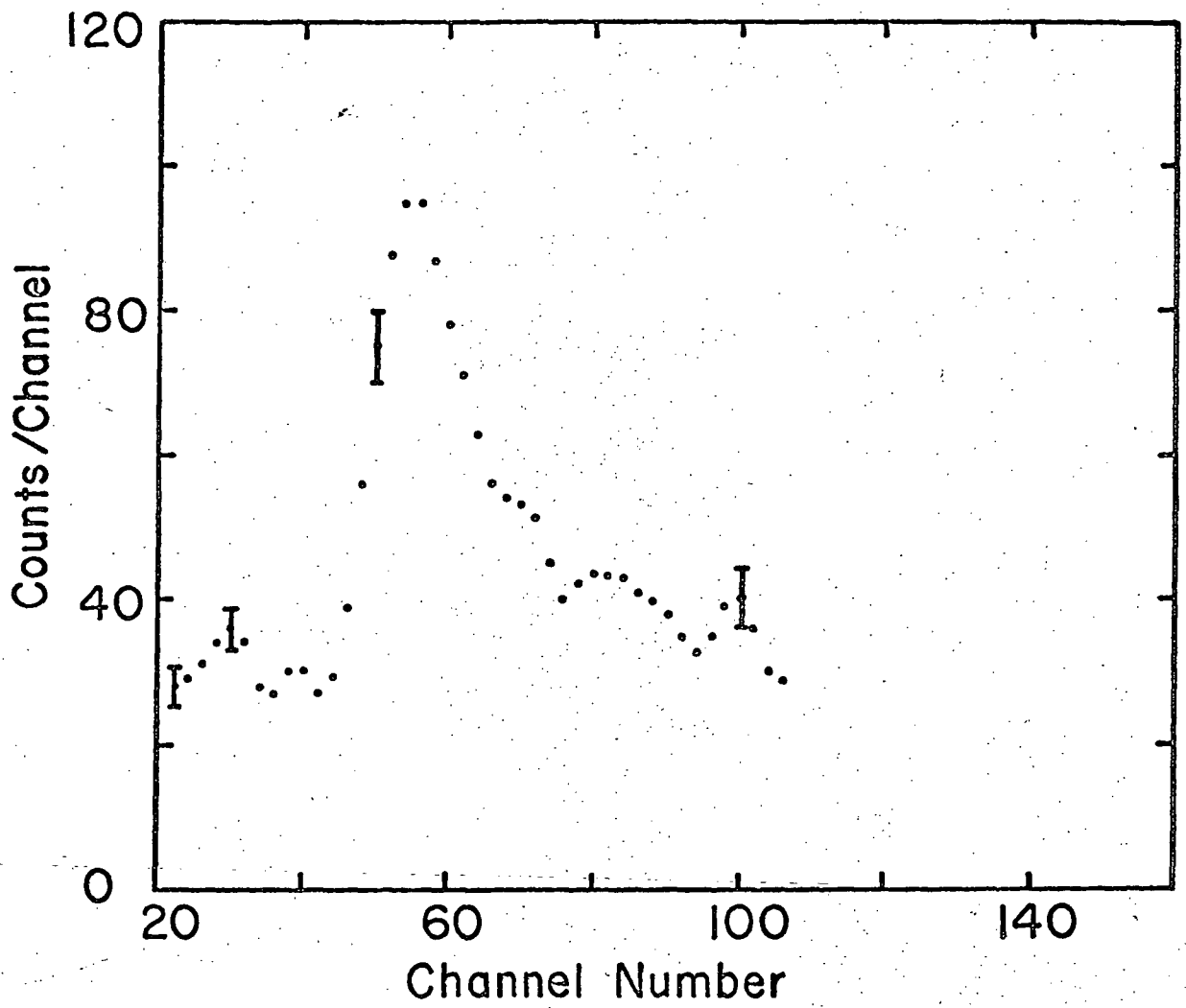


FIGURE 2.4

ENERGY SPECTRUM FROM MICA ONLY

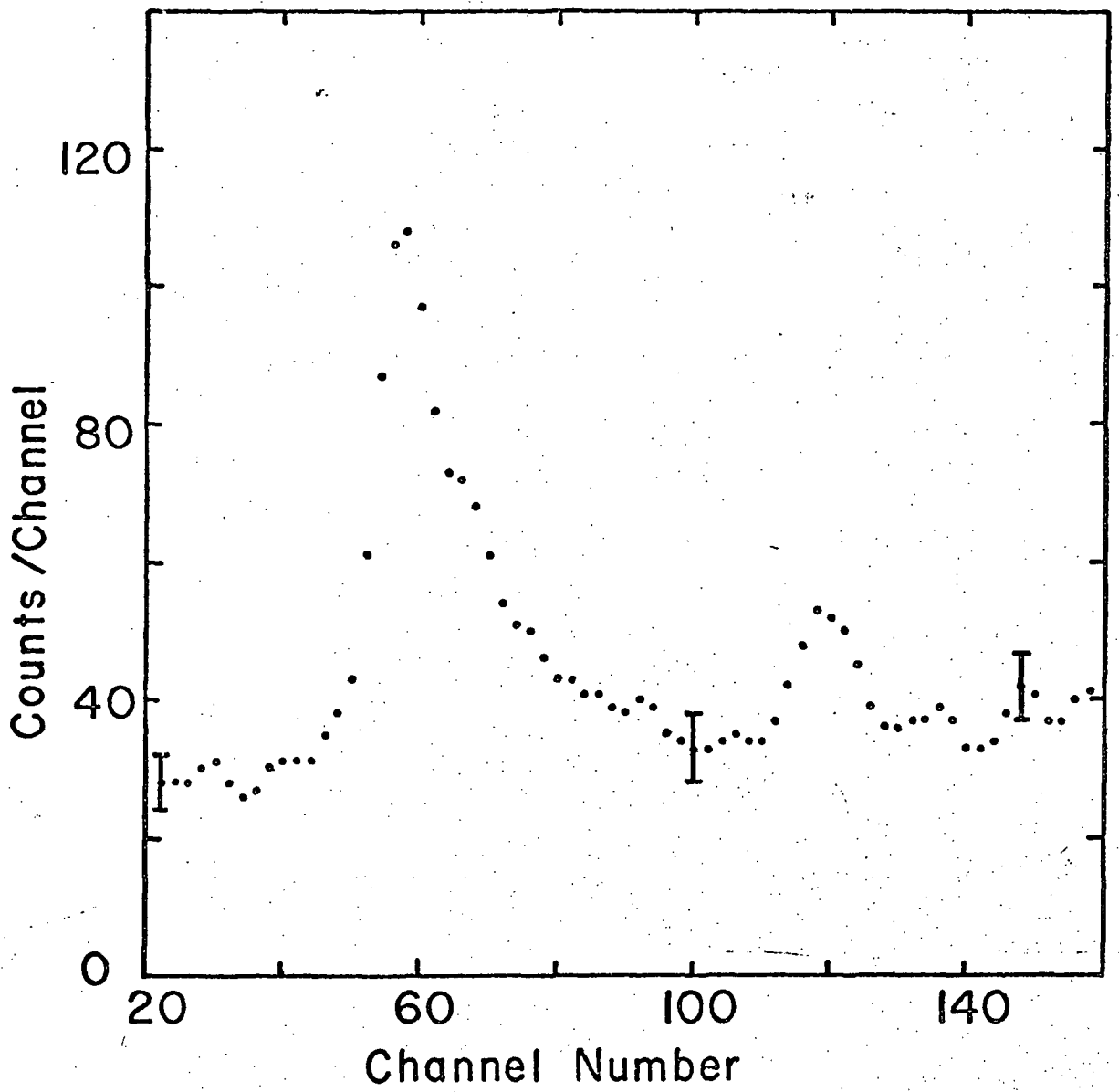


FIGURE 2.5

ENERGY SPECTRUM FROM MICA-GOLD SANDWICH

In addition to this peak attributed to the mica, we observe the increase in intensity of a peak,  $\sim 2.9$  eV above the main mica peak, as the thickness of gold is increased in steps from 20 nm to 320 nm. The peak due to gold also shows pronounced fine structure. Fig. 2.5 shows the results for 160 nm of gold.

The data so far obtained enables us to reach the following conclusions:

- a) The auxiliary structure in the source spectrum is relatively weak, suggesting perhaps the Krylon spray (most probably an amorphous coating) on the source is acting as a moderator. The full width of the peak at half intensity is  $\sim 0.2$  eV, excellent for  $e^+$  scattering.
- b) The copper disc is not acting as the moderator for the  $\text{Co}^{58}$  atoms diffused into it. The  $\text{Co}^{58}$  is electro-deposited on the surface of the Cu disc. The disc is then annealed at  $900^\circ\text{C}$  in an atmosphere of hydrogen for two hours. We expect very little diffusion of  $\text{Co}^{58}$  into the Cu disc as a result and the single energy peaks of the emitted positrons is consistent with our expectation. Substantial diffusion would have resulted in double peaks as in the case of micro-gold moderators. One would be due to Krylon and another due to copper, assuming that the peak energies are well separated. This assumption will be checked by a study, now in progress, of the spectrum of the source without Krylon.



- c) Although the peak due to mica comes very close in energy to that of the source, it has been found that this peak is not due to the slow positrons from the source. A bias is applied between the source and the mica-gold moderator which should produce a shift in the position of the gold peak (Fig. 2.5) from the source peak. No shift has been found. This implies that the slow positrons from the source are annihilated by the thick mica and the residual fast positrons emitted by the source are moderated in mica-gold moderator.
- d) For the first time, positrons have been detected by a secondary-emission process. We are able to infer from our data that single particle detection of positrons by secondary-emission devices (in the present case a Bendix Spiraltron - see Fig. 2.1) is preferable to the conventional  $2\gamma$  detection in terms of signal-to-noise ratio, cost, and efficiency. The efficiency of the  $2\gamma$  detector is limited by the size of the detectors and the solid angle they subtend.
- e) From these results the attenuation length, the thermalization length, and hence the thermalization time for slow positrons in gold (and similarly for other materials) can be obtained. This is the first direct measurement of the thermalization time of positrons.
- f) Results of attenuation lengths for slow positrons will be compared with that of electrons in gold and other

materials. This will enable us to understand the differences and similarities in the interaction of slow electrons and positrons with solids.

- g) Through these experiments the secondary-emission coefficients will be determined for positrons, electrons, and positive ions for the material used in the Spiraltron. The ratio of the secondary-emission coefficient for positrons and electrons from the experiments will be compared with the result obtained by Cherry.<sup>5</sup> The positions of the peaks are relative to the positions of positive ion peaks of 1, 2, 3, and 4 eV.

#### 2.4 Status of the Development of an Operational Positron Beam

Concurrent with the work aimed at understanding the nature of the emission process and its implications for the physics of the solid state, we are involved in a search for the material with the largest yield of slow positrons. So far we have examined only the source itself and the mica-gold system. We expect that what we learn about the physics of slow positron production should enable us to find the most efficient production system without an aimless trial-and-error hunt.

In the present configuration the amplitude of the mica peak is  $94e^+/\text{eV-min}$  for a 2mCi source of fast positrons. Since the width of the peak is approximately 1/2 eV we can estimate approximately  $50 e^+ \text{ min}^{-1}$  in the entire useable peak.

The transmission of the transfer lens has been measured for electrons at >60%, and the estimated detection efficiency is 50%. Thus the total flux at the source is approximately  $3 \text{ sec}^{-1}$ . This means the conversion efficiency is  $\sim 4 \times 10^{-8}$  for fast into slow positrons. Much improvement can be expected, as it is unlikely that the first choice of moderator material and thickness would be the optimum.

## 2.5 Future Studies

2.5.1 The further development of the low energy, mono-energetic, high intensity sources of positrons will require a continuation of the present plan to look at the energy and angular distribution of the emitted positrons as a function of moderator composition, thickness, temperature and geometry. Also, now that we find that the energy distribution of the emitted positrons is quite narrow ( $\sim 0.2 \text{ eV FWHM}$ ) it is important to determine if surface contamination varies the energies of emitted positrons with time.

2.5.2 The implications of structure in the energy spectra:  
a) At this stage it is not possible to explain the origins of the structure mentioned in Section 2.3. Analysis is being carried out to establish the nature of the structure.

b) Inelastic scattering effects of the slow positrons leading to both plasmon and phonon excitation are important. In the case of insulators excitonic transitions induced by positrons cannot be ruled out.

c) Tharp and Sheibner<sup>13</sup> as well as several other workers have observed inelastically scattered electrons from metal surfaces. The loss peaks have been clearly identified as due to bulk and surface plasmon excitations. Nothing precludes one from assuming that positrons in solids and at solid surfaces suffer characteristic energy losses. Indeed, if this is so, perhaps a new chapter in the solid state spectroscopy will be opened up and the traditional role of positrons for the investigation of solids will be expanded.

2.5.3 Further studies will be made to establish the extent of surface and bulk contributions in various materials. To eliminate surface contaminations, self-supporting metal films will be made in the experimental chamber at UHV conditions. The present experiments are carried out in a vacuum better than  $10^{-7}$  Torr. This has to be increased to  $10^{-10}$  Torr or better.

2.5.4 It should be noted that for a monoenergetic incident beam of positrons the inelastic structure occur at lower energies, whereas in the present case the structure is seen on the high energy side of the main peak. The structure cannot be explained by a simple picture of thermalization of positrons in a solid nor by the "negative work function" model.<sup>3,9</sup> Therefore, a new theory for the nature of thermalization has to be developed. Tong has obtained the values of work function in the Jellium model. A more rigorous theory is being developed to include lattice-ion interactions in the Wigner-Bardeen model.

2.5.5 Positrons should be a powerful method of investigating the electric dipoles on insulator surfaces. Muller,<sup>14</sup> for instance, made LEED observations of electric dipoles due to fractional monolayers of potassium ions on the cleaved surface of mica.

Due to polarization fields<sup>15</sup> in an insulator and the associated long relaxation times, it would appear that positrons should not be emitted by non-conducting surfaces. The present experiments indicate that this is not the case. Positrons from insulators need to be investigated more thoroughly.

It should be possible from these experiments to assess to what extent the positron results complement the results obtained by interactions of electrons, photons, and electric and magnetic fields with solids.

### 3. POSITRON STORAGE TECHNIQUES

#### 3.1 Introduction

One method of making fullest possible use of the low flux of positrons presently available from thin-film sources is to store the positrons in a "trap" which has a lifetime much longer than the time interval between emission of particles. H.G. Dehmelt and his students have shown<sup>16</sup> that a Penning configuration can contain electrons for several days, and we are in the process of applying this technique to positrons. A Penning trap (see Fig. 3.1) uses an electrostatic quadrupole field to limit the extent of motion of the particles parallel to the z-axis and a homogeneous magnetic field along the z-axis to provide containment in the perpendicular plane. We plan to store and detect the positrons in a manner identical to that used for electrons, but the problem of introducing positrons into the trap is more difficult than the corresponding process for electrons.

THE PENNING CONFIGURATION

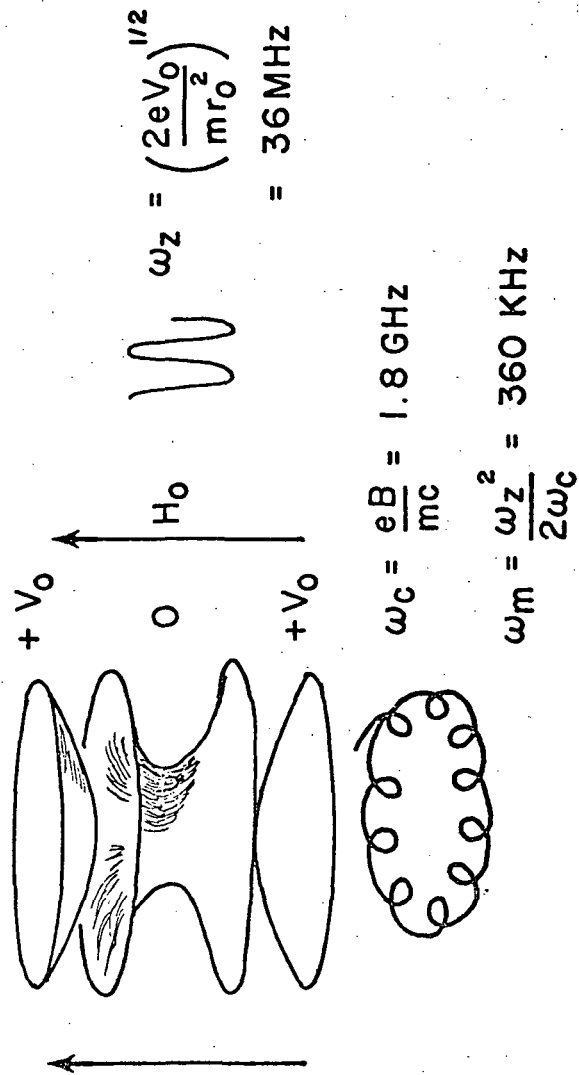


FIGURE 3.1

### 3.2 Experimental Apparatus

The Penning trap has been constructed and is presently undergoing initial testing. It consists of a machined aluminum hyperboloid of revolution with radius approximately 1 cm. The magnetic field is provided by a long solenoid which can maintain a field of approximately 600 G. The motion of charged particles in the region of interest is a combination of three motions. The electric field gives an harmonic motion parallel to the z-axis of angular frequency  $\omega_z = (2eV_0/mr_0^2)^{1/2}$  where  $V_0$  is the well depth in volts and  $r_0$  the trap radius. The magnetic field leads to cyclotron orbits of angular frequency  $\omega_c = eB/mc$ , and the combination of electric and magnetic fields provides a magnetron drift of approximate frequency  $\omega_m = \omega_z^2/2\omega_c$ . In the present case the frequencies are approximately  $\omega_z/2\pi = 36$  MHz,  $\omega_c/2\pi = 1.8$  GHz,  $\omega_m/2\pi = 360$  kHz.

The trap is contained in a bakeable ultrahigh vacuum system pumped with a 100 l/s Orb-Ion pump. Mild baking has allowed  $10^{-9}$  Torr to be reached, but with baking to  $300^\circ\text{C}$  it should be possible to reach the low  $10^{-10}$  Torr region to remove all effects of background gas on positron lifetime.

Electrons are normally introduced into such a trap by directing a beam of electrons into the trap. This beam ionizes residual gas atoms, yielding electrons which are trapped. The trapping of positrons is more difficult, but



should be possible through a two-stage process. The positron source, a radioactive  $\text{Co}^{58}$  emitter covered with suitable moderator, is located on one trap end cap, electrically insulated so that it may be biased at will. The positrons enter the trap with approximately 1 eV kinetic energy, slightly inclined to the z-axis. As Dehmelt has shown, the motion of charged particles in the z-direction may be "cooled" by making the two end caps part of an LC circuit tuned to the z-axis oscillation frequency  $\omega_z$ . See Fig. 3.2. The motion of the charged particles causes currents to flow in the parallel resonant circuit which are damped out by the high impedance of the circuit at resonance. Walls<sup>17</sup> shows that the time constant for this thermalization of z-axis motion to the temperature of the external inductor is  $16md^2/3e^2R$  where d is the separation of the end caps and R is the impedance of the circuit. By correctly designing the external inductor this time can be made approximately 0.2 sec. This is much too long a time to allow initial trapping of the electrons, but, fortunately, it is possible to trap the particles conditionally by transferring some of their momentum into the x-y plane where the phase space provided by the magnetic field is large. Walls also shows that the time constant for coulomb collisions to effect this momentum exchange ( $\tau_{\perp z}$ ) is inversely proportional to the density of trapped particles, and is a few milliseconds for  $10^4$  particles. Other methods of increasing this coupling between motions along the z-axis

THERMODYNAMIC SYSTEM

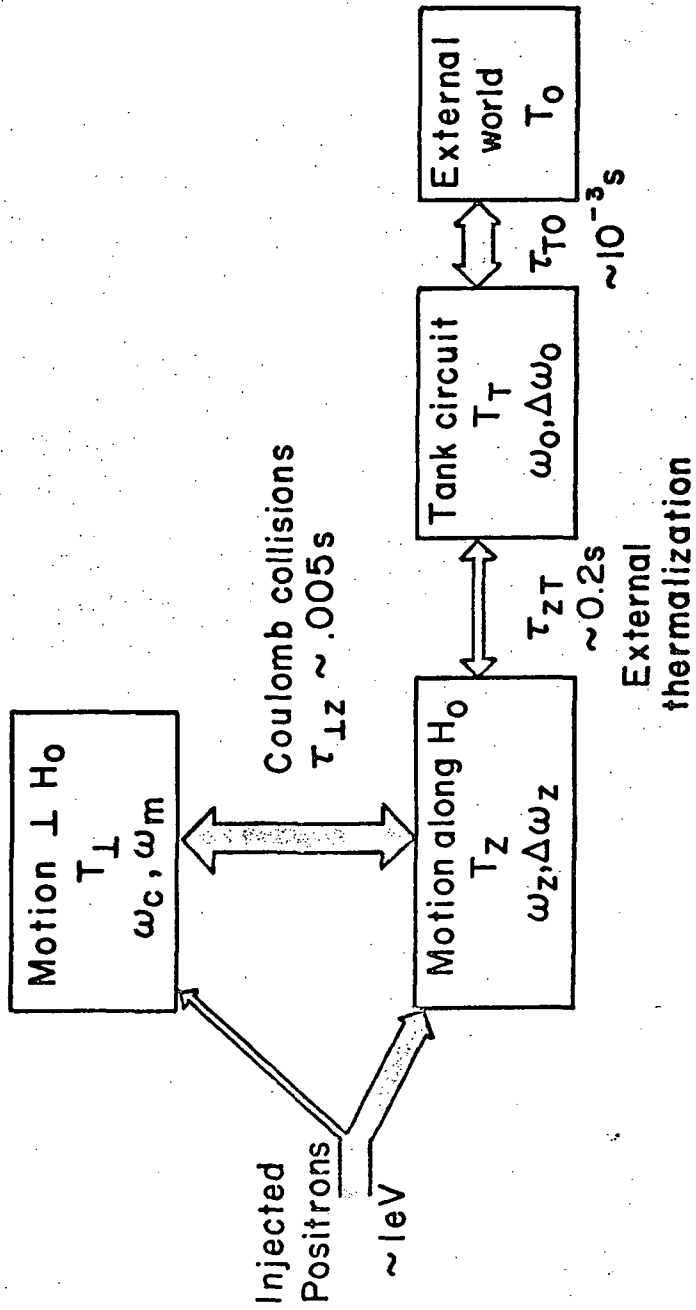


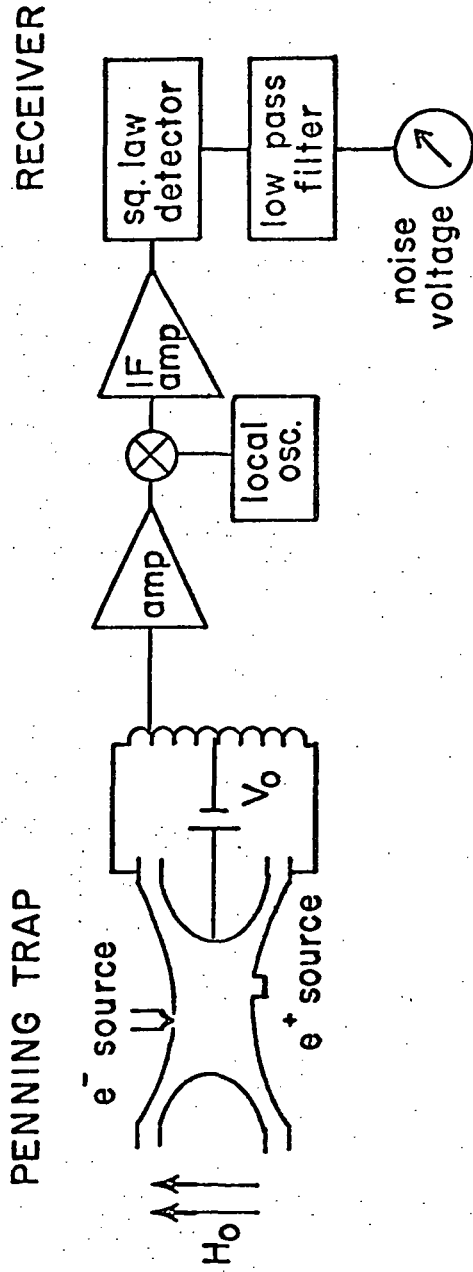
FIGURE 3.2

and the transverse plane are the injection of untrapped electrons and the inclination of the injected positron beam to the z-axis.

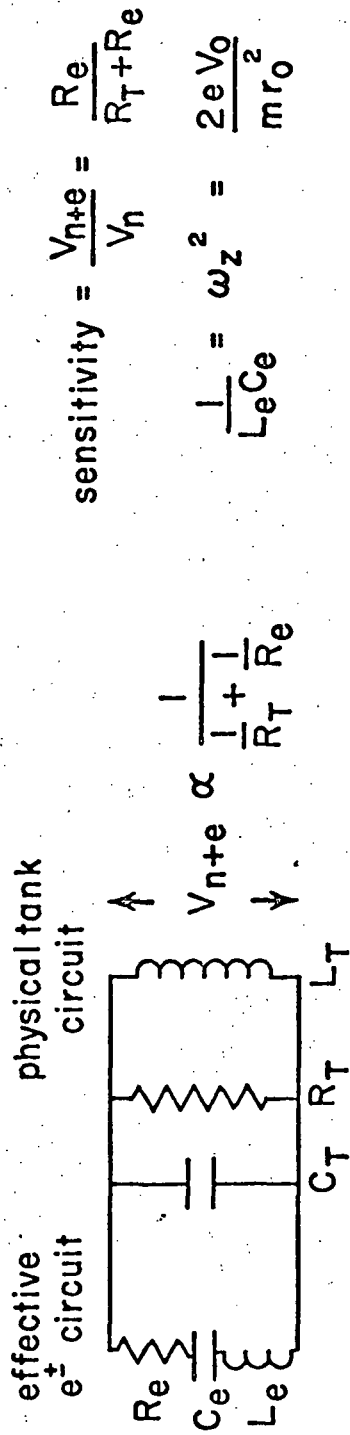
One feature of low-energy positrons that should aid trapping is observation in the General Atomic work that low energy positrons are repelled from metals.<sup>4,6</sup> This effective "negative work function" will aid by erecting higher potential walls than would be the case for electrons. It also makes possible an alternative injection scheme. A thin wire placed along the conical surface asymptotic to the trap surfaces could be coated with a slow positron source. While in an electron trap such a wire would intercept a large number of electrons, the work function barrier should merely add one more randomization mechanism to positrons.

Detection of the positrons involves the same LC circuit that provides thermalization. See Fig. 3.3. At resonance the charged particles in the trap load the LC circuit, causing an impedance  $Z$  to appear across the circuit inversely proportional to the number of particles. Since the noise power is proportional to the effective resistance, a receiver which is sensitive to the integrated noise power can give a dc level proportional to this noise, and thus related to the number of charged particles in the trap. The receiver used includes a MOSFET preamplifier stage, a SP-600 receiver, with

POSITRON/ELECTRON DETECTION SCHEME



ELECTRICAL EQUIVALENT



$$\text{sensitivity} = \frac{V_{n+e}}{V_n} = \frac{R_e}{R_T + R_e}$$

$$\frac{1}{L_e C_e} = \omega_z^2 = \frac{2eV_0}{m r_0^2}$$

FIGURE 3.3

a low-pass filtered dc amplifier connected to the output of the diode detector. It should be possible to detect approximately  $10^4$  positrons by this method.

There is an alternative method of positron detection available. One end cap of the trap can be made of 90% transparent copper gauze, and the trap can be dumped through this gauze, sending the accumulated positrons downstream to a thin annihilation foil. The two 0.511 MeV gammas detected in coincidence record the number of positrons in the trap. This scheme has the disadvantages of being destructive measurement of limited (1%) detection efficiency, and of being specifically for positrons, i.e. excluding testing with electrons.

### 3.3 Planned Program

The initial experiment which will be done with the trap is simply to first trap electrons, then positrons. The various time constants will be measured and the operation of the trap explored.

The lifetime for positrons as a function of residual gas pressure will then be measured. Providing the trap is deep enough to contain elastically scattered positrons, this can provide a measurement of annihilation cross sections for thermal positrons. By progressively reducing the trap depth

to allow collisionally heated positrons to escape, it should be possible to obtain some information about elastic scattering processes. The trapped positrons can be heated by applying power at the cyclotron frequency to reach energies up to about 20 eV for both elastic and inelastic studies.

Another experimental method is that used by Fortson<sup>18</sup> with electrons. He measures the equilibrium temperature at a given pressure of one noble gas, then, after filling with another gas, finds the pressure which gives the same temperature. He claims that this gives a measure of the relative scattering cross sections of thermal electrons by the gases. Such studies should be equally applicable for positrons.

#### 4. CROSSED BEAM EXPERIMENT

##### 4.1 Positron Transport and Analysis

To study the interaction of low energy (1-20 eV) positrons with atoms using the crossed beam technique, an electrostatic lens system has been built and is being tested with electrons. The lens system (see Fig. 4.1) is enclosed in a vacuum chamber which is pumped to  $10^{-7}$  Torr. The chamber construction allows lead shielding to be placed between the source and the detector thus reducing background counting due

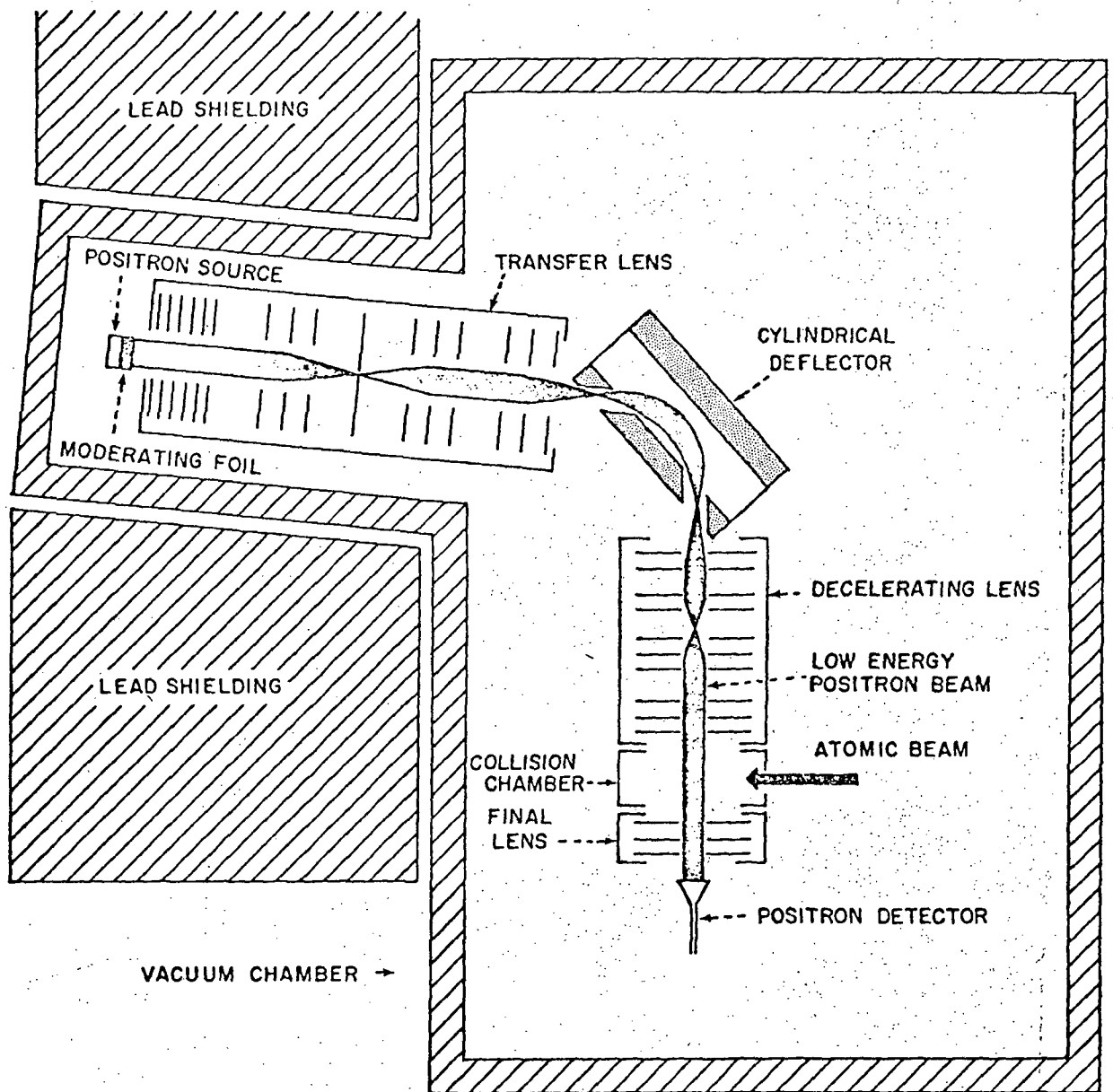


FIGURE 4.1

CROSSED BEAM APPARATUS

to gamma rays. Magnetic shielding has been built and is ready for installation.

The positrons are transported from the moderating foil to the deflector by the transfer lens. The positrons are initially given 200 eV additional energy to make the transfer more efficient. The beam area is defined by the slit aperture in the transfer lens.

The cylindrical deflector is adjusted to transmit the low energy positrons while blocking fast positrons and gamma rays. It was built for maximum transmission rather than for good energy resolution, since the energy spectrum of the positrons emitted by the foil has a narrow peak (FWHM  $\sim$  0.2 eV) at low energy (1 eV).

The decelerating lens focuses the positrons as they emerge from the deflector, decelerates them, and directs them across the collision chamber. The final lens accelerates the transmitted positrons and transports them to the Bendix Spiraltron electron multiplier.

The voltages for the entire lens system are furnished by one power supply used with a voltage divider assembly. To study atomic interactions as a function of incident proton energy, the voltage applied to the positron source and moder-



ating foil is varied. The collision chamber is held at true ground potential. The positron beam remains in focus because the varying potential is also the floating ground of the lens system.

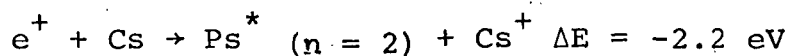
The lens system has been tested for electrons and operates satisfactorily.

#### 4.2 Alkali Beam System

An alkali oven is being designed to utilize the low energy positron beam in atomic collision studies.

Of immediate interest are the elastic and inelastic scattering cross sections of low energy positrons by cesium atoms. A comparison of positron cross sections with electron cross sections could be difficult because there is considerable disagreement in both theory and experiment concerning the elastic scattering cross section for electrons.<sup>19</sup> Therefore, measurements of both electron and positron scattering cross sections will be made.

Subsequently, the charge exchange reaction



will be investigated. We are particularly interested in attempting to detect 2430 $\text{\AA}$  radiation (Ps Lyman- $\alpha$ ) from the decay of excited positronium. In their attempts to measure

the  $2430\text{\AA}$  radiation, previous investigators have used high pressure gas to stop the positrons.<sup>20,21</sup> The failure of these attempts is likely due to de-excitation of the positronium occurring by collision rather than by radiation.<sup>21</sup> The cesium density in the crossed beam region of the present experiment is low enough ( $10^{14}$  atoms/cm<sup>3</sup>) so that  $2430\text{\AA}$  radiation should be the dominant de-excitation mechanism.<sup>21</sup> This experiment is unique in that a large probability for positronium formation is obtained by using low energy positrons rather than by using a high density of atoms.

Cesium was chosen for the first set of experiments because of its properties which include:

- a) Cs is atomic hydrogen - like and therefore amenable to calculation in a way similar to three body systems.
- b) Cs has a large atomic radius ( $2.67\text{\AA}$ ) which should result in a large scattering cross section for positrons.
- c) It has a low ionization potential which increases the probability of charge exchange with positrons, i.e., the Ps formation channel is always open and the formation of excited positronium is energetically preferred.
- d) Cs has a low melting temperature which makes it possible to keep a high density of atoms localized to the collision region by using surfaces at liquid nitrogen temperature to condense the vapor.

An intense ( $\sim 10^{14}$  atom/cm<sup>3</sup>) cesium beam will be formed with a supersonic nozzle or a calibrated hole structure at the mouth of the oven. The oven will be initially charged with 30 grams of cesium and a simple recirculation system will extend the operation time. The flux of cesium atoms will be measured with a hot wire detector.

## 5. ASSOCIATED THEORETICAL STUDIES

### 5.1 P.A. Fraser (Applied Mathematics) and Associates

Recently Y.F. Chan completed a thesis entitled "Scattering of Positrons by H Atoms" where he calculated the R matrix for S-wave scattering in the region 1/2 to 3/4 Ry kinetic energy. His study was in essence a close coupling approach with correlation which has satisfactorily satisfied the bound principle. B. Page is continuing work on (Ps,He) scattering where he is presently extending the early static exchange results of Fraser for this system.

### 5.2 D.F. Gallaher (Physics) and Associates

An investigation of ( $e^+$ ,H) elastic scattering below the Ps formation threshold in a pseudo-state expansion formulation has been carried out with Y.C. Fon for the s, p, d partial

wave phase shifts. The results are found to be in good agreement with those of long range force oriented models. A natural extension of this work requires the incorporation of short range effects due to virtual positronium formation in suitably chosen pseudo states of positronium.

### 5.3 B.Y. Tong (Physics) and Associates

Further consideration is being given to the theory of the negative work function, bulk effects and surface contamination effects in order to help interpret recent results.

### 5.4 J. Nuttall (Physics) and Associates

Work in progress consists of rigorous discussion of behaviour of scattering amplitudes of a three-body threshold in the case of short range forces; study of convergence of Kohn method in more general cases; investigation of asymptotic form of wave function for three charged particles; further study of complex energy method for atomic scattering and attempts to apply it to excitation and ionization in e-H scattering; investigation of further applications of analyticity to atomic scattering, in the hope of proving convergence of Born series at high energies and deriving non-singular integral equations for three-particle scattering; calculation of neutron-deuteron scattering by the complex coordinate method.

6. ROUGH OUTLINE OF PROGRAM

Provided funds are available, the three apparatuses will be operated simultaneously, with the solid state experiment serving to study in detail  $e^+$  source properties, while the two different scattering spectrometers are tried.

- a) Source Experiment - The purpose of this experiment is to learn in detail how the thermalization process works by studying some different moderators as a function of moderator thickness, surface contamination, temperature, etc.
  
- b) Positron Bottling Experiment - With the completion of the trap tests with electrons, attempts will be made to trap measurable numbers of electrons. Once successful attempts to scatter electrons then positrons will be made. Probably  $H_2$  or He will be used as the first scattering gas.
  
- c) Crossed Beam Apparatus - With the completion of the lens tests with electrons, positrons will be used in the transfer system and analyser. The first positron tests will be used to check shielding and the efficiency of  $e^+$  detection. After these tests, the Cs beam system will be installed. Cs and other alkalis will be first tested.

REFERENCES

1. D.G. Costello, D.E. Groce, D.F. Herring, & J. Wm. McGowan, *Can. J. Phys.* 50, 23 (1972)
2. J. Wm. McGowan, Positron Experiments Today: Scattering from Helium, VII ICPEAC Amsterdam, The Netherlands, 26-30 July 1971, to be published North-Holland Pub. Co.
3. R.J. Drachman, Positron Theory, VII ICPEAC Amsterdam, The Netherlands, 26-30 July 1971, to be published North-Holland Pub. Co.
4. D.G. Costello, D.E. Groce, D.F. Herring, & J. Wm. McGowan, *Phys. Rev. B*, 5, 1433 (1972)
5. W.H. Cherry, Ph.D. Thesis (Princeton University 1958)  
(unpublished)
6. D.E. Groce, D.G. Costello, J. Wm. McGowan, & D.F. Herring, *Bull. Am. Phys. Soc.* 13, 1397 (1968); Proceedings of the Vith International Conference on the Physics of Electronic and Atomic Collisions (MIT Press, Cambridge, Mass., 1969)  
p. 757
7. J.M.J. Madey, *Phys. Rev. Letters* 22, 784 (1969)
8. B.Y. Jaduszliwer, T.J. Bowden and D.A.L. Paul, *Bull. Am. Phys. Soc.* 15, 785 (1970)
9. C.E. Kuyatt and J.A. Simpson, *Rev. Sci. Instr.* 38 103 (1967)
10. J.R. Smith, *Phys. Rev.* 181, 522 (1969)
11. N.D. Lang and W. Kohn, *Phys. Rev. B* 3, 1215 (1971)
12. B.Y. Tong, *Phys. Rev. B*, 5, 1436 (1972)
13. L.N. Tharp and E.J. Scheibner, *J. Appl. Phys.* 38 (3320) (1967)

14. K. Muller in *The Structure and Chemistry of Solid Surfaces*, edited by G.A. Somorjai (John Wiley, New York, 1969) p.35-1
15. H.J. Wintle et al, *J. Appl. Phys.* 44, 719 (1972)
16. For review papers see H.G. Dehmelt, "Radio Frequency Spectroscopy of Stored Ions" in Advances in Atomic and Molecular Physics, D.R. Bates, Ed., Vol 3 (1967) and Vol 5 (1969)
17. F.L. Walls, Thesis, Univ. of Washington (1970) (unpublished)
18. M.D. McGuire and E.N. Fortson, *Bull. Am. Phys. Soc.* 17, 131 (1972)
19. J.A. Dayton, Jr., NASA Technical Memorandum TM X-1897 (1969)
20. L.W. Fogg, *Nuc. Inst. and Methods* 85, 53 (1970)
21. M. Leventhal, *Proc. Natl. Acad. Sci.* 66, 6 (1970)

APPENDIX 1

- 1.1 E.L. Chaney, P.W. Zitzewitz, J.Wm. McGowan, "Two Experimental Approaches to the Study of Interactions of Low-Energy Positrons with Thin Targets" VII Int. Conf. on the Physics of Electronic and Atomic Collisions, Amsterdam, The Netherlands, 26-30 July 1971.
- 1.2 R.K. Cacak, R. Caudano, T.D. Gaily, J. Wm. McGowan, "MEIBE Progress", VII Int. Conf. on the Physics of Electronic and Atomic Collisions, Amsterdam, The Netherlands, 26-30 July 1971.
- 1.3 Subrahmanyam Pendyala, P.H.R. Orth, J. Wm. McGowan, and P.W. Zitzewitz, "Experimental Study of the Emission of Low Energy Positrons from Metals", 2nd Int. Conf. on Positron Annihilation, Queen's University, Kingston, Ontario, August 1971.
- 1.4 M.M. Pant, Subrahmanyam Pendyala and J.Wm. McGowan, "A Pseudopotential Approach to the Calculation of Positron Annihilation in Metals and Simple Substitutional Alloys", 2nd. Int. Conf. on Positron Annihilation, Queen's University, Kingston, Ontario, August 1971.



- 1.5 Subrahmanyam Pendyala, M.M. Pant and B.Y. Tong, "Positron Annihilation at F-Centres", 2nd Int. Conf. on Positron Annihilation, Queen's University, Kingston, Ontario, August 1971.
- 1.6 D.G. Costello, D.E. Groce, D.F. Herring, and J. Wm. McGowan, "(e<sup>+</sup>, He) Total Scattering", Can. J. Phys. 50, 23 (1972).
- 1.7 B. Y.Tong, "Negative Work Function of Thermal Positrons in Metals", Phys. Rev. B, 5, 1436 (1972).
- 1.8 D.G. Costello, D.E. Groce, D.F. Herring, and J. Wm. McGowan, "Evidence for the Negative Work Function Associated with Positrons in Gold", Phys. Rev. B, 5 1433 (1972).
- 1.9 Subrahmanyam Pendyala, J. Wm. McGowan, and B.Y. Tong, "A Model Work Function of Positrons in the Wigner Seitz Approximation", Abstract submitted to the American Physical Society Meeting, 24-27 April 1972, Washington, D.C.
- 1.10 Subrahmanyam Pendyala, J.Wm. McGowan, P.W. Zitzewitz, and P.H.R. Orth, "Emission of Low Energy Positrons from Solids", Abstract submitted for the American Physical Society, 24-27 April 1972, Washington, D.C.
- 1.11 P.W. Zitzewitz and J.Wm. McGowan, "The Lifetime of Free

Positrons", Abstract submitted to the CAP Annual Meeting, 26-29 June 1972, Edmonton, Alberta.

- 1.12 S. Pendyalan, J.Wm. McGowan and P.W. Zitzewitz, "Solid State Spectroscopy with Low-Energy Positrons", Abstract submitted to the CAP Annual Meeting, 26-29 June 1972, Edmonton, Alberta.
- 1.13 W.C. Fon and D.F. Gallaher, "Positron-Hydrogen Elastic Scattering with Inclusion of Long Range Effects via a Pseudostate Expansion", accepted for publication J. Phys. B: Atom. Molec. Phys. Vol. 5.
- 1.14 J.Wm. McGowan, "Positron Experiments Today: Scattering from Helium", accepted for publication North Holland Pub. Co., 1972.
- 1.15 Subrahmanyam Pendyala, M.M. Pant and B.Y. Tong, "APW Calculation for Band Structure of Cadmium", Can. J. Phys. 49, 2633 (1971).

TWO EXPERIMENTAL APPROACHES TO THE STUDY OF INTERACTIONS OF  
LOW-ENERGY POSITRONS WITH THIN TARGETS<sup>†</sup>

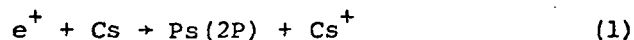
E. L. CHANEY, P. W. ZITZEWITZ, J. Wm. MCGOWAN

The University of Western Ontario, London, Canada.

## I. A Positron-Atom Crossed Beams Apparatus

An intense  $\text{Cu}^{64}$  source ( $\sim$  tens of Curies), with an energy moderating foil in front of the source, provides the low-energy ( $\sim$  leV) positrons.<sup>1</sup> An electrostatic lens system with a cylindrical mirror deflector transports the positrons to the interaction region in a separate chamber where the positron beam is crossed by an intense beam of atoms, which emanate from a specially designed oven incorporating a collimated array of capillaries. A commercial channel electron multiplier is used to detect the positrons.

Due to its hydrogenic character, very low ionization potential and ease of handling, cesium has been chosen for the first set of experiments. We will attempt to observe the charge transfer reaction which leads to excited positronium



by looking for the  $\text{Ps}(2P)$  Lyman- $\alpha$  radiation. A solar-blind detector with a peak sensitivity near  $2430\text{\AA}$  will be used.

Figure 1 shows a schematic of the apparatus, which will be described in detail. Preliminary measurements will be presented.

---

<sup>†</sup> Work supported by the N.R.C. of Canada and the U.S. N.A.S.A. under contract number NGR 52-009-006.

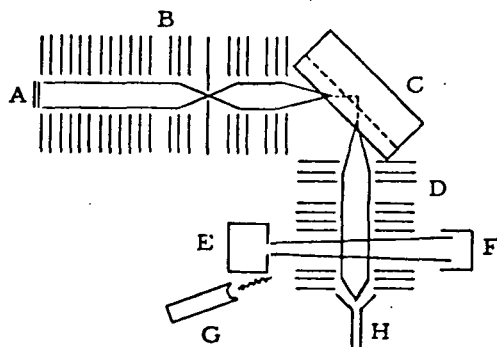


Fig. 1. A -  $\text{Cu}^{64}$  source and moderating foil; B - electrostatic transfer lens; C - cylindrical-mirror deflector; D - accelerating lens; E - Cesium oven; F - hot-wire detector; G - solar-blind detector; H - channel electron multiplier.

## II. A Trapped Positron Apparatus

A method to provide an alternative to a high intensity positron beam is to use an electro-magnetic trap to contain a low-level positron flux for a long time. Using a Penning configuration, a 500G axial magnetic field provides radial confinement while a DC electric quadrupole field limits the axial motion. A small  $\text{Co}^{58}$  source ( $\sim 0.1$  Curie), and an energy-moderating foil,<sup>1</sup> plated consecutively on a fine wire located on the  $V = 0$  surface of the trap, provides the low-energy positrons. The number of positrons in the trap is determined by dumping the positrons out through a highly transparent metal gauze end cap. The positrons are then transported to a thin foil on which only slow positrons will annihilate. Standard coincidence counting techniques are used to detect the positrons. A schematic of the apparatus is shown in Figure 2.

The cross sections for positron annihilation on various gases can be measured by determining the number of positrons

trapped as a function of gas pressure. By making this measurement as a function of trap depth the momentum transfer cross sections can also be determined.

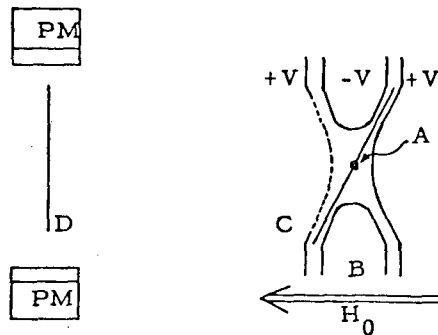


Fig. 2. A -  $\text{Co}^{58}$  source and moderating foil; B - Penning quadrupole field; C - Gauze end cap; D - Annihilation foil.

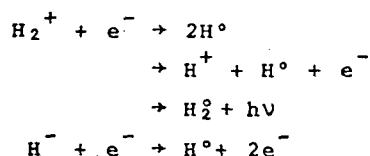
#### References

- <sup>1</sup> Evidence for the Negative Work Function Associated with Positrons in Gold, D. G. Costello, D. E. Groce, D. F. Herring, J. Wm. McGowan. Submitted for publication.

## MEIBE\* PROGRESS

R.K. CACAK, R. CAUDANO<sup>†</sup>, T.D. GAILY, J.Wm. MCGOWAN  
The University of Western Ontario, London 72, Canada

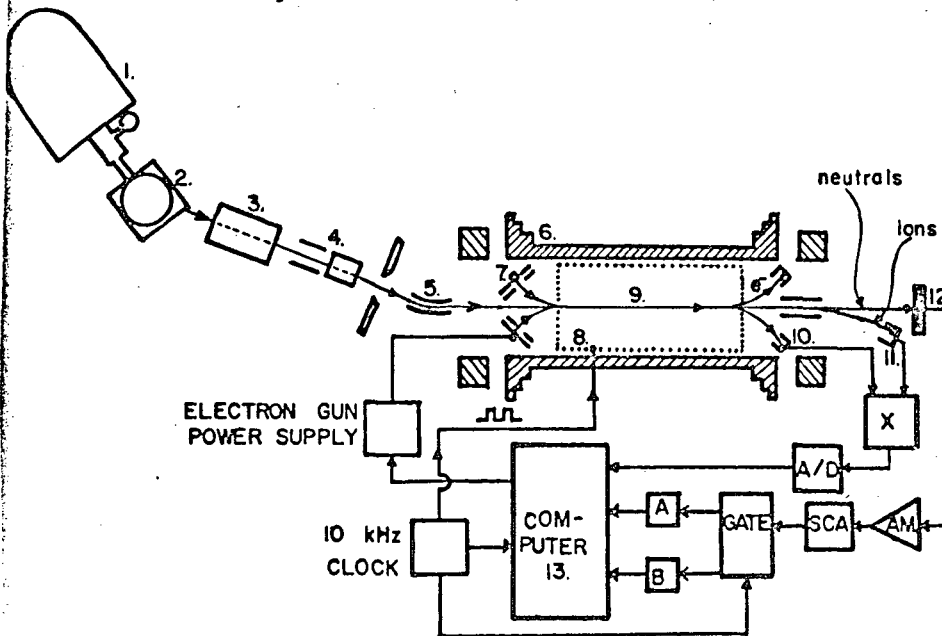
Electron-ion recombination and detachment processes in the energy range 0.0 to 20 eV are being studied in a merging electron-ion beam experiment (MEIBE - pronounced maybe). Among the reactions presently under study are



and recombination and detachment of various other ions of atmospheric and biomedical importance. The MEIBE is unique for several reasons besides being one of the few merged electron-ion beam apparatuses. At the high ion energies used ( $\sim 400$  keV), the reactants may be detected using standard nuclear particle techniques. The experiment is controlled and calculations are made by a small on-line computer. Finally, this is the first merging electron-ion experiment where the effective resolution of the interaction energy is increased by the high laboratory velocity of the electron beam. For 400 keV ions,  $\sim 110$  eV electrons yielding an interaction energy of 1 eV, the energy spread in the center-of-mass is expected to be of the order of 0.1 eV. The ions are formed in an RF discharge ion source and are accelerated to an energy of 400 keV (Figure 1) by a Van de Graaff accelerator (1). After momentum analysis (2) the beam is focused by a magnetic quadrupole lens (3) and is positioned with a set of steering plates (4) before it enters the interaction chamber. Further electrostatic deflection of the ion beam (5) as it enters the interaction chamber removes the charge-transferred neutrals. The ions then enter the center of a long, axially symmetric, solenoidal magnetic field. The field is created by a solenoid (6) approximately 75 cm long, constructed to give uniform fields with small radial components near the center of the coil and a rapidly diverging magnetic field near the ends. The end-field guides a beam of electrons from a ring-shaped electron gun (7) into the ion beam, which passes through the center of the ring. The electrons enter the ion beam from all sides in a conical sheet. The laboratory energy of the electrons for a fixed ion energy determines the center-of-mass energy of the reactions.

During alternate half cycles of a 10 kHz chopped voltage applied to a grid (8) around the interaction region (9)

Figure 1. MEIBE (not to scale).



the electron beam is accelerated to a center-of-mass velocity where the cross section is known to be negligible. Using this modulation technique, the signal may be distinguished from the background of neutrals formed by charge-transfer processes in the interaction region. An interaction region pressure of about  $5 \times 10^{-10}$  Torr further reduces the background to an acceptable value. At the end of the 40 cm. long interaction region, unreacted charged particles are deflected into Faraday cups (10,11) while the energetic neutrals are undeflected and are detected by a lithium-silicon solid state detector (12). The energy resolution of the detector is sufficient to discriminate monatomic ( $\sim 200$  keV) from diatomic neutrals ( $\sim 400$  keV).

The overlap integral of the electron and ion beam densities is measured in three dimensions with a rotating wheel (not shown in Fig. 1). This wheel, in which a spiral arrangement of small holes is drilled, intersects and moves parallel to the beams as it rotates. Each hole allows a different portion of the two beams to pass through, and by simultaneously measuring the two currents, the overlap integral, an important experimental parameter, is determined.

The signals are amplified, analyzed, and digitized and then ultimately collected by a small on-line computer (13)

which gates the information into the proper storage buffer in phase with the chopped electron beam. The computer retrieves the signal from the background and makes a statistically-based decision when to advance the electron gun voltage to the value corresponding to the next center-of-mass energy.

- \* Merging Electron-Ion Beams Experiment. The authors wish to express their gratitude to the National Research Council of Canada for support of the project.
- + Departement de Physique, Facultes Universitaire N-D de la Paix, Namur, Belgium.



Experimental Study of the Emission of Low Energy  
Positrons from Metals\*

Subrahmanyam Pendyala, P. H. R. Orth, J. Wm. McGowan,  
and P. W. Zitzewitz

Department of Physics, University of Western Ontario,  
London, Ontario  
Canada.

The study of slow positrons emitted from the solids used to moderate several hundred keV positrons holds the interest of both atomic and solid-state physicists. The use of these positrons in collision experiments attracts the former, and the elucidation of the mechanism of their production is an interesting problem for the physicist interested in the properties of solids and their surfaces.

Although Madanski and Rasetti<sup>1</sup> failed to find low energy positrons from various materials, Cherry<sup>2</sup> did observe them with energies under 10 eV in 1958. In both these studies a radioactive source provided the fast positrons. Groce *et al*<sup>3</sup> obtained positrons from pair-production by brehmsstrahlung radiation emitted by stopping high energy electrons produced in a linear accelerator. They observed a sharp peak in the positron spectrum near 1 eV and a narrow angular distribution of the slow particles. Paul and co-workers<sup>4</sup> using a radioactive source, reported emission between 300 and 1500 eV, and, more recently, Jadaszliwer *et al*<sup>5</sup> have reported the very low energy positrons with narrow energy and angular distributions. About one slow positron is produced for each  $10^7$  fast positrons. Madey<sup>6</sup> has also observed slow positrons from dielectric films.

Following independent suggestions by Kohn<sup>7</sup> and Callaway<sup>8</sup>, Tong<sup>9</sup> has recently described a theoretical model which suggests that the fast positrons may be thermalized in, and then "thrown" from, the moderating material with an energy equal to the positron or "negative" work function. This model implies that the thin gold foil evaporated on the moderators used by Groce does more than simply provide an equipotential surface. Similarly, it indicates the importance of the chromium coating on the mica in Cherry's experiment and the aluminum film on Madey's polyethylene. However, the model does not predict a peaked positron spectrum.

The present experiment is designed to study the low energy positrons with a view towards understanding the processes of moderation and emission in the foils. In view of the previous experimental results and the theoretical suggestions, we have built our apparatus to allow positrons from a radioactive source, either  $\text{Cu}^{64}$  or  $\text{Co}^{58}$ , to fall upon moderator foils in a movable holder. This enables us to vary the type of material, its thickness, and the angle between the normal to the foil and the axis of the analyzer. By means of a helium cold-finger the foil can be cooled to  $4^\circ\text{K}$ . In addition, a vacuum deposition chamber can be attached to the system so that fresh surfaces may be prepared, annealed, and used without exposure to air. The electrostatic  $180^\circ$  spherical analyzer has been designed with small angle and energy acceptance. Both the standard 2- $\gamma$  coincidence detection scheme and a Mullard channel electron multiplier are used.

The vacuum chamber is stainless steel with copper and greaseless Viton-A O-rings. We have avoided organic materials within the vacuum system and have used oil-free pumping by adsorption fore-pumps and an Orb-Ion electrostatic titanium pump. The system can be baked to  $150^\circ\text{C}$ . Currently the pressure is just under  $10^{-7}$  Torr.

In the present experiments a strong  $\text{Cu}^{64}$  source was used. After transport from the Chalk River Reactor the strength was near 1 Ci. The surface of the copper appears bright and clean, but we plan to make more detailed studies of its microscopic condition. In future runs a  $\text{Co}^{58}$  source with strength near 10 mCi will be employed. Aluminum, copper, and gold moderators of .001 to .020 in. thickness have been used in the holder described above. In addition, since the surface of the  $\text{Cu}^{64}$  source should provide self-moderation for positrons created within the metal, some runs have been made with no additional moderator.

The lenses and spherical analyzer were built of OFHC copper following a design by Chris Kuyatt. They accelerate positrons from the source to 11.2 eV for analysis then transport them to the detector. By maintaining the source at ground potential and placing the analyzer on a voltage ramp between -15 and 0 V, any positron with kinetic energy between 0 and 15 eV can be studied. The energy resolution,  $\Delta E$ , was designed to be 50 meV. Because of low counting rates it was found to be desirable to broaden this resolution for early experiments. Since  $\Delta E/E$  is a function of geometry alone, this broadening can be achieved simply by increasing the

energy,  $E$ , at which the analysis is done. A width of approximately 1 eV has been used. The entire source and analyzer is surrounded by two concentric magnetic shields.

The transfer lens was originally 12" long, but this allowed only a half inch of lead shielding around the photomultiplier tubes, and the background rate was excessive. The most recent run is being made with a transfer lens twice that long. There is at least 4" of lead around the tubes and 16" between the source and detector. The 2- $\gamma$  detection system uses NaI(Tl) scintillators and 56AVP photomultipliers in a fast-fast coincidence circuit. The positrons are accelerated to 1 KeV and focussed on the cone of a Mullard channel electron multiplier<sup>10</sup> placed between the two scintillators. Secondary electrons produced by the collision on the cone should provide a high-efficiency detection signal. It is hoped that this much simpler detector will be found suitable for future positron-atom collision experiments. It is also of interest to confirm Cherry's result that the secondary electron production for positrons is only 40% that of similar electrons. To provide a check on this method of detection we can monitor not only the counting rate for the multiplier, but also the coincidence between these counts and the 2- $\gamma$  coincidence events.

A Kicksort multichannel analyzer allows events from any one of these three detection modes to be recorded as a function of ramp voltage, and thus positron energy.

Two runs have been completed and the third is now underway, with results to be presented at the conference. In the first run we were unable to identify a positron signal because of the high background rate and the low signal caused by the narrow analyzer resolution. In the second, which used the broadened resolution, a few positrons were observed despite electronics problems. Although the energy distribution could not be measured, the signal to background ratio (S/B) increased during the run as the source died, supporting the conclusion that true events were observed. The source of the high background rate is not completely understood. The increase in S/B suggests accidental coincidences between one annihilation gamma and either another annihilation gamma or a degraded or partially stopped 1 MeV gamma from another branch of the  $\text{Cu}^{64}$  decay scheme. The great increase in the amount of lead shielding should reduce both these sources.

There is another possible cause of background, which should not decrease faster than the signal, caused by the large flux of unmoderated positrons produced at the source. Positrons may have a small, but finite, probability of bouncing off metal surfaces and thus a few may reach the detector without being selected by the analyzer. While these positrons cannot

be completely contained without reducing vacuum pumping speed to zero, it is hoped that the longer transfer lens will also help to eliminate this source of background.

\* Supported by the National Research Council and the (U.S.) National Aeronautics and Space Administration.

#### References

- <sup>1</sup> L. Madanski and R. Rasetti, Phys. Rev. 79, 397 (1950).
- <sup>2</sup> W. H. Cherry, Ph.D. Thesis, Princeton University, 1958 (unpublished).
- <sup>3</sup> D. E. Groce, D. G. Costello, J. Wm. McGowan, and D. F. Herring, Bull. A.P.S. 13, 1397 (1968); D. F. Herring, J. Wm. McGowan, D. E. Groce, and V. Orphan, Proc. Vth Int. Conf. on the Physics of Electron and Atomic Coll., Publishing House NAUKA, Leningrad, 1967; D. E. Groce, D. G. Costello, J. Wm. McGowan, and D. F. Herring, VIth Int. Conf. on the Phys. of Elec. and Atomic Collisions, MIT Press, Cambridge, Mass., 1969, p.757.
- <sup>4</sup> D. A. L. Paul, P. W. Hietala, G. F. Celitans, P. G. Stangeby, and J. Maksimov, Bull. A.P.S. 13, 1474 (1968).
- <sup>5</sup> B. Y. Jaduszliwer, T. J. Bowden, and D. A. L. Paul, Bull. A.P.S. 15, 785 (1970); B. Jaduszliwer, W. C. Keever, T. J. Bowden, and D. A. L. Paul, Proc. VIIth Int. Conf. on the Phys. of Electronic and Atomic Collisions, North-Holland, Amsterdam, 1971, p.920.
- <sup>6</sup> J. M. J. Madey, Phys. Rev. Letters, 22, 784 (1969).
- <sup>7</sup> W. Kohn, Private Communication.
- <sup>8</sup> J. Callaway, Private Communication.
- <sup>9</sup> B. Y. Tong, Private Communication.
- <sup>10</sup> Supplied courtesy of Mullard, Ltd.

A PSEUDOPOTENTIAL APPROACH  
TO THE CALCULATION OF POSITRON ANNIHILATION\*  
IN METALS AND SIMPLE SUBSTITUTIONAL ALLOYS.

M.M. Pant, Subrahmanyam Pendyala<sup>†</sup>  
and J. Wm. McGowan

Department of Physics  
University of Western Ontario  
London, Ontario, Canada

Positrons annihilating in solids have been found to be a useful probe for obtaining information about the momentum distribution of the electrons. For pure metals however, this tool cannot compete with other more precise methods of measuring the Fermi Surface parameters. Because the techniques of measuring positron annihilation angular correlation curves do not require specimens with long electron mean free path, it is expected to be a more fruitful way to examine the Fermi Surface and electronic structure of alloys. Another interesting feature of positron annihilation is that although many body effects are important to explain the positron life times reasonably, they influence the angular distribution of  $\gamma$ -rays much less appreciably. It is the study of this correlation curve that yields information about the Fermi Surface.

There have been a few simple minded<sup>1,2,3</sup> and some rather detailed calculations for the angular distribution curves of annihilation gamma rays for metals and semiconductors. Here we describe a scheme based on pseudo wave functions and the positron wave function as a single plane wave. This approximation is reasonable for most of the angular distribution because the positron is largely excluded from the core, where the pseudo wave-function is not correct. This scheme can be easily extended to simple substitutional alloys using approximations similar to those in the pseudo-potential theory of alloys.<sup>(4)</sup> We plan to carry out such calculations for a series of metals and alloys where the constituents have small core.

#### General Theory for Metals

The probability that an annihilation with valence electron will yield two photons of total momentum 'P' is given by<sup>(5)</sup>

$$F^v(P) = \sum_{\underline{R}} \left| \int \psi_+(\underline{r}) \psi_{\underline{R}}(\underline{r}) e^{-i\underline{P}\cdot\underline{r}} d\underline{r} \right|^2 \quad (1)$$

and the counting rate measured by the standard parallel-slit apparatus is proportional to

$$F^v(\theta) = \iint_{-\infty-\infty}^{+\infty+\infty} dk_x dk_y F^v(\underline{k}) \quad (2)$$

where  $\theta = \frac{\hbar p_z}{mc}$ , and  $\psi_{\underline{k}}(\underline{r})$  represents the conduction electron wave function and  $\psi_+(\underline{r})$  is the positron wave function.

We use the form

$$\psi_+(\underline{r}) = \sum_{\underline{g}} b_{\underline{g}} \exp(i \underline{g} \cdot \underline{r}) \quad (3)$$

for the positron wave function and

$$\phi_{\underline{k}}(\underline{r}) = \sum_{\underline{q}} a(\underline{q}, \underline{k}) \exp[i(\underline{k} + \underline{q}) \cdot \underline{r}] \quad (4)$$

for the pseudo wave function of the conduction electron.

The actual conduction electron wave function is related to this pseudo wave function and the wave functions for the core electrons, by the relation

$$\psi_{\underline{k}}(\underline{r}) = \phi_{\underline{k}}(\underline{r}) - \sum_{\underline{R}_i, \alpha} \psi_{\alpha}(\underline{r} - \underline{R}_i) \int \psi_{\alpha}^*(\underline{r}' - \underline{R}_i) \phi_{\underline{k}}(\underline{r}') d\underline{r}' \quad (5)$$

where  $\alpha$  denote the core states and  $\underline{R}_i$  the lattice sites.

In the present calculation we approximate  $\psi_{\underline{k}}(\underline{r})$  by  $\phi_{\underline{k}}(\underline{r})$  and later see if the core orthogonality term is needed for better agreement of our calculations with the experiments. The coefficients  $a(\underline{q}, \underline{k})$  in (4) for  $\underline{q} \neq 0$  are given from the perturbation theory by

$$a(\underline{q}, \underline{k}) = \frac{\langle \underline{k} + \underline{q} | W(\underline{r}) | \underline{k} \rangle}{(\underline{k}^2 - |\underline{k} + \underline{q}|^2)} \quad (6)$$

where  $W(\underline{r})$  is the pseudopotential. The matrix elements for the pseudopotential may be factorized into a structure factor and a form factor to give

$$a(\underline{q}, \underline{k}) = \frac{S(\underline{q}) W(\underline{q})}{(\underline{k}^2 - |\underline{k} + \underline{q}|^2)} \quad (7)$$

with

$$S(\underline{q}) = \frac{1}{N} \sum_{\underline{R}_i} e^{-i \underline{q} \cdot \underline{R}_i} = \delta_{\underline{q}, \underline{K}_m} \quad (8a)$$

where  $\underline{K}_m$  is a reciprocal lattice vector and

$$W(\underline{q}) = \langle \underline{k} + \underline{q} | W(\underline{r}) | \underline{k} \rangle = \frac{1}{\Omega_0} \int_{\Omega_0} e^{-i(\underline{k} + \underline{q}) \cdot \underline{r}} W(\underline{r}) e^{i \underline{k} \cdot \underline{r}} d\underline{r} \quad (8b)$$

where the integration is over the volume  $\Omega_0$  of a single ion.

Therefore

$$\psi_{\underline{k}}(\underline{r}) \sim \phi_{\underline{k}}(\underline{r}) = C_n \left[ \exp(i \underline{k} \cdot \underline{r}) + \sum_{\underline{K}_m \neq 0} \frac{W(\underline{K}_m) \exp\{i(\underline{k} + \underline{K}_m) \cdot \underline{r}\}}{(\underline{k}^2 - |\underline{k} + \underline{K}_m|^2)} \right] \quad (9)$$

$C_n$  is a normalization constant which we set equal to unity for the present. Substituting (3) and (9) for  $\psi_{\underline{k}}(\underline{r})$  and  $\psi_{\underline{k}'}(\underline{r})$  respectively into equ (1) and simplifying gives

$$F^v(\underline{k}) = \sum_{\underline{G}} b_{\underline{G}}^2 \sum_{\underline{G}} \sum_{\underline{K}_m \neq 0} \frac{b_{\underline{G}} b_{\underline{G} - \underline{K}_m} W(\underline{K}_m)}{\{(\underline{p} - \underline{G})^2 - |\underline{p} - \underline{G} + \underline{K}_m|^2\}} \\ + \sum_{\underline{G}} \sum_{\underline{K}_m \neq 0} \sum_{\underline{K}_m' \neq 0} \left\{ \frac{b_{\underline{G}} W(\underline{K}_m)}{[(\underline{p} - \underline{G} - \underline{K}_m)^2 - |\underline{p} - \underline{G}|^2]} \right\} \left\{ \frac{b_{\underline{G} + \underline{K}_m - \underline{K}_m'} W(\underline{K}_m')}{[(\underline{p} - \underline{G} - \underline{K}_m)^2 - |\underline{p} - \underline{G} - \underline{K}_m + \underline{K}_m'|^2]} \right\} \quad (11)$$



One Plane wave Approximation for  $\psi_+$  ( $\underline{r}$ )

We now make a simplifying assumption that  $b_{\underline{g} \neq 0} = 0$  for all  $\underline{g}$  and  $b_0 = 1$ , which implies that we are treating the positron wave function to be a constant. That this may not be a very unrealistic assumption, is seen from the work of Stroud and Ehrenreich<sup>(2)</sup> where they found that  $\sum_{\underline{g} \neq 0} |b_{\underline{g}}|^2 < 0.1$ . With this assumption we have

$$F^v(\underline{k}) = 1 + \sum_{k_m \neq 0} \frac{W^2(k_m)}{\{k_m^2 - 2(k_m^x p_x + k_m^y p_y + k_m^z p_z)\}^2} \quad (12)$$

and

$$F^v(\underline{\theta}) = \int_{-\infty}^{\infty} \int_{-\infty}^{\infty} d p_x d p_y F^v(\underline{k}) \quad (13)$$

The core electron contribution is included in

the usual manner by taking the normalized atomic functions centered on the lattice sites  $\underline{R}_n$  in the tight-binding approximation.

In the present approximation *ie*  $b_0 = 1$

$$F^c(k) = (4\pi)^2 \sum_{n,l} a_{nl} \left| \int_0^\infty dr r^2 j_0(kr) R_{nl}(r) \right|^2 \quad (14)$$

It should be noted here that the core contribution is overemphasized by taking the positron wave function to be constant throughout the crystal, whereas an exact evaluation of positron wave function should exclude it from the core region.

The total contribution to the counting rate is proportional to

$$F(\theta) = \int_{-\infty}^{\infty} \int_{-\infty}^{\infty} dk_x dk_y \{ F^v(k) + F^c(k) \} \quad (15)$$

#### Application to alloys.

In this section we briefly consider the application of this method to simple substitutional alloys, where there are no structural changes. However the method is not restricted because of the above limitation. Equation (6) is now modified due to different ions at the different lattice sites. The matrix element of (6) will become<sup>4</sup>

$$\langle \underline{R} + \underline{q} | W | \underline{R} \rangle = (1-c) \langle \underline{R} + \underline{q}_0 | W^{(1)} | \underline{R} \rangle + c \langle \underline{R} + \underline{q}'_0 | W^{(2)} | \underline{R} \rangle \delta_{\underline{q}\underline{q}'_0} \quad (6a)$$

when  $\underline{q}_0$  is a reciprocal lattice vector, where  $c$  is the concentration of ions of type 2,  $\underline{q}_0$  is reciprocal lattice vector and  $W^{(1)}$  and  $W^{(2)}$  are the ionic potentials of type 1 and type 2 ions. When  $\underline{q}$  is not a reciprocal lattice vector we have

$$|\langle \underline{k} + \underline{q} | W | \underline{k} \rangle|^2 = \frac{1}{N} c(1-c) |\langle \underline{k} + \underline{q} | W^{(2)} - W^{(1)} | \underline{k} \rangle|^2 \quad (6b)$$

Since we only need the modulus square we are not concerned about the phase of the matrix element. The angular correlation curve for a substitutional alloy is obtained by using (6a) and (6b) for the matrix element of (6).

Substituting (6a) and (6b) gives

$$F^v(\underline{k}) = 1 + \sum_{\underline{G} \neq 0} \frac{\{ (1-c) \langle \underline{k} | W^{(1)} | \underline{k} - \underline{G} \rangle + c \langle \underline{k} | W^{(2)} | \underline{k} - \underline{G} \rangle \}^2}{(k^2 - |\underline{k} - \underline{G}|^2)^2} + \frac{c(1-c)}{N} \sum_{\substack{\underline{q} \neq \underline{G} \neq 0 \\ \text{and } \underline{q} \neq 0}} \frac{|\langle \underline{k} | W^{(2)} - W^{(1)} | \underline{k} - \underline{q} \rangle|^2}{(k^2 - |\underline{k} - \underline{q}|^2)^2} \quad (16)$$

where  $\underline{G}$  is any reciprocal lattice vector.

The form factors  $W(\underline{q})$  are given by Harrison and several other authors<sup>(4,6)</sup>. As a check we propose to study the Li Mg system whose angular correlation curves

have been determined by Stewart<sup>(7)</sup>. It has been found that the Alkali-Noble metal systems show metallic to semiconductor transition as the alkali constituents become heavier. We feel there is a good scope to the study of these systems to confirm other calculations.

\* Partially supported by NASA (U.S.) and National Research Council (Canada)

† On leave of absence from Tata Institute of Fundamental Research, Bombay, India

References

1. Proceedings of the Conference on Positron Annihilation, edited by A.T. Stewart and L.O. Roellig (Academic Press, Inc., New York, 1966).
2. D. Stroud and H. Ehrenreich, Phys. Rev. 171, 399 (1968).
3. J.B. Shand Jr., Phys. Letters 30A, 478 (1969).
4. W.A. Harrison, Pseudopotentials in the Theory of Metals (W.A. Benjamin, Inc., New York, 1966).
5. S. De Benedetti, C.E. Cowan, W.R. Konnekev, and H. Primakoff, Phys. Rev. 77, 205 (1950).
6. Solid State Physics, Vol 24, Edited by H. Ehrenreich, F. Seitz and D. Turnbull (Academic Press, Inc., New York, 1970).
7. A.T. Stewart, Phys. Rev. 133, A 1651 (1964).
8. T.L. Liu and H. Amar, Rev. Mod. Phys. 40, 782 (1968).

POSITRON ANNIHILATION AT F-CENTRES

Subrahmanyam Pendyala<sup>†</sup>, M.M. Pant<sup>††</sup> and B.Y. Tong

Physics Department

The University of Western Ontario

London, Ontario, Canada

ABSTRACT

A simple calculation is made of the effect of positrons annihilating at color centres on the angular correlation curve. There is reasonable agreement with reported experimental data for additively colored KCl.

<sup>†</sup> On leave of absence from Tata Institute of Fundamental Research, Bombay, India

<sup>††</sup> Address from 1st Jan. 1972. Physics Department  
Indian Institute of  
Technology, Kanpur, India

There has been considerable recent interest in the problem of positron-annihilation in alkali halides, with color centres [1]. Dupasquier [2] has measured the lifetime spectra of positrons annihilating in additively colored KCl single crystals, and Herlach and Heinrich [3] have measured the angular distribution of photons due to the positrons annihilating in pure and additively colored KCl crystals. Herlach and Heinrich report a large effect of coloring on the angular distribution, and these changes are most pronounced at small angles. Because of the small momenta of F-centre electrons, the experiments clearly suggest that a large number of the positrons are trapped and annihilated at the F-centres. We were therefore prompted to do a simple calculation of the contribution to the correlation curve due to the positrons annihilating with the F-centre electrons.

We use the standard expression [4] for the probability that a positron will annihilate with an F-centre electron to give photons of total momentum  $\underline{p}$ ,

$$f(\underline{p}) = \left| \int \psi_+(r) \psi_e(r) e^{-i\underline{p}\underline{r}} d\underline{r} \right|^2, \quad (1)$$

and the counting rate in the usual parallel slit geometry is therefore

$$N(\theta) = \iint dp_x dp_y f(\underline{p}),$$

where  $\theta = hp_z/mc$  and  $\psi_+(r)$  and  $\psi_e(r)$  are the positron and F-centre wave functions respectively. Since the coulomb potential of the vacancy is screened by the F-centre electron, the positron wave function  $\psi_+(r)$  was taken to be a constant for simplicity. For the F-centre electron we chose a hydrogenic wave function of the form

$$\psi_e(r) = \sqrt{\frac{Z_0^3}{\pi}} e^{-Z_0 r} \quad (3)$$

The angular distribution curve is then given by

$$N(\theta) = \frac{C \cdot 64\pi^2 Z_0^5}{3} \left[ \frac{1}{(P_z^2 + Z_0^2)^3} - \frac{1}{8Z_0^6} \right], \quad (4)$$

for  $P_z < Z_0$  and zero for  $P_z > Z_0$ . The one parameter  $Z_0$  that we have in the calculation can be obtained most simply by relating it to the absorption energy [5] by  $Z_0 = \sqrt{8 E_{abs}} / 3$  and using the experimental results of Gebhardt and Kuhnert [6]. The curve thus obtained with C normalized to the peak value of the experimental difference curve (c) is shown as (e) in Fig. 1. It is seen that the shape of the curve is quite similar to the difference curve of Ref. [3]. However, the cutoff value is considerably smaller than the experimentally observed one. Since the cut-off in the curve is also given by  $Z_0$  alone, we did another calculation by choosing  $Z_0$  to produce the experimentally observed cut-off at 5.5 mrad. As shown in curve (d) of Fig. 1 in this case the calcu-



lated curve falls almost exactly on the experimental curve. It therefore seems that this simple minded calculation gives a good qualitative description of the angular correlation of  $\gamma$ -rays produced by positrons annihilating at F-centres.

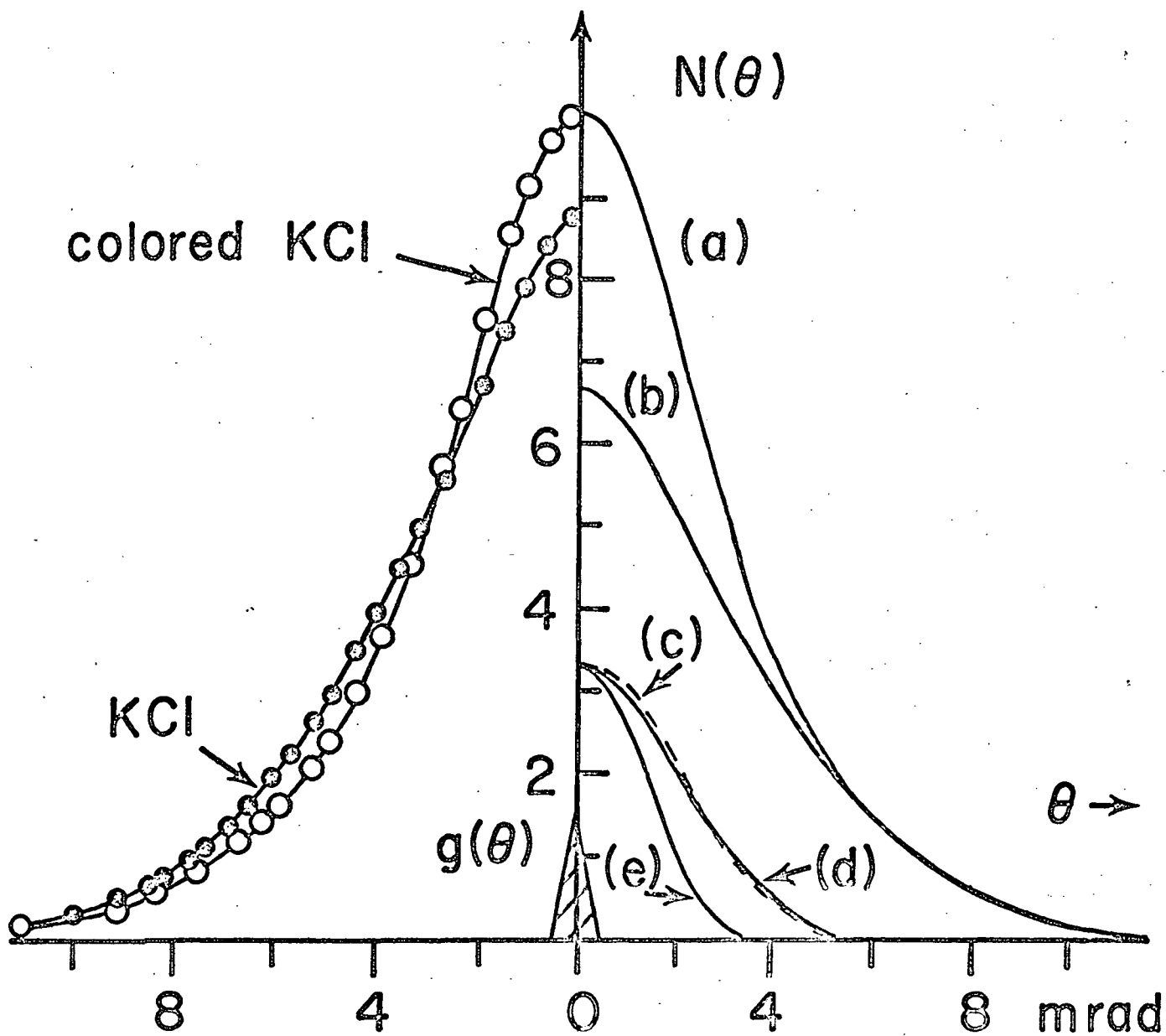
The authors wish to thank Professor P.W.M. Jacobs for a useful discussion.

REFERENCES

1. W.C. Mallard and F.H. Hsu, Positron Annihilation,  
2nd International Conference (1971) Kingston, Canada.
2. A. Dupasquier, Lett. Nuovo Cimento 4 (1970) 13.
3. D. Herlach and F. Heinrich, Phys. Letters 31A (1970) 13.
4. S. De Benedetti, C.E. Cowan, W.R. Konneker and H.  
Primakoff. Phys. Rev. 77 (1950) 205.
5. A.A. Berezin, Int. J. Quantum Chemistry 3 (1969) 485
6. W. Gebhardt and M. Kuhnert, Phys. Letters 11 (1964) 15.

FIGURE CAPTION

Angular correlation  $N(\theta)$  for KCl. (a) Colored crystal (b) pure crystal (c) difference curve. For (d) and (e), see text.



# $(e^+, \text{He})$ Total Scattering<sup>1</sup>

D. G. COSTELLO

*Gulf Energy and Environment Incorporated, P.O. Box 608, San Diego, California 92112*

D. E. GROCE

*JRB Associates Incorporated, La Jolla, California 92037*

D. F. HERRING

*Enviro-Med Incorporated, La Jolla, California 92037*

AND

J. WM. MCGOWAN

*Physics Department, University of Western Ontario, London, Ontario<sup>2</sup>*

Received June 21, 1971

The total scattering cross section for  $e^+$  in He has been measured through two energy intervals, 1 to 4 eV and 17 to 26 eV. Through the lower elastic-scattering interval our results are consistent with the calculations of Drachman. From below the positronium formation threshold, at 17.8 eV to above the He ionization threshold, our results agree qualitatively with the calculations of Kraidy, who includes in his model virtual positronium and positronium polarization. Just below 17.8 eV the cross section is  $0.35 \pm 0.04\pi a_0^2$ . In these experiments a high-current linac has been used as a source of positrons and total beam attenuation has been used to determine the cross section.

La section efficace totale de diffusion de  $e^+$  dans He a été mesurée pour deux intervalles d'énergie: 1 à 4 eV et 17 à 26 eV. Dans l'intervalle le plus bas, les résultats obtenus pour la diffusion élastique sont compatibles avec les calculs de Dreckman. A partir d'au-dessous du seuil de formation du positronium, à 17.8 eV, jusqu'au-dessus du seuil d'ionisation de He, nos résultats s'accordent qualitativement avec les calculs de Kraidy, qui inclut dans son modèle le positronium virtuel et la polarisation du positronium. Immédiatement au-dessous de 17.8 eV la section efficace est de  $0.35 \pm 0.04\pi a_0^2$ . Dans ces expériences un linac à fort courant a été utilisé comme source de positrons, et l'atténuation total du faisceau a été utilisée pour déterminer la section efficace.

Canadian Journal of Physics, 50, 23 (1972)

## 1. Introduction

Studies of electron scattering have progressed to the point where detailed elastic- and inelastic-scattering measurements and theory not only successfully examine simple systems like  $(e, \text{H})$  where the conditions for theoretical investigation are ideal and experimentation awkward, but also systems like  $(e, \text{He})$  and  $(e, \text{Li})$  where experimental conditions are less difficult but theory is less precise. Throughout all of the studies there has been no way to separate from other forces, such as Coulomb and polarization, the effects of the electron exchange force between

the bombarding electrons and the electrons in the target atom since the incoming electron and those in the target are indistinguishable. There are several ways to test the effect of electron exchange: (1) to label the electron by polarizing it and observing the change in polarization after the scattering, and (2) to replace the electron with a positron which is readily distinguishable from the electron. It is this latter approach to the study of elastic electron scattering which we have chosen here.

In the elastic-scattering region and below the onset of any inelastic process, one primarily tests exchange when the negative electron is replaced with a positron. However, even this is somewhat complicated theoretically by the fact that the mean static interaction of an atom with a positron is repulsive while long-range polarization is attractive so that the two effects oppose

<sup>1</sup>Work carried out at Gulf Energy and Environment, Inc., San Diego, California, and supported, in part, by N.A.S.A., Goddard Space Flight Center under contract NAS5-11116.

<sup>2</sup>All enquiries or correspondence to be addressed to the above.

rather than combine as in the case of electron scattering. Furthermore, near the first inelastic threshold, virtual positronium formation must be considered as a real effect although the recent theoretical studies (Fels and Mittleman 1967; Drachman 1968a), suggest that in the case of the  $(e^+, H)$  system at least resonances (compound states) are not important even though other work suggested they might be (Bransden and Jundi 1967). However, in an earlier study, Cody *et al.* (1964) proposed that virtual positronium formation is much less important than is polarization.

Theoretically, the most tractable system is  $(e^+, H)$ ; experimentally something like  $(e^+, Ar)$  has proven more manageable. For the moment  $(e^+, He)$  has become the compromise system for which considerable theory and complementary experiment is now available.

Drachman (1966, 1968b) has applied a modified adiabatic method to  $(e, H)$  scattering without the inclusion of virtual positronium formation and has assumed, by comparison with the  $(e, H)$  system (Schwartz 1961), that if the effective short-range polarization is suppressed nearly exact agreement with the variational  $s$ -wave phase shifts should be obtained. Like Drachman, Massey *et al.* (1966) also used a variation of the polarized-orbital (Temkin and Lamkin 1961) approximation developed for electrons while Callaway *et al.* (1968) made an attempt to adjust the polarization for the kinetic energy of the incoming positron. Kraidy (1967) and Kraidy and Fraser (1967) in the same way essentially have examined the effect of virtual positronium formation as well as polarization.

Using a variational technique similar to that used by Chen and Mittleman (1966) where only the elastic scattering and positronium formation channel are considered. Fels and Mittleman (1969) also derived cross sections above the positronium threshold as a function of the induced polarization.

No experimental values of  $(e^+, H)$  scattering cross section are yet available and until this report no single collision studies of the  $(e^+, He)$  system were reported. However, positronium annihilation studies have been carried on in a drift tube filled to several atmospheres pressure along the axis of which an electric field is applied. From an analysis of the swarm data one can try to extract the momentum-transfer cross section

just below the first inelastic threshold. But remember, when the high-energy tail of the swarm begins to affect the region just below the positronium formation threshold 17.8 eV, the breadth of the swarm is large and the average positron has an energy below 10 eV. Consequently, the estimates of cross section must be inaccurate compared with others at low energies where the swarm is narrow.

The first experimental result to be reported by Marder *et al.* (1956) lies between 5 and 10 times below all theoretical predictions (refer to Table 1). More recent experiments have shown these measurements to be in error by more than a factor of 5 (Lee, Orth, and Jones 1969; Leung and Paul 1969). However, the complexity of the analysis and the need for some detailed information on the nature of the interaction place strong limitations on this experimental method for obtaining elastic (or momentum-transfer) cross sections. Rather, it is suited to determining the consistency of calculated cross sections with the results of annihilation experiments at low energies. It cannot readily be used to give unique results. Even the more sophisticated swarm experiments by Lee, Orth, and Jones (1969) and Leung and Paul (1969) cannot actually obtain the cross section at the positronium threshold, yet they both indicate that results by Marder *et al.* (1956) are much too low.

Under normal conditions, beam experiments should measure the total scattering cross section without reliance upon the theoretical model. However, through the low-energy range of the experiments reported here, the use of a time-of-flight spectrometer with an axial magnetic field makes it necessary to depend upon the theoretical model for complete analysis. But this is the exceptional case rather than the rule.

## 2. Experiment

In this paper and in conference proceedings (Groce, Costello, McGowan, and Herring 1969) we report the results of a time-of-flight scattering experiment (see Fig. 1) where the positrons were produced in a 0.04 in. tantalum target by the bremsstrahlung radiation resulting from the interaction of a 20 ns 55 MeV 1 A peak beam of electrons in a 0.055 in. tantalum converter. The energy of the resulting positrons was then moderated by one of a number of metals and

TABLE I. (e<sup>+</sup>, He) total scattering cross sections in  $\pi a_0^2$

Energy (eV)	Experimental					Theoretical total				
	Momentum transfer		Total This work	C=1 $\alpha=0$ (d)	(e)	(f)	(g)	(h)	(i)	
	(a)	(b)								(c)
Thermal and above		Agrees (d)								
2	—	—	0.03	Large	—	0.07	0.14	—	—	
4	—	—	0.09	0.17	—	0.11	0.24	0.28	—	
10	—	—	0.22	0.12	—	0.15	0.35	0.30	—	
14	—	—	0.24	0.14	—	0.21	0.36	0.36	—	
16.5	0.023 ± 0.006	>(a)	0.25	0.16	—	—	0.36	0.37	—	
			( $\sigma_{\text{res}}$ ) (0.21)	0.17	0.42	—	0.37	0.36	0.35 → 0.48	
					Upper limit s.p.d wave					
18.5	—	—	—	—	—	—	0.38	1.70	—	
19.3	—	—	—	0.40 ± 0.19	—	—	0.38	1.94	—	
21.3	—	—	—	0.60 ± 0.16	—	—	0.37	2.22	—	
26.1	—	—	—	1.0 ± 0.15	—	—	0.36	2.2	0.36 → 0.42	
				1.24 ± 0.27						

References to the above table are as follows.  
 (a) Marder, Hughes, Wu, and Bennett (1956).  
 (b) Lee, Orth, and Jones (1969).  
 (c) Leung and Paul (1969).  
 (d) Drachman (1966; 1968b).  
 (e) Drachman, Private communication.  
 (f) Massey, Lawson, and Thompson (1966).  
 (g) Callaway, LaBarr, Fu, and Duxler (1968).  
 (h) Keady (1967).  
 (i) Fels and Mittleman (1969).

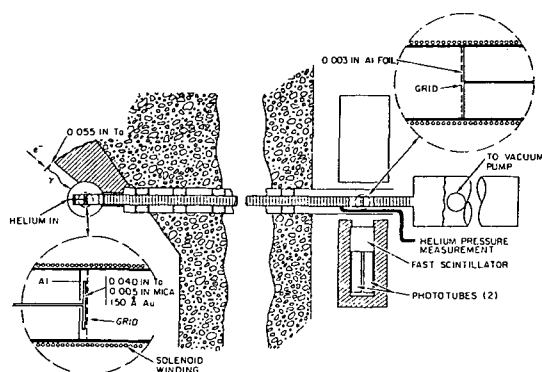


FIG. 1. Scattering chamber and time-of-flight energy analyzer shown with details of positron-source region and positron annihilator.

nonmetals. In Fig. 2, we show the case where a 150 Å mica slab 0.005 in. thick and gold-coated, is used (Costello, Groce, Herring, and McGowan 1972). The bulk of the positrons which came from the moderator have an energy near 1 eV which could be changed by biasing the moderator with respect to the 3 m time-of-flight collision chamber.

A solenoid was wound along the length of the collision region to assure that very-low-energy positrons are not disturbed by stray AC or DC magnetic fields as they traverse the length of the tube. Those positrons which traveled the length of the collision region were detected with a 1.3% efficiency when the two 0.51 MeV annihilation  $\gamma$  rays, which are 180° out of phase, were counted in four-way coincidence upon annihilation in a thin aluminum foil. To eliminate the effect of the after-pulsing resulting from the gamma flash from the source, the coincidence of two dissimilar phototubes looking at each fast liquid scintillator was required. In order to determine where to place the annihilation foil in order to optimize the coincidence counting,  $^{22}\text{Na}$  was moved up and down the flight path. The foil was placed where the coincidence count rate peaked.

The total scattering cross-section in helium gas was obtained by sequentially measuring the number of positrons traversing the collision region evacuated to  $2 \times 10^{-7}$  Torr, and then the number when the pressure in this region was increased, to  $\sim 10^{-3}$  Torr. Because the cross section for helium is smaller than for most impurities, it was necessary to use the boil-off from

liquid helium in a continuously pumped system in order to eliminate an observable effect of contamination. The helium gas came to thermal equilibrium with the room as it passed through at least 3 m of copper pipe before entering the 3 m long collision chamber. No rapid cooling of the gas occurred as it entered the collision chamber.

The attenuation of the 2 eV positron beam is shown in Fig. 2. On the low-energy side of the peak, notice that as the pressure is increased, the number of scattered positrons is apparently larger than the number of primary particles. This is due to the spiralling of the scattered positrons giving rise to a longer flight time and apparently increased number at lower energies. Consequently, at low energies only the high-energy side of the peak was analyzed. Only for positron energies in excess of  $\sim 10$  eV was downscatter negligible. The linearity of positron attenuation as a function of He pressure is demonstrated on a semilog plot in Fig. 3. From the slope of this curve one is able to obtain directly the total scattering cross section.

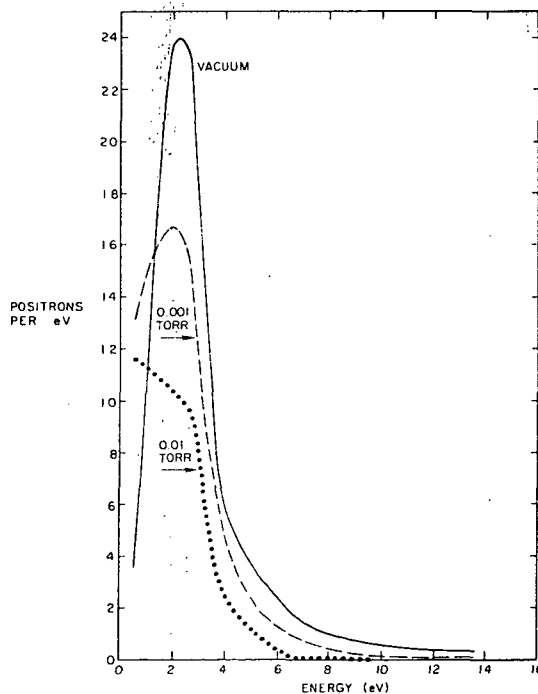


FIG. 2. Dependence of the energy spectrum of positrons which have traversed the collision chamber filled with helium to various pressures.



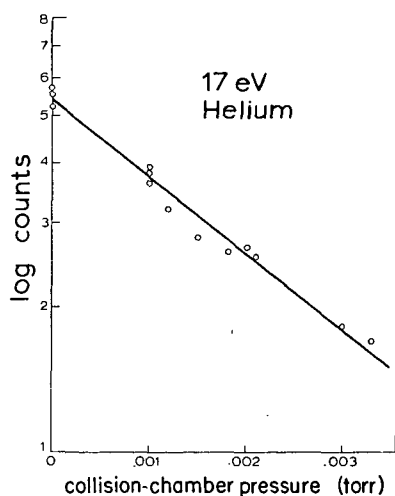


FIG. 3. Decrease in number of positrons reaching the annihilation foil as a function of the helium pressure in the scattering chamber.

Attempts to reproduce results from different runs, however, showed variations of the positron intensity that were considerably outside statistics. A test was devised to assess if these variations were in the electronic equipment used in the experiment. Weak  $^{137}\text{Cs}$  sources were placed near each detector. The counting rate of these sources was low enough so that accidental coincidences from the two detectors during the positron arrival time were negligible, resulting in little or no increase in rate. During an accelerator run the pulses from each detector could be routed into a scaler for a period of time when no positrons were present. In this way it was possible to continuously monitor the gain and discriminator level of the detectors during a run. Although small variations ( $\sim 2\%$ ) in the two detectors were noted, there appeared to be no correlation between the variation in positron intensity and changes in the detector system.

The other possible sources which could contribute to the observed variations are the positron source or the electron-current integrator. At this point it appeared that an extensive investigation would be necessary to determine and eliminate this source. Neither time nor funds permitted such an extensive investigation; it was therefore decided to live with the problem, if at all possible. The rate of variation of positron intensity is relatively slow; large changes take place in a time span of 30 min to an hour. If

gas-in and vacuum runs are made in time intervals short compared to the above time then the effect of the positron-intensity variation can be reduced. On two different dates data were obtained with short running times ( $\approx 15$  min). Furthermore, by making runs in the following order—vacuum, gas, vacuum—and then comparing the two vacuum runs, variations in positron intensity were detected and those runs with large variations were discarded. This, of course, is not a very efficient system of data collection.

On the final accelerator run a much improved system was used. An electrically operated valve was installed in the gas flow line. This modification permitted a much faster cycling of the gas which did not necessitate shutting down the accelerator during the cycling of gas, so that much more uniform beam conditions were possible. The runs were of about 2 min duration. Data collection was discontinued during the time required ( $\sim 30$  s) for the vacuum system to reach stability after a switch. Fortunately, equipment used in neutron-capture work was already available so that the data collection could be automated. Two banks of scalers, as well as two different multichannel analyzer memories, were used. One set was used to collect data from the vacuum runs and one from the gas-in runs. This proved to be a much superior system over the previous manual operation of the gas cycling. Over a long time the variations in positron intensity did average out between gas-in and vacuum data if many of the short 2 min runs were added together.

### 3. Results and Discussion

In this paper we have chosen two energy intervals for consideration. The first lies between 1.0 and 4 eV which overlaps the region where theory predicts a minimum in the total cross section and where the swarm experiments can be used most effectively to verify calculated cross sections. The second which is between 17 and 26 eV includes the onsets of positronium formation in the ground and excited states, He excitation, and ionization. These intervals are discussed separately below.

#### *Cross Section Between 1.0 and 4 eV*

With no accelerating potential on the converter foil the positrons are emitted from the

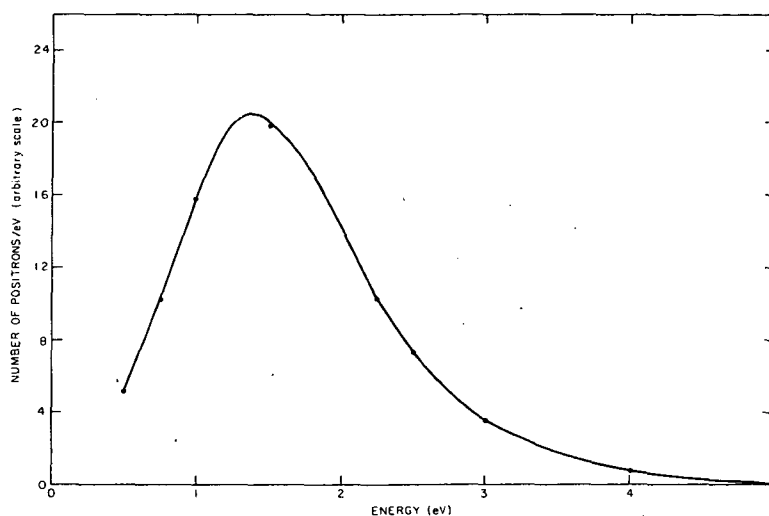


FIG. 4. Positron energy spectrum with no converter-target biasing, using gold-plated aluminum as moderator.

converter with the energy spectrum shown in Fig. 4. This distribution for an aluminum moderator (oxidized covered) with a 200 Å gold film is peaked at approximately 1.5 eV and has a full width at half maximum greater than 1 eV. After background subtraction (the background appears to be due to accidental coincidence from after pulsing of the detectors) there are few positrons above 4 eV in the low energy spectrum.

Because the positrons are in a solenoidal magnetic field the analysis of the experimental data is not simple. A positron may be elastically scattered and then trapped by the magnetic field, and still arrive at the annihilation foil at a later time. This effect, illustrated in Fig. 2, which we have termed "downscatter", can cause an apparent negative attenuation, *i.e.*, in the low energy region more positrons may be detected with gas in the flight path than under vacuum conditions. To obtain the correct attenuation this downscatter must be calculated and removed from the gas-in runs. This calculation, however, requires a knowledge of the angular distribution of the scattering which implies a knowledge of the total cross section, the quantity which we wish to obtain from the measured attenuation.

A much simpler approach is to calculate the yield curve from various assumed sets of phase shifts and for a given gas pressure compare the calculated yields with those obtained experi-

mentally at the same gas pressure. (This approach, like swarm studies, simply verifies the consistency of our data with various theoretical calculations.) These comparisons should indicate which set of phase shifts fit the experimental data best, then the total scattering cross section can be calculated from the phase shifts. No information is lost in this method, as a matter of fact we gain information about the angular distribution of the scattering. Information concerning the angular distribution, of course, is contained in the downscatter part of the yield.

A simple calculation assuming only one collision with a He atom before detection may not be of sufficient accuracy to yield the desired results. This can be seen from the following argument. A reasonable running time ( $\sim 1$  h) for a gas-in run typically yields from 10 to 15% counting statistics over the peak of the distribution. For reasonable tests of excellence of fits the attenuation needs to be at least 2 times this statistical uncertainty. The gas pressure should be adjusted so that the positrons are attenuated by 20 to 30%.

Now, if we consider a positron travelling down the flight path in the direction of the magnetic field, and then consider a collision with an atom, this collision changes its direction with respect to the magnetic field and the positron's path is now a helix. Because of this helical motion, the distance the positron travels in the gas before

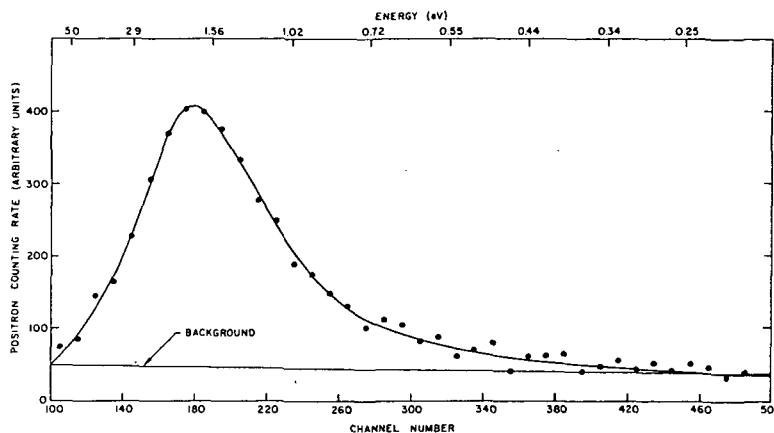


FIG. 5. Positron time spectrum with no converter-target biasing and under vacuum conditions, using gold-plated aluminum as moderator.

it reaches the annihilation foil may be many times the straight-ahead path length; it will thus be almost assured of having a second collision. It is apparent then that the calculation should include the possibility of multiple collisions.

A simple way in which this problem can be solved is by the use of a computer Monte Carlo program in which multiple collisions may be very easily taken into account.

A brief description of the computer program which was used in the analysis follows. Since the experimental data are in terms of positron flight times, it was decided to perform the calculation in terms of time rather than energy. In this way the output of the program can be compared directly with the experimental data.

The assumed phase shifts are fed into the computer memory as tables of phase shifts versus the energy of the positron. The present calculations include phase shifts for  $l = 0, 1, 2,$  and  $3$ . Higher values of  $l$  could be included but for the present energy range higher values are probably not needed for suitable accuracy. The shape of the positron yield under vacuum condition is also needed. This was obtained from the smooth curve drawn through the data points after background subtraction as shown in Fig. 5. This curve was fed into the program as a table of vacuum yield versus the channel number of the multichannel analyzer. Channel number was selected as a convenient unit of time so that the program output could be more easily compared with the experimental data.

The pressure was also entered in the input information to calculate the yield for the various pressures. The computer calculates the energy corresponding to the first channel numbers considered, then the phase shifts  $\delta_0, \delta_1, \delta_2,$  and  $\delta_3$  are determined at the channel energy by a simple interpolation from the input phase-shift tables. The angular distribution of the scattering as well as the total cross section for the time channel can be calculated from the set of phase shifts corresponding to that channel. The program then follows a positron with an energy corresponding to the time channel down the flight path. The computer is asked to supply a random number  $X_1$  between 0 and 1 from a uniform distribution. The path length  $S$  the positron will travel before a collision with a gas atom is given by

$$S = \ln \left( \frac{1}{1 - X_1} \right) / \sigma_T N$$

where  $\sigma_T$  is the total cross section and  $N$  is the number of atoms per  $\text{cm}^3$ .

The distance  $Z$  travelled down the flight path is given by

$$Z = \frac{S}{\cos \theta}$$

where  $\theta$  is the angle between positron velocity vector and the magnetic field. If  $Z$  is greater than the length of the flight path then a count which is weighted by the vacuum yield is recorded in the appropriate time bin. If  $Z$  is less than the flight path then a new angle  $\theta$  is selected by two random numbers in such a way as to give the proper

angular distribution which was calculated from the input phase shifts. A new  $S$  is found and the computer goes through the above process until the positron is either lost from the system by being scattered backwards to a point past the source or is counted. If it is counted, a weighted (weighted according to the vacuum yield curve) count is stored in a time bin which corresponds to the total flight time of the positron. After the positron is counted or lost from the system another positron is followed through the system. The present program followed 1000 positron histories for each input time channel. In this way a yield curve can be obtained for a given set of phase shifts and pressure.

The input phase-shift information to the program was taken from calculations by Drachman (1966). The results of these calculations are given in terms of two parameters,  $\alpha$  and  $C$ . The use of the more recently calculated phase shifts (Drachman 1968b) to correct for positron backscatter tends to decrease the cross section at low energies but not change  $\alpha$  and  $C$ . Any increase in these phase shifts will increase the cross section. The changes will be within the estimated errors. The parameter  $\alpha$  measures the amount of monopole correlation retained in the scattering wave function, and would be the only parameter in the theory if it were possible to use an exact wave function for the helium atom.

The parameter  $C$  is selected to give the measured polarizability once an approximate wave function is selected. Drachman has calculated four sets of phase shifts corresponding to the extreme values of  $\alpha$  and  $C$  ( $\alpha = 0$  or  $1$  and  $C = 1$  or  $1.24$ ). The difference in the phase shifts is not great between the two values of  $C$  for a given value of  $\alpha$ . Between the two values of  $\alpha$ , however, there is a much larger difference, especially in  $\delta_0$ . The correct value of  $\alpha$ , for this reason, should be more easily obtained than the correct value of  $C$ .

Figures 6, 7, and 8 show the comparison between the Monte-Carlo calculations and the experimental data. Only at the highest pressure shown in Fig. 8 is there sufficient difference in the two values of  $\alpha$  to make a good judgment by the fit. In the cases studied here it is evident that the value  $\alpha = 0$  gives the best fit to the data. The difference in the two values of  $C$  was not sufficient to make an accurate judgment with the present experimental data, although the value  $C = 1$  seems to give the best fit.

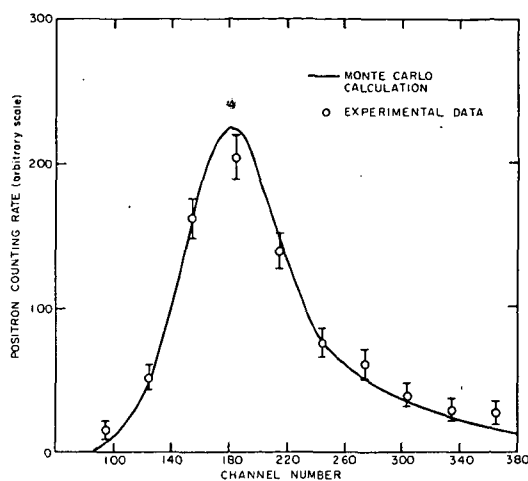


FIG. 6. Positron time spectrum for  $1 \times 10^{-3}$  Torr He gas pressure. Solid curve is the Monte Carlo calculated curve for  $\alpha = 0$  and  $C = 1$ .

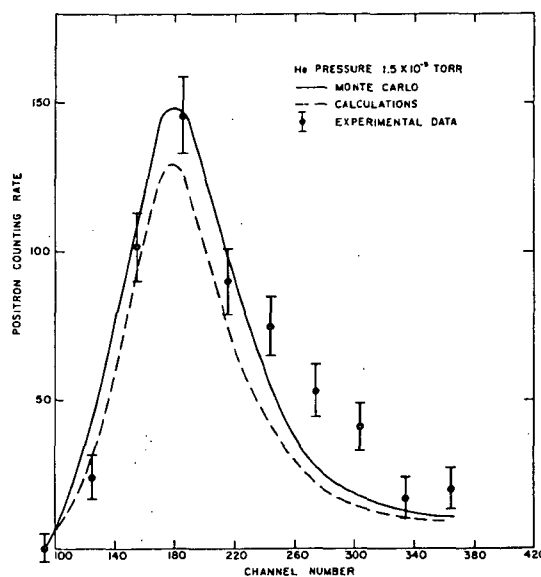


FIG. 7. Positron time spectrum for  $1.5 \times 10^{-3}$  Torr He gas pressure. Solid curve is the Monte Carlo calculated curve for  $\alpha = 0$  and  $C = 1$ . Dashed curve is calculated curve for  $\alpha = 1$  and  $C = 1.24$ .

The fit to the data for the two higher pressures in the energy region below about 1 eV (time channel 220) is not as good as above 1 eV. The measured number of positrons below 1 eV are considerably above the calculated curves. The reasons for this are not known. Two assumptions were made in the calculations to try to explain

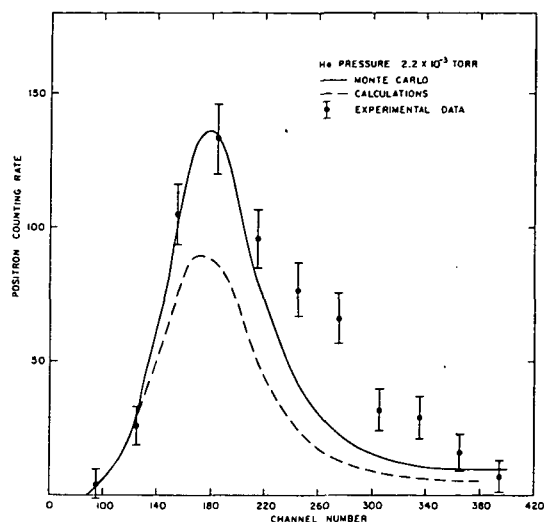


FIG. 8. Positron time spectrum for  $2.2 \times 10^{-3}$  Torr He gas pressure. Solid curve is the Monte Carlo calculated curve for  $\alpha = 0$  and  $C = 1.24$ .

this result. First it was assumed that those particles which collide with the walls of the flight path are not lost but bounce off the wall or continue down the flight path. This assumption was put into the calculations. There was a slight increase in the yield but it was not enough to explain the measured results. The second assumption, which also failed, was to assume that there was an initial angular spread of the positrons leaving the converter. No change in the yield curve was noted with the second assumption. The lack of agreement between the calculated and experimental results in Figs. 7 and 8 associated with longer flight times might also reflect a need for an increase in the calculated scattering cross section at lower positron energies. Allowing for the downscatter as a result of the collisions of these positrons would lead to an increase in the theoretical curve in better agreement with our experimental results.

The conclusion of the analysis from the fits to the experimental data is that the value of  $\alpha$ , the monopole correlation, is  $\alpha \approx 0$ . The parameter  $C$  in Drachman's calculations for  $\alpha = 0$  is  $C = 1$ . The calculated curve for this set of parameters is shown in Fig. 9, marked D (for Drachman (1966)). Some values are given in Table 1. The cross-hatched portion of the curve indicates the region of fit with experiment, with an estimated error of  $\pm 30\%$ . These results are consistent with

the swarm data by Lee *et al.* (1969) and Leung and Paul (1969).<sup>2</sup>

Two sources of systematic error must be considered which are associated with the large gamma flash accompanying the linear-accelerator pulse. They come from the production of ions and electrons in the bulk of the helium gas and the production of secondary electrons from the wall of the time-of-flight tube. Because of the large cross sections associated with charge-charge scattering, 1% ions could give rise to a cross section a factor of 2 too high. However, estimates based upon 1 J energy dumped into the gas per pulse lead to ion-

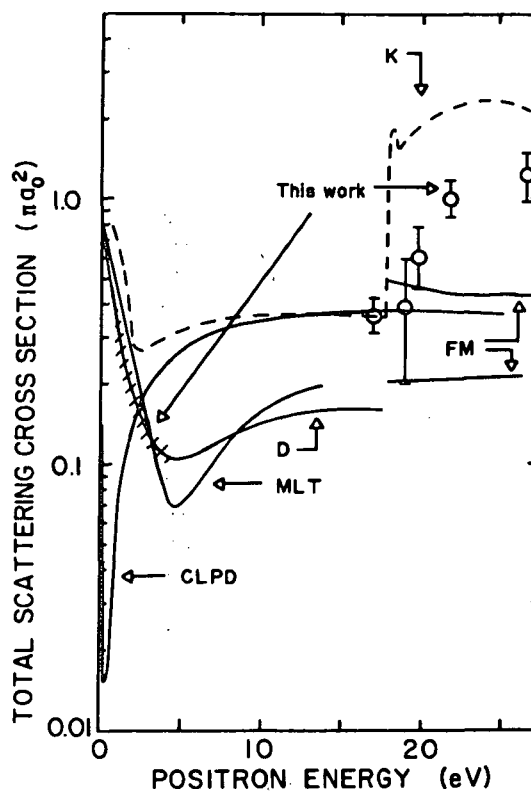


FIG. 9. Experimental results shown in comparison with the various calculated total scattering cross sections for positrons on helium. The results marked "CLPD" refer to Calloway, LaBahn, Pu, and Duxler; "MLT" to Massey, Lawson, and Thompson. Those marked "D" refer to Drachman (for  $\alpha = 0$  and  $C = 1.24$ ). "FM" refers to Fels and Mittleman and "K" to Kraidy. The uncertainty bars identify the experimental results at high energies while at lower energies the hatched line superimposed on the Drachman results identifies the region over which our experiments agree reasonably well with theory.

electron pair densities  $\ll 0.01\%$  of the helium-atom density. The more serious problem appears to be associated with the secondary electrons. If one assumes a 1% yield of electrons along the walls of the chamber, immediately after the pulse, the density of electrons in the gas will be less than  $10^8$  electrons/cm<sup>3</sup> which even without diffusion is  $\ll 0.01\%$  of the helium-atom density. One estimates that the total systematic error associated with this effect is  $< -2\%$  of the total cross section.

#### Cross Section Between 17 and 26 eV

When a positive potential is applied to the converter foil, those positrons which are formed in the converter-moderator sandwich are accelerated to higher energies. These positrons then may be used to investigate the cross section at higher energies than the region offered by the low-energy distribution. For He one energy region is of particular interest, namely above 17.8 eV, where positronium formation is possible. A series of short runs were made with a +15 V bias on the converter-moderator foil. This bias produced a beam of positrons with energies near 16 eV (15 V accelerating potential plus initial energy of the positrons from the moderator surface). Six or more different gas pressures were used in these runs with vacuum runs interspersed with the gas in runs so that changes in the positron intensity could be detected. The logarithm of the ratio of a gas-in yield to vacuum yield was plotted versus the pressure of the He gas (example Fig. 3).

The cross section was found from the slope of a straight line fitted to the points using the method of least squares. Leaving out three points which were in doubt because of variation in intensity during the run, the cross section was found to be  $0.346 \pm 0.035$  in units of  $\pi a_0^2$  at a positron energy of 16.5 eV, which is just below the positronium formation threshold.

A series of runs were also made at positron energies above the positronium formation threshold, 18.5, 19.3, 21.3, and 26.1 eV. Unfortunately, during these runs there were large changes in positron intensity leading to the assignment of large errors to the data points. These changes could be detected by the changes in the intensity of low-energy positrons which were not accelerated, since they originate at points other than the converter (accelerating

grid, flight path walls, etc.). The shape of this low-energy distribution was calculated for different gas pressures in a manner similar to that in the previous section. By normalizing the low-energy peaks one could minimize the fluctuations in the high-energy peak. Once this was done a cross section was obtained again using the method of least squares. Table 1 and Fig. 9 give the results of the analysis.

The increase in the cross section above 18 eV is unequivocally associated with the onset of



but the triplet systems cannot be excited through exchange and the possibility of excitation through magnetic or electric-multipole interaction is small. The first state which may be excited with reasonably large probability is the  $2^1S$  state with an onset at 20.6 eV. The sharp onset in our data is below this point.

It was hoped that our experiments would allow us to unequivocally pick the best theoretical model for positron scattering just below the positronium formation threshold. However, as can be seen in Fig. 9 and Table 1, the inclusion of virtual positronium with the polarization of helium as calculated by Kraidy (1967) is nearly equivalent to the results obtained by Callaway *et al.* (1968) with their extended polarization-potential approach where virtual positronium is not explicitly included. Judging from a comparison with Armstead's (1968) work for hydrogen, Drachman's phase shifts for  $\delta_0$  are likely to be too small near the Ps threshold; this may be due to omission of virtual Ps in these states.

However, just above 17.8 eV only the calculations of Kraidy, who includes the polarization of the positronium, show the proper trend, though they are a factor of 2 higher than the experimental values. The addition of He polarization tends to drop his values in this region. The shape resonance in the  $^1P$  channel predicted by Kraidy was not found. More data are necessary to tell conclusively whether or not it exists. At threshold the experimental values agree with the best of Fels and Mittleman (1969); however, their slope is unquestionably wrong.

#### 4. Concluding Remarks

We have been able to demonstrate clearly that the positron scattering cross section is

decreasing in the interval 1–4 eV in agreement with the Drachman model, where the amount of monopole correlation retained in the scattering wave function is characterized by  $\alpha = 0$  and the approximate ground-state target wave function is best represented by  $C = 1$ . This is consistent with the conclusions drawn from swarm measurements.

Just below 17.8 eV, the positronium formation threshold, our experimental value is 3 times higher than the lower bound set by swarm studies. It also exceeds the Drachman value by a factor of 2. The inclusion of virtual positronium by Kraidy (1967) tends to give results in agreement with experiment. Effectively, the same thing is found in the Callaway *et al.* case, where the approximation is quite different and the individual phase shifts disagree. Above the Ps formation threshold the Kraidy calculations which include the polarization of Ps show the trend we find, but tend to lie a factor of 2 above our results. This disagreement would seem to disappear when some He polarization is included. His predicted  $p$ -wave shape resonance was not found. Our data are sparse in this important region.

ARMSTEAD, R. L. 1968. *Phys. Rev.* **171**, 91.

BRANDSEN, B. H. and JUNDI, Z. 1967. *Proc. Phys. Soc. (London)*, **92**, 880.

CALLAWAY, J., LABAHN, R. W., PU, R. T., and DUXLER, W. M. 1968. *Phys. Rev.* **168**, 12.

CHEN, J. C. Y. and MITTLEMAN, M. H. 1966. *Ann. Phys. (N.Y.)*, **37**, 264.

CODY, W. J., LAWSON, J., MASSEY, H. S. W., and SMITH, K. 1964. *Proc. Phys. Soc. (London)*, **A**, **278**, 479.

COSTELLO, D. G., GROCE, D. E., HERRING, D. F., and MCGOWAN, J. WM. 1972. *Phys. Rev.* In press.

DRACHMAN, R. J. 1966. *Phys. Rev.* **144**, 25.

——— 1968*a*. *Phys. Rev.* **171**, 110.

——— 1968*b*. *Phys. Rev.* **173**, 190.

——— 1969. *Phys. Rev.* **179**, 237.

FELS, M. F. and MITTLEMAN, M. H. 1967. *Phys. Rev.* **163**, 129.

——— 1969. *Phys. Rev.* **182**, 77.

GROCE, E. E., COSTELLO, D. G., MCGOWAN, J. WM., and HERRING, D. F. 1968. *Bull. Am. Phys. Soc.* **13**, 1397.

——— 1969. *Proc. Vth Int. Conf. Phys. Electron. At. Collisions (MIT Press, Cambridge)*, p. 757.

HERRING, D. F., MCGOWAN, J. WM., GROCE, D. E., and ORPHAN, V. 1967. *Proc. Vth Int. Conf. Phys. Electron. At. Collisions (Publ. House Nauka, Leningrad, USSR)*.

KRAIDY, M. 1967. Ph.D. Thesis, Univ. of Western Ontario, London, Ontario.

KRAIDY, M. and FRASER, P. A. 1967. *Abstracts of Papers Vth Int. Conf. Phys. Electron. At. Collisions (Publ. House Nauka, Leningrad, USSR)*.

LEE, G. F., ORTH, P. H. R., and JONES, G. 1969. *Phys. Lett. A*, **28**, 674.

LEUNG, C. Y. and PAUL, D. A. L. 1969. *J. Phys. B*, **2**, 1278.

MARDER, S., HUGHES, V. W., WU, C. S., and BENNETT, W. 1956. *Phys. Rev.* **103**, 1258.

MASSEY, H. S. W., LAWSON, J., and THOMPSON, D. G. 1966. (Academic Press, New York), p. 203.

SCHWARTZ, C. 1961. *Phys. Rev.* **124**, 1468.

TEMKIN, A. and LAMKIN, J. C. 1961. *Phys. Rev.* **121**, 788.

## Negative Work Function of Thermal Positrons in Metals

B. Y. Tong

*Department of Physics, University of Western Ontario, London, Ontario*

(Received 3 May 1971)

Theoretical study shows that thermalized positrons are thrown out of a metal with an energy of the order of several eV. This phenomenon is shown to be closely related to the electron work function of metals. Since energy is emitted when positrons leave the metal surface, it is named "negative work function." The negative work function of thermal positrons is  $\Phi^p \approx \Delta\phi^e - \mu_c^p + O(N_p/N)$ , where  $N_p$  and  $N$  are the total number of positrons and electrons, respectively, in the metal.  $\Delta\phi^e$  is the electrostatic potential across the metal surface due to the double layer taken from the electron work-function calculation, and  $\mu_c^p$  is the correlation contribution to the positron chemical potential at the mean electrostatic potential.

Recently observations of low-energy positrons of several eV emitted from metallic surfaces when a high-energy positron source is directed onto the other side of the slab were reported.<sup>1,2</sup> Up to now the accuracy of such experiments<sup>2</sup> only allows us to take these results as qualitative indications of the existence of such low-energy positron sources. Metals and dielectrics like mica or polyethylene were used. Without realizing that such emission is mainly a surface phenomenon, in nearly all cases the material has been coated with a layer of metal, usually gold or chromium. The only quantitative measurement is reported in Ref. 1.

It is well known that high-energy positrons are easily thermalized in metals after a few collisions.<sup>3</sup> The low-energy emission of several eV, which is

much larger than the kinetic energy of thermal positron ( $\sim 0.025$  eV), must therefore be related to the energy that a positron receives when it leaves the metallic surface. We call this the negative work function of the thermal positrons in metals. It is qualified by the word "negative" because unlike the electrons, energy is emitted on leaving the metal.

Let us first return to our understanding of the ordinary work function of a metal. The jellium model used in such theory says that the positive ions are replaced by a rigid uniform positive jelly. The electron cloud fills up the whole interior of the metal but it spills over a little near the edge [Fig. 1 (a)]. This leakage of electrons and the excess positive background form a double layer [Fig. 1 (b)] first suggested by Frenkel<sup>4</sup> and used by Wigner and



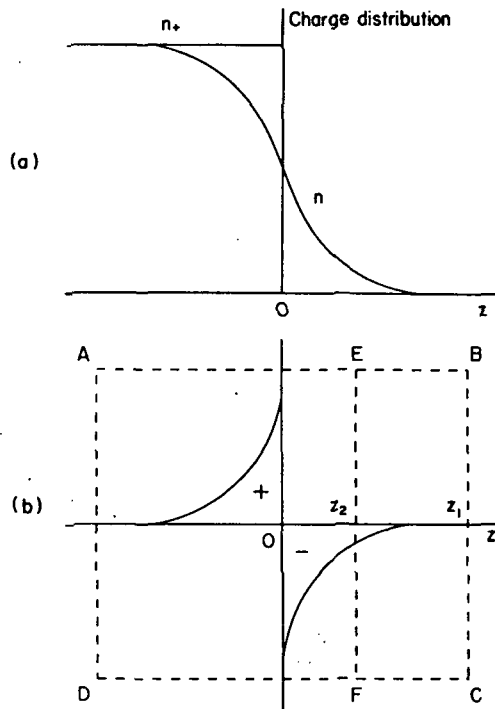


FIG. 1. (a) Charge distribution of a semi-infinite metal with surface at  $z=0$  in the jellium model.  $n_+$  is the positive background and  $n$  is the electron density. (b) Double layer. The field at  $z_1$  is zero because there is no net charge inside the box ABCD when  $z_1 \gg 0$ . At a point  $z_2$  close to the surface the net charge in the box AEFB is positive. The double layer attracts an electron but repels a positron.

Bardeen.<sup>5</sup> The thickness of the double layer is only a few Å.

The double layer attracts an electron when the electron is very close to the surface. This can be seen if we use Gauss's theorem [Fig. 1(b)]. This attractive potential of the double layer is only one of the contributions to the work function of an electron. Fermi statistics and exchange and correlation effects must be included in a good self-consistent calculation. Only in recent years have techniques been developed to successfully calculate the work function.<sup>6-9</sup> Values obtained from a full theoretical calculation and from experiment are in good agreement (5-10%).

A positron, on the other hand, is repelled by the double layer near the surface. There is no exchange effect of the positron with the electron. Of course, Fermi statistics and exchange and correlation effects among the electrons are still the major contributors in determining the true electron-density distribution in the metal.

Let us now examine the above statements more quantitatively. We refer to Lang and Kohn<sup>9</sup> for the proof of an exact expression of the work function  $\Phi^e$  of an electron in a metal:

$$\Phi^e = \Delta\phi^e - \mu^e, \quad (1)$$

where  $\Delta\phi^e$  is the rise in mean electrostatic potential across the metal surface (double layer), and  $\mu^e(n)$  is the bulk chemical potential of the electrons at the mean electron density  $n$  of the metal interior relative to the mean electrostatic potential.  $\mu^e$  consists of three terms: the Fermi energy  $k_F^2/2m$ , the exchange  $\mu_x^e(n)$ , and the correlation  $\mu_c^e(n)$  contributions. In all metals, the work function  $\Phi^e$  is positive.

We can derive a similar expression for the positron work function:

$$\Phi^p = \Delta\phi^p - \mu^p, \quad (2)$$

where  $\Delta\phi^p$  is the lowering of the mean electrostatic potential across the metal surface as described above, and  $\mu^p$  is the chemical potential of the positron in the metal interior relative to the mean electrostatic potential. This is valid in the small ( $n_p/n$ ) limit, where  $n_p$  and  $n$  are the positron and electron densities, respectively.

It should be emphasized here that in these expressions, all many-body effects including the image forces have been taken into account.<sup>9</sup>

In the evaluation<sup>6-9</sup> of  $\Delta\phi^e$ , the only parameter entering the calculation is the mean electron density  $n$  in the bulk. In the positron case,  $n$  is not changed much since the mean density of positrons,  $n_p$ , is of the order  $n_p/n \approx 1/N$ . We can talk of mean density of positrons, because we know both from experiments and from theory that at metallic densities positrons do not form bound states with electrons.<sup>10-13</sup> It is quite true that electrons crowd around a positron locally, but this does not affect the "mean" electron density in the bulk. Neglecting all contributions coming from terms proportional to  $n_p$ , as compared to those containing  $n$ , we find  $\Delta\phi^p(n) \approx -\Delta\phi^e(n)$ . Another way of saying the same

TABLE I. Negative work functions for thermalized positrons in metals. For the sake of reference, we give here a list of common metals and their  $r_s$  values: Al (2.1); Mg(2.7); Cu(2.7); Au(3.0)<sup>a</sup>; Na(4.0); K(4.9); Cs (5.6).

$r_s$	$\Delta\phi^p$ <sup>b</sup> (eV)	$\mu^p$ (eV)	$\Phi^p$ (eV)
2.0	-6.80	-1.89	-4.91
2.5	-3.83	-1.69	-2.14
3.0	-2.32	-1.55	-0.77
3.5	-1.43	-1.43	0
4.0	-0.91	-1.34	0.43
4.5	-0.56	-1.26	0.70
5.0	-0.35	-1.20	0.85

<sup>a</sup> $\Phi^p$  for gold is -2.26 eV. If we use Smith's value for  $\Delta\phi^e$ , then  $\Phi^p \sim -1.93$  eV. It may be of interest to compare these theoretical values with the measured value reported in Ref. 1.

<sup>b</sup>From Table I in Ref. 9.

thing is that neglecting corrections of  $O(1/N)$ , the chemical potential of an electron  $\mu^e(n)$  is not changed.<sup>14</sup> Since  $\mu^e(n)$  is a unique functional of the density  $n$ , it means that to  $O(1/N)$ ,  $n$  is not changed, implying

$$\Delta\phi^p(n) = \Delta\phi^e(n) + O(1/N).$$

$\Delta\phi^e(n)$  have been calculated by various authors<sup>7-9</sup>; a listing of values calculated by Lange and Kohn<sup>9</sup> are shown in Table I. They are of the order of several eV.

We shall now estimate the chemical potential  $\mu^p$  of positron. The kinetic energy of the thermal positron is taken to be zero. Again neglecting terms proportional to  $n_p$ , we have  $\mu^p(n) \sim \mu_c^p(n)$ . To get a rough estimate of  $\mu_c^p$ , let us evaluate the ring diagram (Fig. 2) with screened potential

$$v = -(e^2/r)e^{-\alpha r}, \quad (3)$$

where the screening constant  $\alpha$  can be chosen<sup>15</sup> as either the Thomas-Fermi value  $\alpha \sim 0.81 r_s^{-1/2} k_F$  or the random-phase-approximation (RPA) value  $\alpha \sim 0.353 r_s^{-1/2} k_F$ . We shall use the former to get an estimate of the magnitude. In addition to the small-momentum-transfer approximation, we shall assume  $n_p$  approach zero. This gives the correlation energy

$$\epsilon_c^p(\text{RPA}) \sim -\frac{13.6}{2\pi} \frac{k_F}{\alpha} = -2.68 r_s^{-1/2} (\text{eV}), \quad (4)$$

where  $r_s$  is the dimensionless parameter  $a_B^{-1} (3V/4\pi N)^{1/3}$  and  $a_B$  is the Bohr radius. Now

$$\mu_c^p = \frac{d}{dn_p} (n_p \epsilon_c^p) \sim \epsilon_c^p$$

for small  $n_p$ . The RPA (static) estimates are listed in Table I. In real situations as compared to the jellium model, there is a local concentration of electrons near a positron.

Even if we suppose this local concentration in electron density is as high as 100 times greater, the above estimates in the static contribution to  $\mu_c^p$  cannot be off by a factor more than 3. The small-momentum-transfer approximation, however, over-

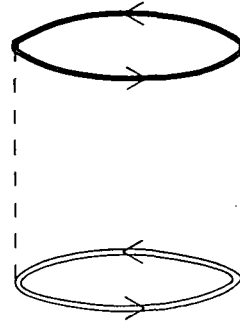


FIG. 2. Ring diagram. The double lines are positron and positron-hole lines, the solid lines are the electron and electron-hole lines, and the broken lines represent the screened interaction [Eq. (2)].

estimates the value. A more accurately calculation of  $\mu^p$  has been made by Bergersen and Carbotte,<sup>16</sup> and their values are close to these estimates. Because of the arbitrariness in both estimates of  $\mu^p$  and  $\Delta\phi^p$ , the values in Table I should only be taken as an indication of the existence of negative work function for thermal positrons in some high electron density metals.

To this date, experiments yielding definite results were carried out at room temperature and pressure.<sup>1,2</sup> As has been indicated in this theoretical study, such observed low-energy positrons of several eV are most likely to be related to the "negative work function." It is a surface phenomenon. We learn from the work-function physicists that surface phenomena are very sensitive to the surface condition, to the purity of the metal, as well as to the presence of absorbed impurities and gases. High vacuum and low temperature are required. Measurements by Pendyala, Orth, Zitzewitz, and McGowan are being carried out under conditions closer to these requirements.<sup>17</sup>

The author wishes to thank Professor J. W. McGowan for suggesting the problem, and Professor W. Kohn, Dr. N. D. Lang, Professor J. Carbotte, Dr. B. Bergersen, Dr. C. K. Majumdar, and S. Pendyala for continuous discussions and critical comments. Partial financial support by a Frederick Gardner Cottrell Grant from the Research Corp. and from the National Research Council of Canada are gratefully acknowledged.

<sup>1</sup>D. E. Groce, D. G. Costello, J. W. McGowan, and D. F. Herring, *Proceedings of the Vth International Conference on the Physics of Electronic and Atomic Collisions* (MIT Press, Cambridge, Mass., 1969), pp. 757-759.

<sup>2</sup>Qualitative observations were reported by L. Madansky and F. Rasetti, *Phys. Rev.* **79**, 397 (1950); W. H. Cherry, Ph. D. dissertation (Princeton University, 1958) (unpublished); J. M. J. Madey, *Phys. Rev. Letters* **22**, 784 (1969); and D. Paul (private communication).

<sup>3</sup>G. E. Lee-Whiting, *Phys. Rev.* **97**, 1157 (1955); E. J. Woll, Jr. and J. P. Carbotte, *ibid.* **164**, 985 (1967); and J. P. Carbotte and H. L. Arora, *Can. J.*

*Phys.* **45**, 387 (1967).

<sup>4</sup>J. Frenkel, *Z. Physik* **51**, 232 (1928).

<sup>5</sup>E. Wigner and J. Bardeen, *Phys. Rev.* **48**, 84 (1935); J. Bardeen, *ibid.* **49**, 653 (1936).

<sup>6</sup>A. J. Bennett and C. B. Duke, in *Structure and Chemistry of Solid Surfaces*, edited by G. Somorjai (Wiley, New York, 1969).

<sup>7</sup>J. R. Smith, *Phys. Rev.* **181**, 522 (1969); **B 1**, 2363 (E) (1970).

<sup>8</sup>N. D. Lang, *Solid State Commun.* **7**, 1047 (1969); N. D. Lang and W. Kohn, *Phys. Rev.* **B 1**, 4555 (1970).

<sup>9</sup>N. D. Lang and W. Kohn, *Phys. Rev.* **B 3**, 1215 (1971).

<sup>10</sup>J. Callaway, *Phys. Rev.* **116**, 1140 (1959).

<sup>11</sup>A. Held and S. Kahana, *Can. J. Phys.* 42, 1908 (1964).

<sup>12</sup>H. Kanagawa, Y. H. Ohtsuki, and S. Yanagawa, *Phys. Rev.* 138, A1155 (1965).

<sup>13</sup>C. K. Majumdar and A. K. Rajagopal, *Progr. Theoret. Phys. (Kyoto)* 44, 26 (1970).

<sup>14</sup>C. K. Majumdar, Ph. D. thesis (University of Cali-

fornia, San Diego, 1965) (unpublished).

<sup>15</sup>D. Pines, *Solid State Phys.* 1, 373 (1955).

<sup>16</sup>B. Bergersen and J. Carbotte (private communication).

<sup>17</sup>S. Pendyala, R. Orth, P. Zitzewitz, and J. W. McGowan (private communication).

## Evidence for the Negative Work Function Associated with Positrons in Gold<sup>†</sup>

D. G. Costello

*Gulf Energy and Environment Incorporated, P. O. Box 608, San Diego, California 92112*

and

D. E. Groce

*JRB Associates Incorporated, La Jolla, California 92037*

and

D. F. Herring

*Enviro-Med Incorporated, La Jolla, California 92037*

and

J. Wm. McGowan\*

*Physics Department, University of Western Ontario, London, Ontario, Canada*

(Received 3 May 1971)

Positrons which have been thermalized in various moderators and coated with  $\sim 200\text{-\AA}$  gold leave the gold surface with an energy which peaks between 0.75 and 2.90 eV. This energy is thought to be associated with a positron or "negative" work function of gold.

### INTRODUCTION

Until we reported<sup>1</sup> our observation of low-energy positrons, the negative results of Madanski and Rasetti<sup>2</sup> had been widely quoted as evidence for the lack of emission of low-energy positrons from surfaces of various materials. In their experiments, they used a  $^{64}\text{Cu}$  positron source and looked for the emission of positrons with energies less than 150 eV from various metallic and dielectric materials. Later, in an unpublished thesis, Cherry<sup>3</sup> did observe positrons from a  $^{22}\text{Na}$  source with energies less than 10 eV transmitted through mica which had been coated with a thin conducting layer of chromium. Following the method of Cherry, Madey<sup>4</sup> found emission of slow positrons from polyethylene with energies peaked near 20 eV. He speculated that the emission process was enhanced by an electric field built up within the dielectric by stopped positrons and their annihilation  $\gamma$  rays.

Our interest in the problem of emission of slow positrons first came from a desire to use them as projectiles in a study of positron-atom-scattering cross sections. On the basis of the experiments on the slowing-down spectrum of positrons with energy above 10 keV of Birkhoff and Wilkie<sup>5</sup> and the "continuous-slowning-down" theory of Spencer and Fano,<sup>6</sup> it was felt that, with a moderated high-energy source, one might be able to produce sufficient flux with energies below 100 eV to measure total scattering cross sections for various target gases.<sup>1</sup>

Repeated attempts to observe positrons in the interval 10–100 eV were unsuccessful although Paul *et al.*<sup>7</sup> using a very similar approach, found a signal associated with positrons between 0.3 and

1.5 keV. Following the independent suggestions of Kohn<sup>8</sup> and Callaway<sup>9</sup> that the positrons may be thermalized and then "thrown" from the material with several eV, attention was focussed on the energy interval  $\sim 1.0\text{--}10.0$  eV. It was in this interval that we did find positrons, all in a peak near 1 eV. We associate this energy with what we call the positron work function or "negative" work function. This is the energy of the positrons which has been thermalized in the moderator and thrown out of a material. Detailed calculations of the mechanism have recently been completed by Tong.<sup>10</sup> A comparison of our results with his theory follows. More recently Jaduszliwer *et al.*<sup>11</sup> have verified the existence of this low-energy peak.

### EXPERIMENT

Rather than using a radioactive source as our source of positrons, we used a 1-A peak current 55-MeV electron linear accelerator (LINAC). The positrons were created through pair production by the bremsstrahlung from a 20-nsec burst of electrons, at a repetition rate of 500 Hz. Energy analysis of the positrons was accomplished by fast time-of-flight techniques using a 3-long flight path. The coincident  $\gamma$  radiation from annihilation in a metal target at the end of the flight path determined the time of arrival of a positron. A schematic diagram of the source and flight path are shown in Fig. 1.

The bremsstrahlung target consisted of a water-cooled 0.3-radiation-length-thick tantalum target within a lead collimator. The forward-directed bremsstrahlung radiation impinged on the converter where the positron-electron pair was formed. This normally consisted of a "sandwich" of tantalum, in

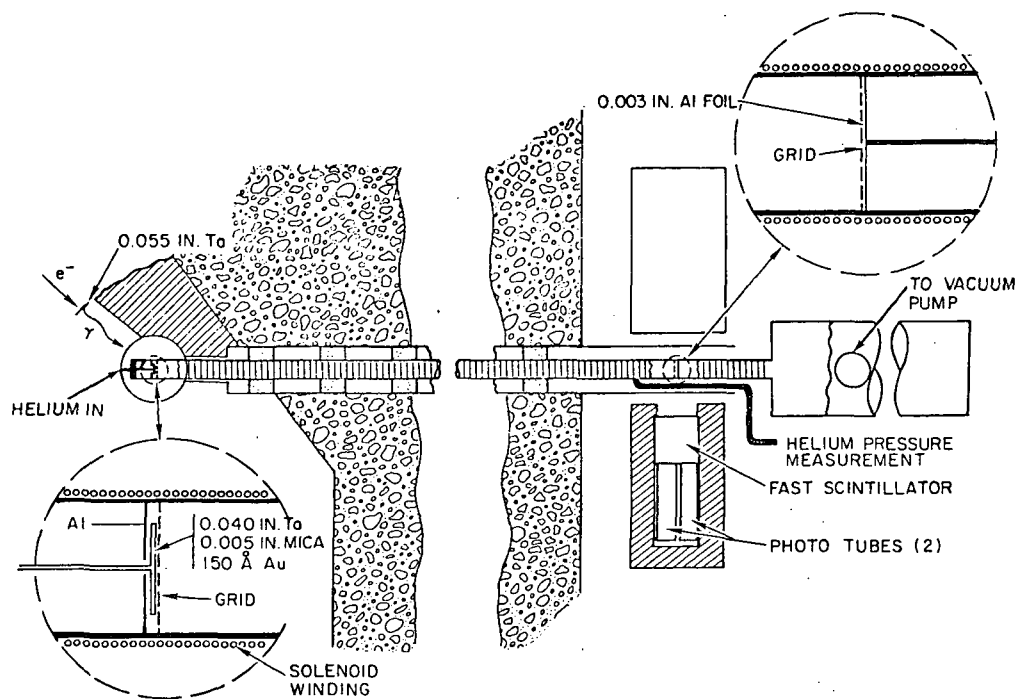


FIG. 1. Scattering chamber and time-of-flight energy analyzer, shown with details of positron-source region and positron annihilator.

which positrons were born, and a low- $Z$  material, in which the positron energy was moderated and from which they were emitted. Several materials have been used for the moderator: aluminum (with an oxide coating of undetermined thickness) with a 200-Å gold coating; mica with a 150-Å gold coating; a CsBr crystal with a 150-Å gold coating. It was our thought at the time of the experiment that we were dealing with a bulk process and that the gold coating simply gave a gold equipotential surface. To make sure this was so, the coating was made as thin as possible so that it would still have a good uniform-conducting surface but not appreciably thermalize the positrons coming through it. However, Tong<sup>10</sup> has shown that the negative work function is largely a surface process. Thus we would expect all of our results to be somewhat similar and to reflect primarily the gold coating.

Because the positrons leave the moderator with essentially one energy, the converter-moderator sandwich could be biased at various potentials with an external power supply (refer to Fig. 2 for an example). A grounded aluminum plate immediately behind the converter target served as part of a 20-pF vacuum capacitor to prevent fluctuations in the potential on the converter target due to Compton and/or photoelectron currents. A grounded gold-plated copper grid was placed on the downstream side of the converter target. With this arrangement it was possible to accelerate or decelerate any positrons coming from the surface of the converter target. However, many of the positrons (between

30 and 60%) which appeared in the low-energy peak (near 1 eV) came from the gold-coated copper grid, perhaps the end of the flight tube, and other sources. For this reason, we separated the positrons coming through the gold-plated moderator from the others by appropriately biasing the target.

In Fig. 2, we show the positron spectrum when +15.00 V were placed on a tantalum converter with a gold-coated mica moderator. When one subtracts 15 eV from the energy of the distribution, a few positrons appear to come from energies less than 0 eV. This reflects only the resolution of the time-of-flight apparatus. It was unfortunate that we had to bias the converter moderator with respect to the grid, since in the time-of-flight experiment the resolution of the emitted positrons was approximately 25 times worse at 15 eV than it was just below 1 eV.

Although the flight path was magnetically shielded, a weak solenoidal field was required to prevent any residual ac or dc magnetic fields from deflecting the low-energy positrons into the walls of the flight tube. The annihilation target at the end of the flight path was also biased with respect to a grounded grid at its upstream side. This bias was required to drive the positrons into the surface of the annihilation foil. The target was an aluminum foil with a thin coating of gold black used to minimize back scattering. High-energy positrons,  $\gamma$  rays, neutrons, etc., could pass through the annihilation foil and proceed into a beam dump downstream.

The vacuum along the flight path was maintained

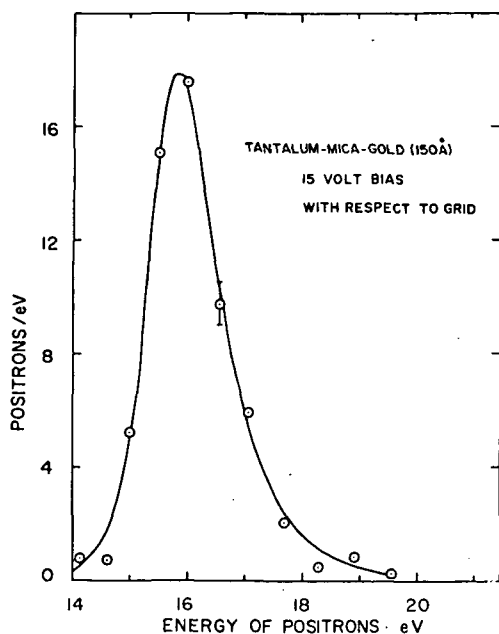


FIG. 2. Average positron energy distribution coming from a tantalum-mica-gold moderator sandwich biased 15 V with respect to the collision chamber. The error is the standard deviation associated with the average of eight runs.

at  $2 \times 10^{-7}$  Torr or better. Large amounts of lead and heavy concrete shielding separated the converted end of the flight path and the detectors. Each detector was a 6-in.-diam  $\times$  6-in.-long Ne 211 fast-liquid scintillator that was viewed by both a 56 AVP and a 6810-Å phototube. The multiple phototubes were required to suppress the effects of spurious "after pulses" from the prompt bremsstrahlung flash. The detectors had an efficiency of 1.3% for annihilation radiation for fourway phototube coincidence.

#### RESULTS AND DISCUSSION

As has been seen in Fig. 2, the energy at which the plot of the number of positrons/eV peaks with a 15-V bias on the moderator corresponds to a negative work function peaking near 1 eV. When displayed as a function of the time of flight, the number of positrons/time interval peaks closer to 2 eV. This apparent discrepancy originally led to some confusion.<sup>1</sup> The values from many runs for various (gold-coated) moderators are summarized in Table I in comparison with other calculated and measured values. The agreement for gold is good when one allows for the incomplete thermalization of the positrons in the thin gold layer.

In essence, the simple theory of the "negative" work function, which is discussed in the following paper,<sup>10</sup> describes the surface of the metal as a dipole layer with the electron density extending

beyond the surface, resulting in residual positive charge within the surface. As the positron is brought from infinity into the dipole it eventually feels only the residual repulsive potential, which primarily sets the value of the "negative" work function. In the treatment by Tong,<sup>10</sup> allowance is also made for electron-positron correlation. It is important to realize that the value for gold can be related to part of the electron work function for the same material. This fact allows us to separate the electrostatic part and perhaps some of the electron-electron correlation parts of the work function from other quantum effects such as electron exchange which does not exist for positrons.

It has also been observed experimentally by us that the angular distribution of the positrons leaving the surface appears to be less than  $\pm 2^\circ$ , much less than the  $(1/40)^{1/2} [= (kT/1 \text{ eV})^{1/2}]$  rad one might expect for electrons in thermal equilibrium with the solid and "thrown" from it with an energy of  $\sim 1 \text{ eV}$ . This limit follows from experiments where the axial magnetic field was changed drastically without changing the time-of-flight distribution of the transmitted positrons. If the positrons had a larger angular distribution, then the transmitted peak would shift towards lower energies with increased magnetic field strength. This results from the fact that positrons which would normally be lost to the walls of the time-of-flight spectrometer would now spiral down the tube and be collected. This was not found. The reason for the small angle of emission is not yet understood.

The energy distribution of transmitted positrons near 1 eV is  $\sim 1 \text{ eV}$  full width at half-height with a tail on the high-energy side. This width, unlike the case where the positrons are accelerated to higher

TABLE I. Values for gold-coated moderators in comparison to calculated and theoretical values.

Material	Values of negative work functions $\Phi^P$	
	Experimental (eV)	Theoretical (eV)
Gold	...	$-0.77^a$
Mica (150 Å) gold	$-0.75 \pm 0.5^b$ $< 5^c$	...
CsBr (150 Å) gold	$-2.90 \pm 1.0^{b,d}$	...
Al (200 Å) gold	$-1.25 \pm 0.5^b$	...
Mica-chromium	$< 5^e$	...
Polyethylene	$-20.7^f$	...
Cu	...	$-1.8^g$

<sup>a</sup>B. Y. Tong in Ref. 10.

<sup>b</sup>This work.

<sup>c</sup>D. A. L. Paul (private communication).

<sup>d</sup>The accuracy of this measurement is small due to experimental factors. However, the higher value may reflect the CsBr substrate since the gold foil is thin.

<sup>e</sup>W. H. Cherry in Ref. 3.

<sup>f</sup>J. M. J. Madey in Ref. 4.

energies, is not likely to be instrumental since at 1 eV the resolution of the spectrometer is very much smaller than the measured width. One can deduce a width of this magnitude if one assumes that the positrons leave an oscillating platform with a mass near that of the electron and with an energy near 1/40 eV. Then in the laboratory frame, the energy of the positrons would be  $\sim 1 \pm 2(1 \times 0.025)^{1/2}$  eV. Accurate measurements of this width, the an-

gular distribution, and the energy as functions of the source temperature and film thickness are needed. Since the negative work function is largely a surface effect, extreme care with surface conditions will have to be taken.

The yield of positrons was between 1 and 10 positrons/sec, or between  $10^{-7}$  and  $10^{-6}$  of the total positron yield from the source. This is in essential agreement with the unpublished results of Cherry.<sup>3</sup>

†Work carried out at Gulf Energy and Environment, Inc., San Diego, Calif., and supported, in part, by NASA, Goddard Space Flight Center under Contract No. NAS5-11116.

\*All enquiries or correspondence to be addressed to the above.

<sup>1</sup>D. E. Groce, D. G. Costello, J. Wm. McGowan, and D. F. Herring, *Bull. Am. Phys. Soc.* **13**, 1397 (1968); *Proceedings of the VIth International Conference on the Physics of Electronic and Atomic Collisions* (MIT Press, Cambridge, Mass., 1969), p. 757.

<sup>2</sup>L. Madanski and F. Rasetti, *Phys. Rev.* **79**, 397 (1950).

<sup>3</sup>W. H. Cherry, Ph.D. thesis (Princeton University, 1958) (unpublished).

<sup>4</sup>J. M. J. Madey, *Phys. Rev. Letters* **22**, 784 (1969).

<sup>5</sup>W. H. Wilkie and R. D. Birkhoff, *Phys. Rev.* **135**, A1133 (1964).

<sup>6</sup>L. V. Spencer and U. Fano, *Phys. Rev.* **93**, 1172 (1954).

<sup>7</sup>D. A. L. Paul, P. W. Hietala, G. F. Celitans, P. G. Stangeby, and J. Maksimov, *Bull. Am. Phys. Soc.* **13**, 1474 (1968).

<sup>8</sup>W. Kohn (private communication).

<sup>9</sup>J. Callaway (private communication).

<sup>10</sup>B. Y. Tong, following paper, *Phys. Rev. B* **5**, 1436 (1971).

<sup>11</sup>B. Y. Jaduszliwer, T. J. Bowden, and D. A. L. Paul, *Bull. Am. Phys. Soc.* **15**, 785 (1970).

Abstract Submitted  
for the Washington D.C. Meeting of the  
American Physical Society  
24-27 April 1972

Physical Review  
Analytic Subject Index  
Number 46

Bulletin Subject Heading  
in which Paper should be placed  
Solids: Theory, Metals

A Model Work Function of Positrons in the Wigner Seitz Approximation. \* SUBRAHMANYAM PENDYALA, J. Wm. McGOWAN and B. Y. TONG, Univ. of Western Ontario. -- Several experiments have established that slow positrons diffuse out of solids with characteristic energy, which is now called the "negative work function". The work function of the positron is defined in the usual sense as the difference of energy of the positron in the metal and the vacuum. The bottom of the band energy is calculated in the Wigner-Seitz approximation, the moment of the surface dipole and the correlation energy of the positron<sup>1</sup> are estimated at metallic densities. The results are compared with the experiments and with calculations based upon the jellium model.

\*Supported by NRC (Canada) and NASA Goddard under Grant NGR 52-029-006

<sup>1</sup>B. Bergerson and J. P. Carbotte. To be published.

Submitted by



---

J. Wm. McGowan  
Department of Physics  
University of Western Ontario  
London 72, Ontario



Abstract Submitted

for the Washington D.C. Meeting of the  
American Physical Society

24-27 April 1972

Physical Review  
Analytic Subject Index  
Number 46, 42

Bulletin Subject Heading  
in which Paper should be placed  
Solids: Experimental, Metals

Emission of Low Energy Positrons from Solids. \*

SUBRAHMANYAM PENDYALA, J. Wm. McGOWAN, P. W. ZITZEWITZ and P. H. R. ORTH<sup>+</sup>, Univ. of Western Ontario. -- It is now well established<sup>1, 2</sup> that slow (1eV) positrons with a sharply defined energy diffuse out of solids used as moderators of fast (400keV) positrons. The present experiment uses a 180° electrostatic energy analyzer to study the distribution in energy and angle of positrons emitted from thin films of gold, aluminum, and copper backed by mica and pure foils of gold, copper and mica. Studies of the effects of moderator thickness will be reported and models for the energy spectra will be discussed. The characteristic<sup>3</sup> energy has been named the "negative work function".<sup>1, 3</sup>

\*Supported by NRC (Canada) and NASA Goddard under Grant NGR 52-029-006

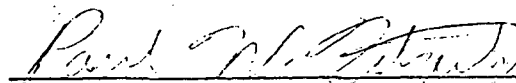
<sup>+</sup> Now at University of British Columbia

<sup>1</sup> D. Costello, et al, Phys. Rev. B5 (Feb. 1972)

<sup>2</sup> B. Y. Jaduszliwer, et al, Bull. APS 15, 785 (1970)

<sup>3</sup> B. Y. Tong, Phys. Rev. B5 (Feb. 1972)

Submitted by



Signature of APS Member

Paul W. Zitzewitz  
Department of Physics  
University of Western Ontario  
London 72, Ontario, Canada

Abstract Submitted  
for the CAP Annual Meeting  
Edmonton, Alberta  
June 26-29, 1972

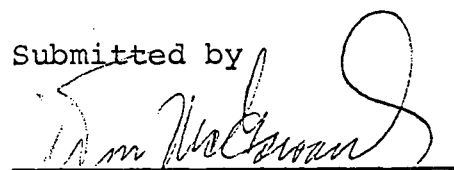
The Lifetime of Free Positrons.\* P.W. ZITZEWITZ and J.WM. MCGOWAN, Univ. of Western Ontario.--An experiment has been designed which will allow storage of thermal positrons for several days. The combination of electrostatic and magnetic fields in the Penning configuration has allowed containment of electrons for 500 hours,<sup>1</sup> and a similar system has been built for the slow positrons emitted by thin film moderators.<sup>2</sup> The theory and equipment will be described and preliminary results presented. Applications to positron-atom collision studies will be discussed.

\* Supported by NRC and NASA Goddard (USA) under grant NGR-52-029-006.

<sup>1</sup>H.G. Dehmelt and F.L. Walls, Phys. Rev. Letters 21, 127 (1968)

<sup>2</sup>D.G. Costello et al, Phys. Rev. 5, 1433 (1972)  
S. Pendyala, et al, Bull. Am. Phys. Soc. 17  
(April 1972)

Submitted by



J. Wm. McGowan

Chairman  
Department of Physics  
University of Western Ontario  
London 72, Ontario

March 30, 1972

Abstract Submitted  
for the CAP Annual Meeting  
Edmonton, Alberta  
June 26-29, 1972

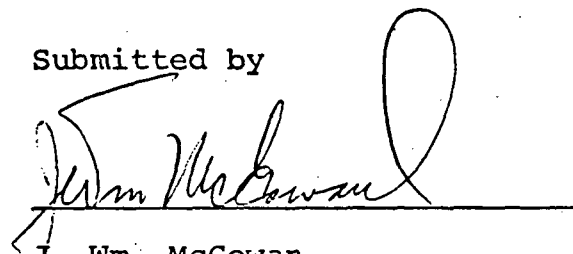
Solid State Spectroscopy with Low-Energy Positrons\*, S.PENDYALA, J.WM. MCGOWAN AND P.W. ZITZEWITZ, U. of Western Ontario.--While developing a source of  $1_{1-2}eV$  positrons for atomic scattering studies, we have found a new method of studying the bulk and surface properties of solids. Slow positrons which leave a moderator placed in front of a source of fast (200 KeV) positrons are then analyzed by an electrostatic  $180^\circ$  analyzer with 0.05 eV resolution. The spectrum obtained consists of a principal peak with considerable structure. In preliminary studies, we have examined Au evaporated on mica and find one peak due to the mica and another due to to the Au. From the variation in intensity of these peaks as a function of film thickness the attenuation length is found directly. Similar studies will be reported for Al and Cu. Implications to be drawn from the fine structure of the peaks will also be discussed.

\*Supported by the NRC and NASA Goddard under grant NGR-52-029-006

<sup>1</sup>D.G.Costello et al, Phys.Rev. 5, 1433 (1972)

<sup>2</sup>S.Pendyala et al, Bull.Am.Phys.Soc.17 (Apr. 72)

Submitted by



J. Wm. McGowan  
Chairman, Department of Physics  
University of Western Ontario  
London 72, Ontario

April 4, 1972

## Positron-hydrogen elastic scattering with inclusion of long range effects via a pseudostate expansion

WC FON and DF GALLAHER

Department of Physics, University of Western Ontario, London, Canada

MS received

**Abstract.** A complete calculation of positron-hydrogen elastic scattering in a pseudo-state expansion formulation is made and results obtained for s, p, d, etc., partial wave phase shifts. Good agreement is found between these calculations and those of long range force oriented models for energies below the positronium formation threshold.

### 1. Introduction

The positron-hydrogen collision is an atomic collision as fundamental as that of the exhaustively investigated electron-hydrogen collision but because of the opposite sign of the projectile charge it has notable differences and in some ways may be a more complex system to analyse. Positronium formation in either the ground or excited states as either a real or virtual process is the analogue of electron exchange in the electron-hydrogen problem and should be included in some manner in any complete formulation; for energies below the positronium formation threshold as is the case here, this is clearly a virtual process. There is an excellent review article by Drachman and Temkin (1971) which includes an extensive discussion of positron-hydrogen scattering and may be consulted with profit.

The other important effect which requires incorporation into the model is that of the distortion of the target state by the electric field of the incoming positron. A special difficulty which is present in the positron collision and not in its electron counterpart is that in the adiabatic approximation appropriate at low energies where one neglects the kinetic energy of the incoming positron, the effective potential seen by the positron consists of two parts; a static potential and a polarization potential which, in this case, have opposite signs, tending to cancel one another, and demanding great delicacy in the choice of an expansion basis for the total wavefunction; in the electron case these potentials add and are further masked at short-distances by the dominant effects of electron exchange. One would ultimately like to include these two important effects of virtual positronium formation and atomic distortion as fully as possible. The distortion or polarization effect is a long range effect and we attempt to include it by expanding the total wavefunction in a pseudo-state basis with the pseudo-states chosen to account for the polarizability of the target as proposed by Damburg and Karule (1967) and recently applied to the elastic electron-hydrogen problem by Burke *et al* (1969).

In the results obtained here we have incorporated only the long range effects in this manner; the important short range effects associated with virtual positronium formation are being currently studied and will be reported on in a subsequent paper.

0/2

Table 1. S-wave  $e^-$ -H phase shifts in various approximations

	a	b	c	d	e	f	g	h	i	j	k
K											
0.1	0.1483	0.151	-0.0580	0.036	0.0072		0.07990	0.128	0.163	0.080	0.0996
0.2	0.1877	0.188	-0.1145	0.0137	-0.0251	0.0745	0.0826	0.158	0.213	0.085	0.1187
0.3	0.1677	0.168	-0.1682	-0.0352	-0.0748		0.0459	0.135	0.201	0.053	0.0938
0.4	0.1201	0.120	-0.2181	-0.0939	-0.1295	-0.011	-0.0073	0.089	0.164	0.005	0.0488
0.5	0.0624	0.062	-0.2635	-0.1539	-0.1829		-0.0654	0.034	0.115	-0.048	-0.0043
0.6	0.0039	0.007	-0.3042	-0.2112	-0.2317	-0.1252	-0.1225	-0.022	0.067	-0.099	-0.0540
0.7	-0.0512	-0.054	-0.3400	-0.2638	-0.2746		-0.1756	-0.074	0.020	-0.147	-0.1038

- (a) Rigorous lower bound results of Bhatia *et al* (1971)
- (b) Variational results of Schwartz (1961)
- (c) Static approximation (Hartree)
- (d) Extended polarization (Callaway *et al* 1968)
- (e) (1s-2s-2p-3s-3p-3d) close coupling (McEachran and Fraser 1965)
- (f) (1s-2p'-3d') pseudo-state results of Perkins (1968)
- (g) (1s-2s-2p-2p'-3d) pseudo-state results of present work
- (h) Rigorous lower bound results of Drachman (1968)
- (i) Adiabatic (monopole + dipole + quadrupole) results of Bransden and Jundi (1966)
- (j) Dipole potential results of Cody *et al* (1964)
- (k) Optical potential formulation of Matese and Fund (1971).

Fung

Table 2. P-wave  $e^+$ -H phase shifts in various approximations

K	a	b	c	d	e	f	g	h
0.1	0.009	0.008	0.0073	0.0072	0.0083	0.0054	0.007	0.0086(1)
0.2	0.033	0.0289	0.0263	0.0226	0.0281	0.0162	0.030	0.032(1)
0.3	0.065	0.0548	0.0518	0.0370	0.0513	0.0257	0.058	0.066(4)
0.4	0.102	0.0801	0.0764	0.0458	0.0714	0.0300	0.084	0.11(1)
0.5	0.132	0.0994	0.0952	0.0468	0.0848	0.0282	0.103	0.14(1)
0.6	0.156	0.112	0.106	0.0408	0.0912	0.0210	0.115	0.17(2)
0.7	0.178	0.119	0.109	0.0290	0.0922	0.0102	0.119	0.19(2)

- (a) Variational results of Armstead (1968)
- (b) Rigorous lower bound results of Kleinman *et al* (1965)
- (c) Rigorous lower bound results of Drachman (1968)
- (d) Extended polarization results of Callaway *et al* (1968)
- (e) (1s-2s-2p-2p'-3d) pseudo-state results of present work
- (f) (1s-2s-2p-3s-3p-3d) close-coupling results of McEachran *et al* (1965)
- (g) Adiabatic (monopole + dipole + quadrupole) results of Bransden and Jundi (1966)
- (h) Extrapolated values of Kleinman *et al* (1965)

and 3 hearten us where comparison is made with other theoretical calculations. Suppose we include the short range effects via, for example, virtual positronium pseudo-states to allow for polarization of the positronium atom by the proton. Considering our long range results we may expect this to enhance our values to close agreement with the variational values.

where

$$Y_{l_1 l_2}^{LM}(\hat{r}, \hat{x}) = \sum_{m_1 m_2} C_{m_1 m_2 M}^{l_1 l_2 L} Y_{l_1 m_1}(\hat{r}) Y_{l_2 m_2}(\hat{x}) \quad (6)$$

and in which the  $S_{nl}(r)$  are radial pseudo-state functions to be specified later; introducing a projection operator  $P_v(r, \hat{x})$  with the property that

$$P_v(r, \hat{x}) \Psi(r, x) = \Phi_v^*(r, \hat{x}) \int \Phi_v^*(r', \hat{x}) \Psi(r', x) dr' d\hat{x} \quad (7)$$

and multiplying (2) by  $\Phi_v^*(r, \hat{x})$  and integrating over the coordinates  $r$  and  $\hat{x}$ , we obtain the final radial equations

$$\begin{aligned} & \left( \frac{d^2}{dx^2} - \frac{l_2(l_2+1)}{x^2} - \frac{2}{x} + 2(E - \epsilon_{nl_1}) \right) F_v(x) \\ & + 2 \sum_{\lambda} \sum_{v' \neq \text{IC}} \{ f_{\lambda}(l_1 l_2 l_1' l_2'; L) Y_{\lambda}(S_{nl_1}, S_{n'l_1'; x}) \} F_{v'}(x) \\ & = -2x \int \Phi_v^*(r, \hat{x}) \left( \frac{1}{|r-x|} - P_v(r, \hat{x}) \frac{1}{|r-x|} \sum_{v' \neq \text{IC}} P_{v'}(r, \hat{x}) \right) \Psi(r, x) dr d\hat{x} \end{aligned} \quad (8)$$

L.C.  
↓  
ψ<sub>λ</sub>(S<sub>nl<sub>1</sub></sub>, S<sub>n'l<sub>1</sub>'</sub>; x)

(IC stands for incident channel) where we have imposed the two conditions

$$\begin{aligned} & \int_0^{\infty} S_{nl_1}(r) \left( \frac{d^2}{dr^2} - \frac{l_2(l_2+1)}{r^2} + \frac{2}{r} \right) S_{n'l_1}(r) dr = -2\epsilon_{nl_1} \delta_{nn'} \\ & \text{out } \rightarrow \int_0^{\infty} S_{nl_1}(r) S_{n'l_1}(r) dr = \delta_{nn'} \end{aligned} \quad (9)$$

L.C.  
↓  
ψ<sub>λ</sub>

as in Burke *et al* (1969) on the radial pseudo-states  $S_{nl}(r)$ , introducing the pseudo-thresholds  $\epsilon_{nl_1}$ , and where the functions  $f_{\lambda}$  and  $Y_{\lambda}$  were first defined by Percival and Seaton (1957).

We have left the total wavefunction unexpanded on the right hand side of (8) under the integral sign. Using the property (7) of the projection operator and the orthonormality of the basis one can see that if  $\Psi(r, x)$  is expanded again as in (4) the second term on the right hand side of (8) (that is, the term involving the projection operators) will vanish and we recover the usual pseudo-state expansion equations. It is these equations which have been solved here and give us our present long range results.

### 3. Results and conclusions

We have presented our calculated results for the s, p, d etc phase shifts in  $1s-2s-\overline{2p}$ ,  $1s-2s-\overline{2p}-\overline{2p}$ ,  $1s-2s-\overline{2p}-\overline{3d}$  and  $1s-2s-\overline{2p}-\overline{2p}-\overline{3d}$  expansions wherein the pseudo-states  $\overline{2p}$ ,  $\overline{2p}$  and  $\overline{3d}$  are those employed by Burke *et al* (1969). It must be at once emphasized that these are purely long range results and so ought not to be expected to approach the accurate variationally obtained values for small  $L$ . Rather, it is hoped to demonstrate here how important is the influence of the neglected short range effects mentioned above, and to show how far long range forces can carry one towards a complete solution.

14

## References

- Armstead R L 1968 *Phys. Rev.* **171** 91-3
- Bhatia A K, Temkin A, Drachman R J and Eiserike H 1971 *Phys. Rev. A* **3** 1328-35
- Bransden B H and Jundi Z 1966 *Proc. Phys. Soc.* **89** 7-11
- Burke P G, Gallaher D F and Geltman S 1969 *J. Phys. B: Atom. molec. Phys.* **2** 1142-54
- Callaway J, Labahn R W, Poe R J and Duxler W 1968 *Phys. Rev.* **168** 12-21
- Cody W J, Lawson J, Massey H S W and Smith K 1964 *Proc. R. Soc. A* **278** 479-89
- Damburg R J and Karule E 1967 *Proc. Phys. Soc.* **90** 637-40
- Drachman R J and Temkin A 1971 *Case Studies in Atomic Collision Physics* Vol 3 to be published
- Drachman R J 1968 *Phys. Rev.* **173** 190-202
- Fon W C 1970 *PhD Thesis* Manchester Canada — out
- Kleinman C J, Hahn Y and Spruch L 1965 *Phys. Rev. A* **140** 413-25
- Matese J J and Fung A C 1971 *Phys. Rev. A* **3** 928-37
- McEachran R P and Fraser P A 1965 *Proc. Phys. Soc.* **86** 369-73
- O'Malley T F, Rosenberg L and Spruch L 1962 *Phys. Rev.* **125** 1300-10
- Percival I C and Seaton M J 1957 *Proc. Camb. Phil. Soc.* **53** 654-62
- Perkins J R 1968 *Phys. Rev.* **173** 164-71
- Schwartz C 1961 *Phys. Rev.* **124** 1468-71

Their inclusion will be critical towards increasing our present phase shift values towards accurate variationally calculated values. Even so, the s, p and d etc phase shifts shown graphically in figures 1(a), (b), (c) and 2(a) and (b) and in tabulated form in tables 1, 2

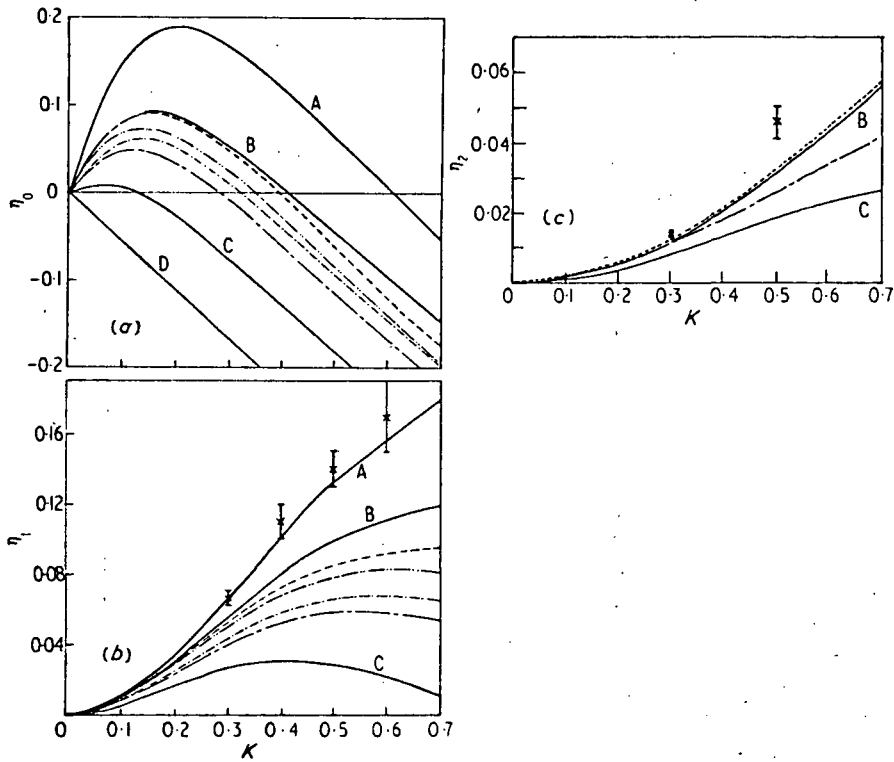


Figure 1. ———  $1s-2s-2\bar{p}$ ; - - -  $1s-2s-2\bar{p}-\bar{p}$ ; - · - · -  $1s-2s-2\bar{p}-3\bar{d}$ ; - - -  $1s-2s-2\bar{p}-2\bar{p}-3\bar{d}$ . (a) curve A, rigorous lower bounds (Bhatia *et al* 1971); curve B, static + polarization (Cody *et al* 1964); curve C, 6 states coupling (McEachran *et al* 1965); curve D, static (Cody *et al*). (b) and (c)  $\{$ , extrapolated estimates of Kleinman *et al* (1965); curve A, variational (Armstead 1968); curve B, rigorous lower bounds (Kleinman *et al*); curve C, 6 states coupling (McEachran *et al*).

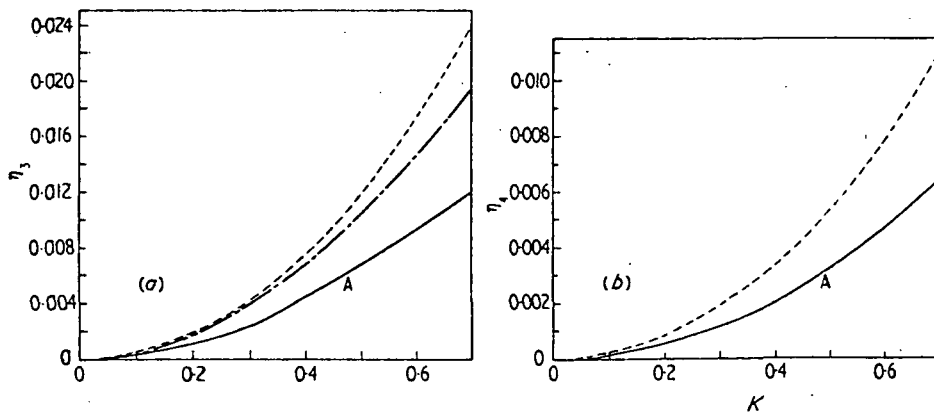


Figure 2. ———  $1s-2s-2\bar{p}$ ; - - -  $1s-2s-2\bar{p}-2\bar{p}-3\bar{d}$ . (a) and (b) curve A, 3 states coupling (repeated by ourselves).



Table 3. D wave  $e^+ - H$  phase shifts in various approximations

K	a	b	c	d	e
0.1	0.0012	0.0013	0.0009	0.0014	0.0013(0)†
0.2		0.0050	0.0038	0.0055	
0.3	0.01181	0.0109	0.0082	0.0123	0.014(1)
0.4		0.0175	0.0134	0.0215	
0.5	0.03134	0.0242	0.0186	0.0326	0.046(5)
0.6		0.0299	0.0231	0.0447	
0.7	0.05700	0.0337	0.0265	0.0578	0.1(1)

(a) Rigorous lower bound results of Kleinman *et al* (1965)

(b) Extended polarization (Callaway *et al* 1968)

(c) 6 state (1s-2s-2p-3s-3p-3d) close coupling (McEachran and Fraser 1965)

(d) 5 state (1s-2s-2p-2p-3d) pseudo-state results of present work

(e) Extrapolated values of Kleinman *et al* (1965)

† The numbers within the brackets are the uncertainty values of the last digits

## 2. Theory

Following Fon (1970), we discuss briefly the derivation of the scattering equations. All equations are written in the usual atomic units. The target proton is assumed infinitely heavy and fixed at the origin and we denote the position vectors of the positron and bound electron respectively by  $x$  and  $r$  relative to it. Our total wavefunction  $\Psi(r, x)$  satisfies the nonrelativistic Schrödinger equation

$$\left( -\frac{1}{2}\nabla_{r^2} - \frac{1}{2}\nabla_{x^2} - \frac{1}{r} + \frac{1}{x} - \frac{1}{|r-x|} - E \right) \Psi(r, x) = 0 \quad (1)$$

which we rewrite in the form

$$\left( \nabla_{r^2} + \nabla_{x^2} + \frac{2}{r} + \frac{2}{x} + k^2 + 2\epsilon_0 \right) \Psi(r, x) = -\frac{2}{|r-x|} \Psi(r, x) \quad (2)$$

where

$$E = \frac{k^2}{2} + \epsilon_0 \quad (3)$$

is the total energy,  $\epsilon_0$  being the ground state eigenenergy of hydrogen and  $k^2/2$  the incident kinetic energy of the positron.

In the interests of simplicity and succinctness of notation we represent the channel quantum numbers  $(nl_1l_2)$  and  $(n'l_1'l_2')$  by  $v$  and  $v'$  respectively. By expanding  $\Psi(r, x)$  on the left hand side of (2) in a complete discrete orthonormal set as

$$\Psi(r, x) = \sum_v \Phi_v(r, \hat{x}) \frac{F_v(x)}{x} \quad (4)$$

with

$$\Phi_v(r, \hat{x}) = \frac{S_{nl_1}(r)}{r} Y_{l_1l_2}^{LM}(\hat{r}, \hat{x}) \quad (5)$$

Numerous previous calculations of this process exist so that we have, in an endeavour to be fairly comprehensive, displayed the results graphically and also in tabular form, including representative values on the curves of figures 1 and 2 and a fuller set in tables 1, 2 and 3. These calculations embody a variety of approximations. For  $L = 0$  we regard the recent rigorous lower bound calculation of Bhatia *et al* (1971) as definitive, superseding the earlier long standing result of Schwartz (1961). For  $L = 1$  the variational result of Armstead (1968) is likewise regarded as definitive.

We note with encouragement that our purely long range results do not suffer too greatly by contrast to these other calculations. All of our results provide lower bounds to the true phase shifts and as the value of  $L$  increases the  $\eta_L$  improve accordingly. This is simply a reflection of the fact that the calculation incorporates the correct long range dipole polarization potential and the resulting phase shifts for sufficiently large  $L$  will follow the effective range formula of O'Malley *et al* (1962)

$$k^2 \cot \eta_L = \frac{8(L+3/2)(L+1/2)(L-1/2)}{\pi\alpha} + \text{higher order terms} \quad (10)$$

which should be substantially exact for larger  $L$  values ( $L \geq 3$ ).

For smaller values of  $L$  as in the case of  $L = 1$ , our best (1s-2s-2p-2p-3d) phase shifts, though a long way from the exact values, however, agree reasonably well with the rigorous lower bounds of Drachman (1968) and the adiabatic (monopole ~~and~~ <sup>plus</sup> dipole ~~and~~ quadrupole) results of Bransden and Jundi (1966). Both of these calculations are long range oriented models.

In the case of S-wave phase shifts, our best calculations are poor compared with those of Bhatia *et al* (1971). However, it is instructive to compare our results with the dipole polarization potential results of Cody *et al* (1964) as is shown in figure 1(a). It is to be noted that these two sets of results tend to coincide with each other. We observe with satisfaction that for low energies, the long range forces are predominantly of dipole polarization nature and that inclusion of long range forces by the pseudo-state expansion is essentially adequate.

The poorness of our results for small values of  $L$  can only suggest that long range forces alone cannot give us the desired goal and short range attractive forces are needed to bring us up to the exact results. Physically, we visualize the collision between a slow positron and a hydrogen atom as follows. For low energies the incident positron at larger distances experiences firstly an attractive force due to the long range polarization potential; as it speeds up and approaches the atom it then (in a simplified picture) encounters the repulsive static potential. These attractive and repulsive forces will now compete and an equilibrium will tend to result describable in the language of 'virtual positronium formation'. The impact of this situation is most strongly reflected in the case of a head on (S-wave) collision between  $e^+$  and H.

In conclusion if we can make up for the loss of short range attractive forces while taking care of the long range forces by the pseudo-state expansion, our model may well prove to be a systematic way to attack positron-atom scattering problems.

#### Acknowledgments

We are deeply indebted to Professor P G Burke for his generosity in making available to us his electron scattering close-coupling code and to Professors P A Fraser and R J Drachman for many helpful and instructive discussions.

130,1

*Positron-hydrogen elastic scattering*

*Positron-hydrogen elastic scattering*

*Positron-hydrogen elastic scattering*

*W C Fon and D F Gallaher*

*W C Fon and D F Gallaher*

*W C Fon and D F Gallaher*

2 DEC: 1971

20P

2024/10/18

1 XXX

2 X

3 X

4 X

5 X

6 X

7 X

8 X

9 X

10 X

11 X

12 X

13 X

14 X

15 X

16 X

17 X

18 X

19 X

20 X

21 X

22 X

23 X

24 X

25 X

26 X

27 **I. Introduction**

28 X

29 X One of the primary problems we have in electron scattering is to test the

30 effects of the electron exchange force between the bombarding electrons and

31 the electrons in the target atom or molecule, since these electrons are com-

32 pletely indistinguishable. One way to eliminate the problem is to replace one

33 electron with an anti-electron, i.e. a positron. This is perhaps most meaningful

34 in the elastic-scattering region, below the onset of any inelastic processes.

35 However, even this study is somewhat complicated theoretically by the fact

36 that the mean static interaction of an atom with a positron is repulsive while

37 the long-range polarization is attractive so that the two effects oppose rather

38 than combine as in the case of electron scattering. Furthermore, we do not

39 yet know if ( $e^-e^+$ ) pair annihilation has a direct effect upon scattering cross-

40 sections. Although we have eliminated exchange, at higher scattering energies

**POSITRON EXPERIMENTS TODAY:  
SCATTERING FROM HELIUM**

J. William McGOWAN

*Department of Physics, University of Western  
Ontario, London, Canada*

Considerable sophistication has developed in instrumentation asso-  
ciated with the swarm techniques which permit studies of the annihilation  
of a free positron with a bound electron, ortho-positronium quenching,  
measurements of the cross-sections for total momentum transfer at ener-  
gies well below the positronium-formation threshold, measurements of  
 $Z_{eff}$ , and so on. However, swarm techniques become less effective as the  
velocity of the colliding positron approaches that for the formation of pos-  
itronium.

Recently, it has been shown that a source of positrons can be fabricated  
which gives a narrow energy distribution [FWHM = 1.0 eV]. As a result,  
complimentary beam experiments can be attempted. In this progress report  
( $e^+, He$ ) scattering experiments and -results are reviewed as an example of  
work possible using both swarm- and beam techniques.

**I. Introduction**

One of the primary problems we have in electron scattering is to test the  
effects of the electron exchange force between the bombarding electrons and  
the electrons in the target atom or molecule, since these electrons are com-  
pletely indistinguishable. One way to eliminate the problem is to replace one  
electron with an anti-electron, i.e. a positron. This is perhaps most meaningful  
in the elastic-scattering region, below the onset of any inelastic processes.  
However, even this study is somewhat complicated theoretically by the fact  
that the mean static interaction of an atom with a positron is repulsive while  
the long-range polarization is attractive so that the two effects oppose rather  
than combine as in the case of electron scattering. Furthermore, we do not  
yet know if ( $e^-e^+$ ) pair annihilation has a direct effect upon scattering cross-  
sections. Although we have eliminated exchange, at higher scattering energies

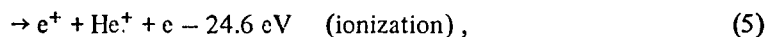
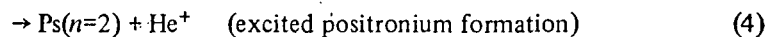
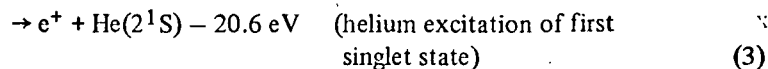
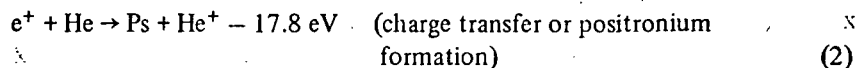
there are the unique problems of positronium formation both in the ground- and excited state, and the formation of compound states which must be added to those of excitation and ionization of the target atom or -molecule.

Theoretically, the most tractable system is  $(e^+, H)$  [1]; experimentally,  $(e^+, Ar)$  has proven more manageable [2,3]. For the moment,  $(e^+, He)$  has become the compromise system for which considerable theory [1] and complementary experimental data are now available. It is this system which will receive the most detailed review in this report. Limited work has been reported on positron collisions with neon, krypton, xenon, nitrogen, hydrogen and a large number of organic and inorganic compounds. See refs. [3-9] for an introduction to this work.

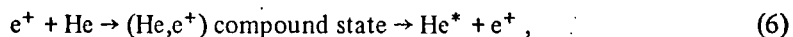
Essentially, two types of experiments have been carried out. The first type includes variations on swarm experiments which the atomic-scattering community readily associates with electron scattering. The second type is a beam experiment involving the collision of energy-resolved positrons with a gas target. This is a new method, and while only one experiment is as yet reported, several others will be reported soon. Clearly, in the future, there will be many more swarm- and complementary beam experiments covering energies from the elastic-scattering region, i.e.,



through the onsets of the inelastic channels (cf. fig. 1):



possibly:



and so on. Competing with all of these processes is the direct annihilation of the positron with the bound electron in the atom,

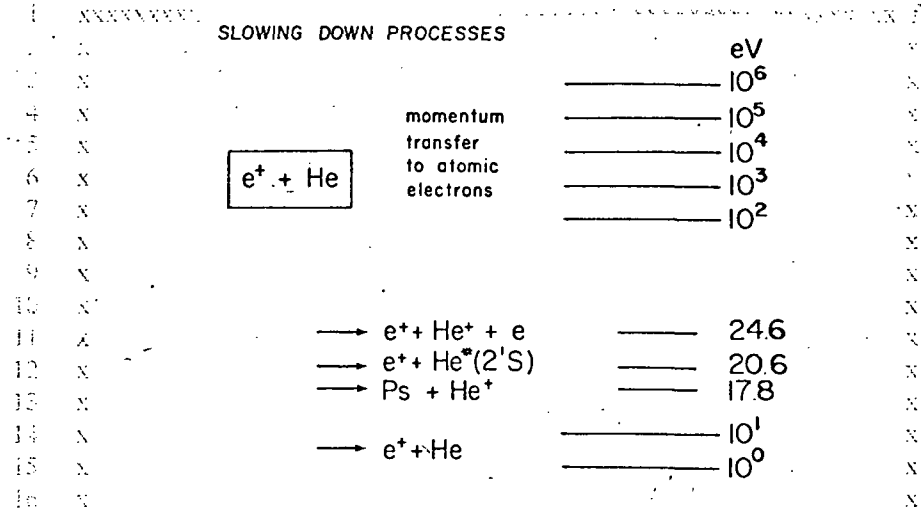


Fig. 1. Slowing down processes for positrons in helium gas, the energy ranges over which they apply, and the threshold energies for the processes involved.

$$e^+ + He \rightarrow \text{gamma rays} + He^+ \quad (7)$$

2. Swarm experiments

Conceptually, the electron- and positron swarm experiments are similar, but as you will see, in many ways the positron swarm studies are much richer. One may introduce a pulse of electrons into the typical gas-filled electron drift tube [10] at  $t = 0$  by flashing a photo-cathode or otherwise gating an electron source. One then measures the time  $t$  it takes for the electrons to traverse the gas cell, as a function of gas pressure,  $p$ , and axial electric field,  $E$ . In these experiments the drift velocity is proportional to  $E/p$ . Normally the pressure range studied is  $0.1 \leq p \leq 20$  Torr.

In order to determine the total momentum-transfer cross-section,  $\sigma_{TMT}$ , it is necessary to solve the diffusion equation,

$$\partial f(v)/\partial t = F[\sigma_{TMT}, v, f(v)] \quad (8)$$

where  $F$  refers to a complicated functional dependence, in order to determine the electron-velocity (energy) distribution function  $f(v)$  and derive  $\sigma_{TMT}$

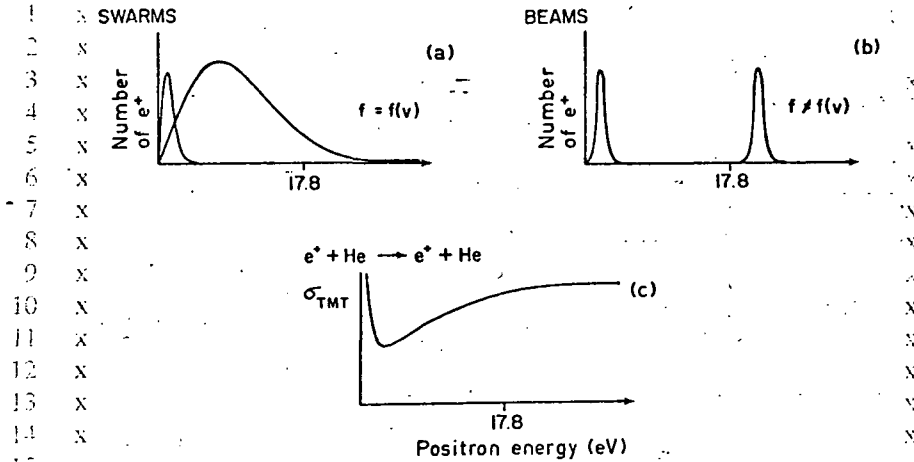


Fig. 2. Representative changes in energy (velocity) distributions of positrons as a function of the mean energy of the positrons (a) for swarms (b) for beams. In both cases, a low and high energy case is shown. The predicted shape of the  $(e^+, \text{He})$  total momentum-transfer cross section through the Ramsauer-like dip is given in (c).

from the analysis. At low mean velocities,  $f(v)$  is very narrow. As the electron velocity is increased through an increase of  $E/p$  or of gas temperature,  $f(v)$  broadens rapidly [10]. This behavior, shown schematically in fig. 2, represents one of the prime characteristics of a swarm experiment.

A variation on this type of experiment allows the study of the formation and destruction of  $(X, e^-)$  complexes as a function of  $E/p$  and  $p$  [11]. In these cases, the negative ions  $X^-$  are usually detected by means of a mass spectrometer and a gating system which enables an experimentalist to measure accurately the number of ions present and their velocity distribution after a given period of time,  $t$ .

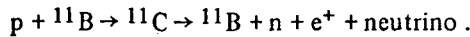
With positrons the situation is similar in that there is a drift tube with an axial electric field  $E$ , but normally the pressure range covered is much higher,  $1 \leq p \leq 100$  atm. (Note: the unit used in positron drift experiments is the amagat — 1 amagat = 1 mol/22.4 litre =  $4.46 \times 10^{-5}$  mol/cm<sup>3</sup>.) But unlike the electron-swarm case, positrons do not come from sources which have a reasonably narrow energy distribution or are convenient for drift studies as far as their half-life is concerned (cf. table 1). Normally, they are obtained from either long-lived natural radioactive sources like <sup>22</sup>Na, <sup>64</sup>Cu, <sup>58</sup>Co, or short-lived machine-made sources like <sup>11</sup>C, which has a 22.5 min natural lifetime toward  $\beta^+$  decay, or from the conversion of bremsstrahlung into a  $(e^+, e^-)$

Table 1  
Characteristics of positron sources

Source	Half life	Percent $\beta^+$ decay	Method of production
$^{11}\text{C}$	20.5 min	100	$^{11}\text{B}(p,n)^{11}\text{C}$ , $^{12}\text{C}(\gamma,n)^{11}\text{C}$
$^{22}\text{Na}$	2.6 yr	89	$^{27}\text{Al}(^3\text{He},2\alpha)^{22}\text{Na}$
$^{55}\text{Co}$	18.2 hr	60	$^{58}\text{Ni}(p,\alpha)^{55}\text{Co}$ , $^{56}\text{Fe}(p,2n)^{55}\text{Co}$
$^{57}\text{Ni}$	36.0 hr	50	$^{56}\text{Fe}(^3\text{He},2n)^{57}\text{Ni}$
$^{58}\text{Co}$	71.3 days	15	$^{58}\text{Ni}(n,p)^{58}\text{Co}$ , $^{55}\text{Mn}(\alpha,n)^{58}\text{Co}$
$^{64}\text{Cu}$	12.7 hr	19	$^{63}\text{Cu}(n,\gamma)^{64}\text{Cu}$
$^{68}\text{Ge-Ga}$	280 days	85	
$^{90}\text{Nb}$	14.7 hr	54	$^{90}\text{Zr}(pn)^{90}\text{Nb}$ , $^{90}\text{Zr}(d,2n)^{90}\text{Nb}$

$\alpha, n$

pair. The source of the radiation may be a LINAC or an electron Van de Graaff. To-date and to my knowledge, no bremsstrahlung source has been used in swarm studies. Shortly, other accelerator sources may be available such as that proposed for Wayne State University, where proton bombardment of  $^{11}\text{B}$  will produce  $e^+$  through the sequence



From radioactive sources, let's say  $^{22}\text{Na}$  for example, the energy distribution of  $e^+$ 's is typically broad (FWHM > 0.1 MeV) with a maximum energy of 0.54 MeV, a peak intensity near 0.17 MeV and a spectrum which reaches down to very low energies. In other words, most positrons are produced with energies much in excess of those needed to study low-energy elastic and inelastic processes. As a consequence, the high pressures referred to above are first needed to moderate the positron energy.

The action of thermalizing high-energy positrons (fig. 1) requires many collisions. From the MeV to keV range, slowing down is essentially described by the Spencer-Fano [12] theory of momentum-sharing between the positron and atomic electrons. Below this, the various inelastic channels summarized by eqs. (3) and (5), and perhaps (6), take over. Notice in fig. 1 that elastic scattering is neatly separated from the positronium-formation threshold and that there is 2.8 eV between the positronium-formation threshold and the first allowed transition. (Note: the  $2^3\text{S}$  state cannot be excited readily, since there is no electron exchange possible). In cases like  $(e^+, \text{Li})$  the positronium formation threshold is at 0 eV. For  $(e^+, \text{He})$  below 17.8 eV,



positrons can only slow down through momentum-transfer collisions. Once thermalized in dense gaseous targets in a time  $\leq 10^{-10}$ s, the positron can be accelerated in the field  $E$  in a gas chamber at pressure  $p$ , and the lifetime  $\lambda$  of the free positron can be measured readily.

One danger with high pressures is that a large variety of processes that have a second- or perhaps even higher-order dependence on gas pressure, may occur. The list of second-order processes known already includes the quenching of excited positronium states due to electron-exchange collisions,  $(X, e^+)$ , compound state formation- and destruction, etc.

The usual positron swarm experiment calls for the measurement of the  $e^+$  destruction or annihilation rate as a function of  $E/p$ ,  $p$ , impurity content, etc. If a  $^{22}\text{Na}$  positron source is used, accompanying the birth of each positron and delayed by only  $10^{-12}$ s is a 1.28 MeV gamma-ray coming from the de-excitation of the excited  $^{22}\text{Ne}$  which is formed during the  $\beta^+$  decay process, cf. fig. 3.

*Stable P  
as in E/p*

Also shown in fig. 3 is a very rough schematic diagram of the typical swarm apparatus. Counter #1 is tuned to the 1.28 MeV gammas. When one is detected,  $t = 0$  is set in the time-to-amplitude converter. A time  $t$  later, counter #2 detects a 0.51 MeV gamma-ray associated with the annihilation of the positron in the gas. Nearly all the useful data are drawn from the analysis of the resulting lifetime spectrum.

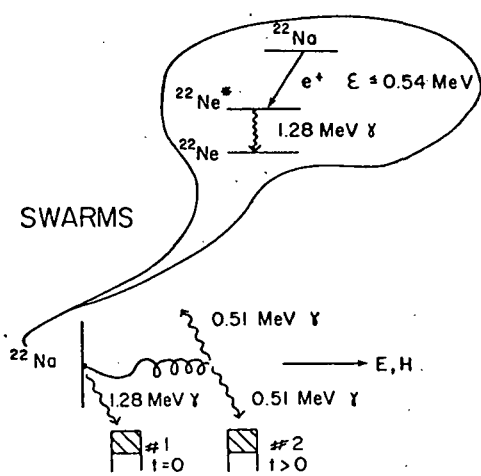


Fig. 3. A schematic representation of a swarm apparatus in which a  $^{22}\text{Na}$  positron emitter is used. In the balloon, the decay scheme for  $^{22}\text{Na}$  is given.

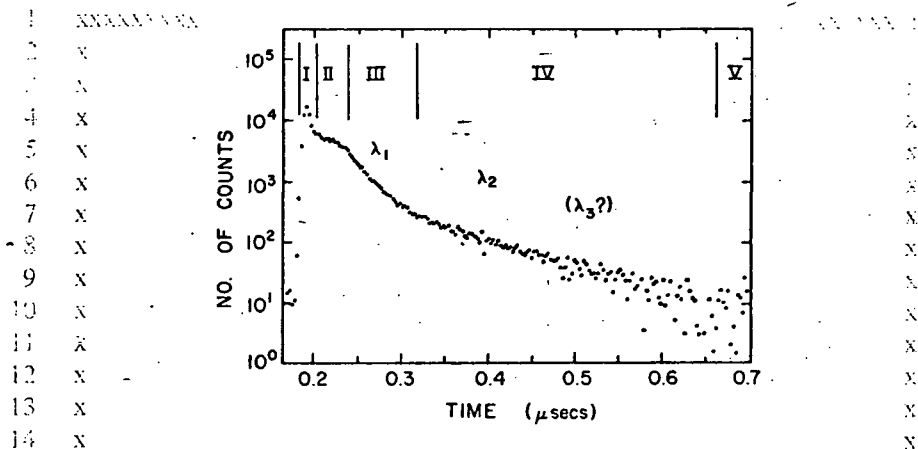


Fig. 4. A representative time spectrum for positron annihilation in argon for  $E/p = 0$  and  $p = 8.9$  amagat. I, prompt peak; II, shoulder region which is sensitive to  $E/p$ ; III, annihilation of the free positron with atomic electrons; the apparent annihilation rate is a function of  $E/p$  and gas temperature; IV, annihilation of  $1^3S$  state of o-Ps; slope is a function of  $p$ ; V, background of random coincidences.

In fig. 4, I show a typical lifetime spectrum for  $(e^+, Ar)$ . I chose this instead of the  $(e^+, He)$  system because the usually recognizable features are more pronounced. These features include:

Region I: A prompt peak at  $t = 0$  which includes a) annihilations in the source, b) annihilations of fast positrons in the process of being slowed down by collisions with gas atoms, c) unresolved two-gamma annihilations of para-positronium with electron- and positron spins anti-parallel, lifetime  $t_p \approx 1.25 \times 10^{-10}$  s, and, d) possible annihilation of  $(Ar, e^+)$  complexes.

Region II: A broad shoulder which is sensitive to  $E/p$  and which reflects the  $\sigma_{TMT}$  cross-section and the Ps formation cross-section.

Region III: An exponential decaying section which is attributed to annihilation of the free positron in flight through the gas cell. The apparent decay rate (reflected in the slope of the exponential) is found to be both a function of  $E/p$  and of the gas temperature.

Region IV: An exponential decay attributed to the annihilation of the  $1^3S$  state of Ps. Angular momentum considerations indicate that this is three-gamma decay. The decay rate is pressure dependent and is thought to reflect the quenching of ortho-positronium primarily through electron exchange  $(o-Ps) + Ar \rightarrow (p-Ps) + Ar^*$ .

Region V: A background due to random coincidences of counts in counter #1 and counter #2.

It is generally felt that the time spectrum associated with regions III, IV, and V can be fitted with a curve of the form  $n = n_{10} \exp(-\lambda_1 t) + n_{20} \exp(-\lambda_2 t) + b$ , where  $n_{10}$  is the amplitude of free component extrapolated to  $t = 0$ ;  $n_{20}$  is the amplitude of o-Ps extrapolated to  $t = 0$ ; and  $b$  is the constant background.

From the exponential portion III associated with the annihilation of the free positron, if the spins of the free positron and the bound electron which make up the annihilation pair are antiparallel, the free-singlet annihilation rate  $\lambda_1$  is shown to be:

$$\lambda_1 = 4.51 \times 10^9 (\rho/M_A) Z_{\text{eff}} (\text{s}^{-1}), \quad (9)$$

where  $Z_{\text{eff}}$  is the effective number of annihilation electrons available in the atom (or molecule) of molecular weight (mass units)  $M_A$ . As expected, the probability that the electron and positron are at the same point in the atom is zero when the gas pressure or density  $\rho$  is zero, cf. refs. [2,6,13-18]. The results of various experiments for  $e^+$  in helium are summarized in table 2. As too often is the case, the uncertainties associated with each experiment are sometimes smaller than the variation between the different measurements. This probably reflects a systematic error associated with impurities in the gaseous targets which, through much effort, has been minimized in the most recent investigations, which tend to agree.

It was not realized in earlier experiments in argon, as well as in helium, that a shoulder was present (region II of fig. 4) in the time spectrum, so sufficient care may not have been taken to account for the non-exponential character of the curve in this region.

An unweighted average of the three most recent measured values [16-18] of  $Z_{\text{eff}}$  for helium at room temperature gives  $Z_{\text{eff}} = 3.7 \pm 0.1$ , in excellent agreement with the variational calculation of Drachman [23], but in poorer agreement with the most recent calculations by Houston and Drachman [27] based upon the Harris method. A similar analysis of the last three measurements for argon [2c,d,e] gives  $Z_{\text{eff}} = 26.4 \pm 0.5$ . As the energy of the positron is increased, the value of  $Z_{\text{eff}}$  must approach the number of electrons in the atom.

Calculated values of  $Z_{\text{eff}}$  are very sensitive to the theoretical model used, therefore a comparison of measured and calculated values of  $Z_{\text{eff}}$  is a good test of the theory. It has been demonstrated both theoretically and experimentally that  $Z_{\text{eff}}$  is a decreasing function of  $E/p$ . Lee et al. [28] and Leung

Table 2

Experimental and theoretical ( $e^+$ ,He) scattering cross sections.  $\sigma_{TMT}$  is the total momentum-transfer cross-section and  $\sigma_{TS}$  the total scattering cross-section; both are indicated in units of  $\pi a_0^2$ . The data are from the references indicated in the corresponding column.

Energy (eV)	Experimental					Theoretical $\sigma_{TS}$		
	$\sigma_{TMT}$		$\sigma_{TS}$			[23,24]	[25]	[26]
	[4,5]	[19]	[17]	[20,21]	[22]			
Thermal			1.05					
2			0.10		0.17		0.17	0.28
4			0.13		$\pm 0.06$		0.12	0.30
10			0.20		$\pm 0.06$		0.14	0.36
14			0.22			0.36	0.16	0.37
16.5	0.023	0.26	0.22	0.35	$\pm 0.04$	0.17	0.42	0.36
	$\pm 0.006$	$\pm 0.03$		$\pm 0.04$	$\pm 0.04$		Upper limit	
19.3				0.60			s,p,d-wave	1.94
				$\pm 0.16$				
21.3				1.0				2.22
				$\pm 0.15$				
26.1				1.24				2.2
				$\pm 0.27$				

*$\sigma$ 's larger as in text*

and Paul [17] have shown that  $Z_{\text{eff}}$  falls more than 10% as the average energy of the positrons is increased to 1 eV. In the case of argon it has further been shown [2f] that  $Z_{\text{eff}}$  is a function of the gas temperature in a way which suggests that the dependence is similar to that found when  $E/p$  is varied.

One may also derive from a measurement of  $\lambda_1$  an annihilation cross-section per atom:

$$\sigma_a = (c/(137)^2 v) Z_{\text{eff}} \pi a_0^2, \quad (10)$$

where  $c$  is the velocity of light. This cross-section is seen to be small even for positrons in equilibrium with liquid He. Near 4K,  $\sigma_a \approx 5\pi a_0^2$ .

Measurements of  $\lambda_2$ , the ortho-positronium quenching rate associated with the portion of the time spectrum labelled IV, are a function of the pressure  $p$  as one would expect. Upon extrapolation to  $p = 0$  one obtains values which

are reasonably consistent from one experiment to another:  $\lambda_2 \cong 7.5 \mu\text{s}^{-1}$ . There is an exciting group of studies on o-Ps formation in high-density He gas and in liquid He, associated with what is called bubble formation. For an excellent introduction to the literature of this field refer to the 1968 review by Fraser [29].

There has been some suggestion by Leung and Paul [17] that region IV of the time spectrum may contain a third exponential term with a deactivation rate  $\lambda_3$  associated perhaps with the quenching of the long-lived 2s state of ortho-positronium. This is an interesting possibility but, as the authors point out, highly speculative.

What is known of  $\sigma_{\text{TMT}}$  in the region below the threshold of positronium formation, i.e. below 17.8 eV for the  $(e^+, \text{He})$  system, comes from the solution of the diffusion equation (cf. ref. [17] for example),

$$\frac{\partial f(v,t)}{\partial t} = \frac{1}{v^2} \frac{\partial}{\partial v} \left[ \alpha(v, \sigma_{\text{TMT}}) \frac{\partial f(v,t)}{\partial v} + \beta(v, \sigma_{\text{TMT}}) f(v,t) \right] - [r_a(v) + r_f(v)] f(v,t),$$

through regions II and III of the lifetime spectrum. Here the mean velocity  $v$  is proportional to  $E/p$ ,  $\alpha$  and  $\beta$  are complex functions of  $v$  and the total momentum transfer cross-section  $\sigma_{\text{TMT}}$ ,  $r_a$  and  $r_f$  are the rates of positronium annihilation and formation which are zero for  $v \ll \bar{v}$ , the threshold velocity for positronium formation.

The values of  $\sigma_{\text{TMT}}$  derived from an analysis of the diffusion equation for higher velocities are very model-dependent. However, a detailed knowledge of the general shape of the cross-section curve and its approximate magnitude make possible a computer fit of the diffusion equation to the time spectrum. This has effectively been done by Leung and Paul [17] for helium, while Orth and Jones [2d] have analytically been able to derive the distribution function  $f(v)$  as a function of  $E/p$  for argon. Leung and Paul used several models. Their final results closely parallel but exceed the theoretical results of Drachman [23] through most of the energy interval from the thermal region to the positronium-formation threshold.

In table 2, I have listed the available experimental cross-sections available for total momentum transfer,  $\sigma_{\text{TMT}}$ , and for total scattering,  $\sigma_{\text{TS}}$ , related through the differential elastic scattering cross-section,  $\sigma(\theta)$ , in the following way:

$$\sigma_{\text{TS}} = 2\pi \int \sigma(\theta) \sin \theta \, d\theta \quad (11)$$

and

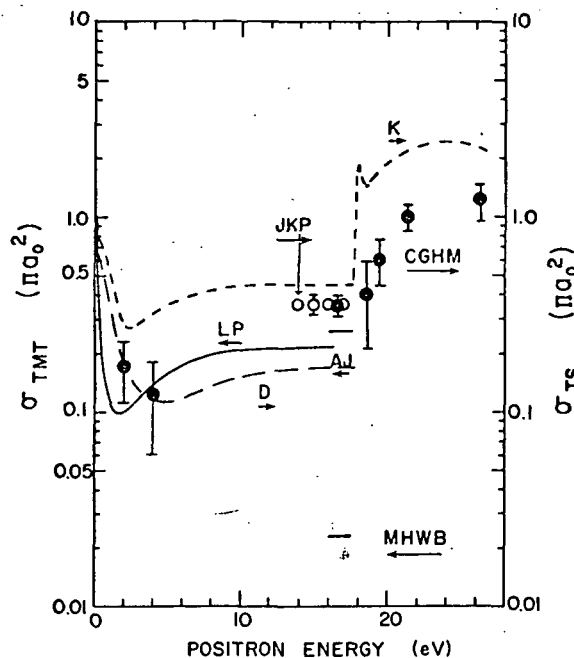


Fig. 5. Measured values of  $\sigma_{TMT}$  where MHWB [4] and AJ [19] are data from similar swarm experiments. In both instances the gray area is an indication of the uncertainty. The  $\sigma_{TMT}$  swarm data by LP [17] are also given. Measured values of  $\sigma_{TS}$  by CGHM [20,21] (closed circles) and JKP [22] (open circles) are shown in comparison with two very different theoretical results D [23,24] and K [26].

$$\sigma_{TMT} = 2\pi \int \sigma(\theta) (1 - \cos\theta) \sin\theta \, d\theta. \quad (12)$$

In fig. 5, I have plotted the experimental and some theoretical values of  $\sigma_{TMT}$  and  $\sigma_{TS}$ . Note that the first data reported by Marder et al. [4], based on the analysis of Teutsch and Hughes [5], are more than an order of magnitude below theory and recent experiments at the positronium formation threshold. This was a dilemma for many years. As time has passed, measured values have increased, in fact theory and experiment are converging rapidly in the elastic-scattering region [30].

It is not at all surprising that there has been difficulty in obtaining good values of  $\sigma_{TMT}$  just below the positronium threshold, since in the analysis of

1 the diffusion equation one assumes that positronium formation and destruc-  
 2 tion are negligible, thus restricting one to choose mean velocities correspond-  
 3 ing to  $\approx 5$  eV, far removed from 17.8 eV. The number of positrons in the  
 4 high energy tail of the distribution is small so that the solution of the diffu-  
 5 sion equation must be relatively insensitive to the choice of  $\sigma_{TMT}$  at higher  
 6 energies.

7 x The strength of the swarm technique lies in the determination of cross-  
 8 sections as a function of  $E/p$  at low energies. In these cases the energy distri-  
 9 bution is narrow, the approximation that positronium production and loss ~~is~~ *are*  
 10 negligible is strictly adhered to, and virtual positronium most likely makes ~~as~~ *an*  
 11 insignificant contribution. As I will report below, it appears that both virtual  
 12 positronium- and positronium formation make a large contribution to total  
 13 scattering cross-sections at higher energies.

14 x For ( $e^+$ ,Ar), it is clear from the data of Jones and his collaborators, and of  
 15 Paul et al., that the variation of the shoulder width with  $E/p$  is consistent with  
 16 a  $\sigma_{TMT}$  function which is somewhat similar in shape to that found for elec-  
 17 tron-inert gas scattering i.e., it shows a Ramsauer character, with a minimum  
 18 in the cross-section at low energies.

19 x Nearly all investigators of the ( $e^+$ ,He) system have remarked on the ex-  
 20 treme effect of impurities on their measurements of  $\sigma_{TMT}$ ,  $Z_{eff}$ , o-Ps lifetime  
 21 and shoulder width. It was also clear in the one beam experiment reported by  
 22 Costello et al. [20,21] that  $\sigma_{TS}$  was very sensitive to impurities.

23 x

24 x

### 25 3. Beam experiments

26 x

27 x For the purpose of this progress report, I have chosen as the primary charac-  
 28 teristic of beam experiments that the electron- or positron velocity distribution  
 29 function,  $f(v)$ , is not a strong function of the energy of interaction of the  
 30 projectile and target (cf. fig. 2). Furthermore, one normally considers the gas  
 31 targets to be thin so that multiple scattering is not a problem.

32 x In principle, electron- and positron beam experiments are the same; the  
 33 largest difference lies in the electron- and positron sources. Relatively large  
 34 numbers of electrons of reasonable energy spread are readily available, where-  
 35 as positrons in small numbers come with an enormous energy spread. In 1958  
 36 W.H.Cherry [31] reported in his thesis that positrons from  $^{22}\text{Na}$ , when  
 37 moderated by mica with a thin layer of chromium, gave an apparently narrow  
 38 peak of positrons with energies less than 5 eV which could serve as an excel-  
 39 lent source of positrons for beam studies (cf. fig. 6). This lay domant until *dormant*  
 40 Groce et al. [21,32] re-discovered the effect for a number of moderating sys-

1  
2  
3  
4  
5  
6  
7  
8  
9  
10  
11  
12  
13  
14  
15  
16  
17  
18  
19  
20  
21  
22  
23  
24  
25  
26  
27  
28  
29  
30  
31  
32  
33  
34  
35  
36  
37  
38  
39  
40

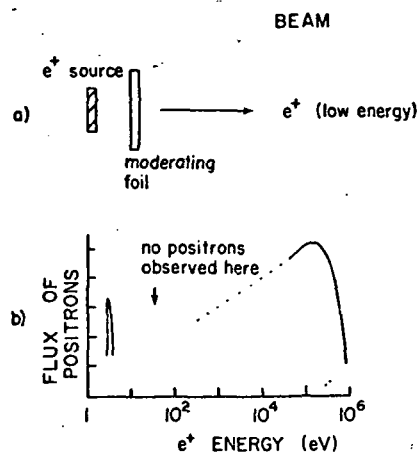


Fig. 6. a) Schematic representation of  $e^+$  source and moderator. b) Characteristic representation of positrons coming through a moderator.

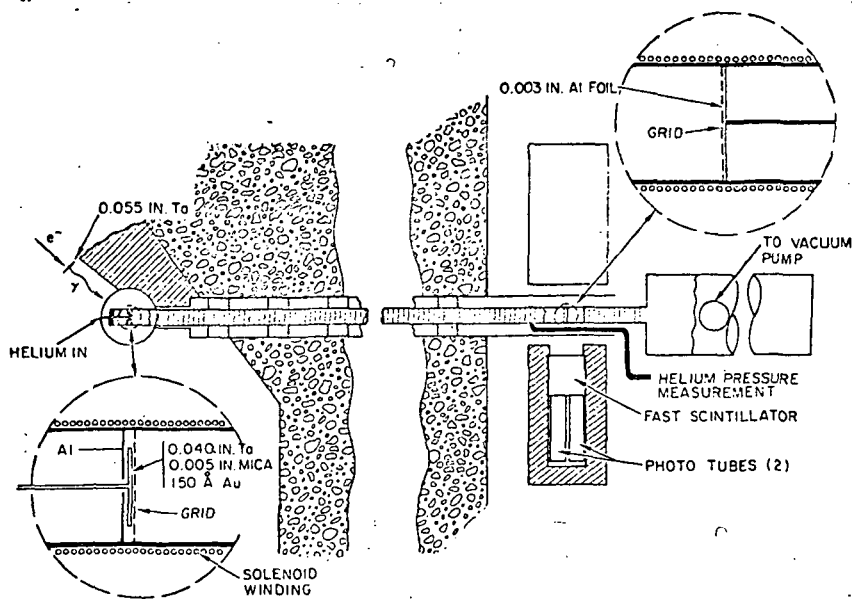


Fig. 7. Time-of-flight apparatus used in the General Atomic beam experiment, showing the time of flight spectrometer (collision chamber), details of the  $e^+$  source and moderator, and details of the annihilation foil.



Table 3

Systems used to moderate positrons in beam experiments. a) A negative value corresponds to a positron coming from the surface with energy; b) The accuracy of this measurement is small due to experimental factors; however, the higher value may reflect the CsBr-substrate since the gold-foil is thin.

Material	Values of negative work function <sup>a</sup>		
	Experimental (eV)	Theoretical (eV)	Refs.
Gold	-	-2.26	[33]
Mica (150 Å) gold	$-0.75 \pm 0.5$	-	[32]
( $\geq 1000$ Å) gold	$< 0$	-	[22]
CsBr (150 Å) gold	$-2.90 \pm 1.0^b$	-	[32]
Al (200 Å) gold	$-1.25 \pm 0.5$	-	[32]
Mica-chromium	$> -5$	-	[31]
Polyethylene	-20.7	-	[34]
Graphite	$\sim -1.5$	-	[22]
Cu	-	-3.1	[33]

tems where the source of positrons was pair production with a 35 MeV LINAC as the source of bremsstrahlung (cf. fig. 7).

In table 3, I have listed all systems thus far studied. Also given are values of the peak energies of the positrons emitted from the surfaces plus some calculated values [33]. In the experiments of Costello et al. [32], no positrons could be found with energies in the interval 2–100 eV. The above findings have now been verified by the group at the University of Toronto [22] who have used gold-covered mica as the moderator of  $^{22}\text{Na}$  positrons. Along with Tong [33] who has done the only theory, Groce et al. [21,32] have described the phenomenon as the "negative work function".

Now we have a narrow energy-band of low-energy positrons, but only a few of them. Approximately one out of every  $10^7$  positrons born in the source survive the trip through the moderator sandwich and emerge in the low-energy bundle. These particles, because they are in a narrow-energy bundle, can be biased to whatever energy is desired. The full width at half maximum is  $\approx 1$  eV, with the peak in the distribution coming between 0.5 and 5 eV (cf. ref. [32]). Laboratories at University College, London, University College, Swansea, University of Toronto, Wayne State University, and our own at the University of Western Ontario, are already designing, building

insert in paragraph:

The group at the University of Western Ontario has further demonstrated that not only the mica-gold moderator but gold and aluminum moderators work as well while the efficiency for copper now appears to be considerably worse.

1 and even operating scattering experiments dependent upon positron sources  
2 based upon the negative work function. As scattering experiments proceed,  
3 complementary experiments dealing with the yield from the moderator, the  
4 energy distribution of the positrons in the low-energy peak, the angular distri-  
5 bution of the emitted particles, and the effect of moderator temperature on  
6 the energy distribution of the emitted positrons, etc., are under way.

7 In the next few paragraphs, I have summarized some of the qualities of  
8 and problems associated with positron beam experiments:

9 I. Long-term stability. There is definite merit associated with the elimination  
10 of hot filaments from an electron scattering experiment, since filament  
11 stability is often a problem. However, one replaces the problems of short-  
12 term stability of electron emitters with problems of very long term stability  
13 of electronics, positron emitting surfaces, surfaces of lens elements, apparatus  
14 temperature and so on.

15 II. Detection of positrons. Because there are so few positrons, one would like  
16 to detect them with high efficiency. At first one imagines this <sup>is</sup> no problem  
17 because so much energy (1.02 MeV) is available for detection when a positron  
18 annihilates. But there are problems:

19 (a) Detection of annihilation  $\gamma$ -rays in coincidence [32]. To conserve mo-  
20 mentum, a ground-state para-positronium annihilates releasing two 0.51 MeV  
21  $\gamma$ -rays which, when identified and detected in coincidence, provide a flawless  
22 way to detect a positron. However, the efficiency is normally between 2 and  
23 10 percent because of geometric effects and the finite thickness of the scin-  
24 tillators. Furthermore, it is necessary to drive the low-energy positrons into a  
25 surface to overcome the negative work function and to minimize reflection  
26 which appears to be large. Two geometries have been used which preferentially  
27 detect low-energy positrons. In the first, an annihilation foil of aluminum is  
28 used with a thickness such that fast positrons pass through while low energy  
29 ones are stopped in it. In the second, a biased rod is used to attract low energy  
30 positrons while allowing higher energy particles to pass by.

31 (b) Well detector [35]. A higher-efficiency method of detection is the well of  
32 scintillant like NaI, where the total energy associated with the annihilation  
33  $\gamma$ -rays is absorbed in the scintillator. The original efficiency is good, and the  
34 discrimination against degraded or infested  $\gamma$ -rays is excellent because one can  
35 preferentially detect the 1.02 MeV peak. Well-type Ge(Li) detectors may be  
36 available in the near future.

37 (c) Electron multiplier. Pendyala et al. [36] have unsuccessfully tried to use  
38 the channel electron-multiplier to detect slow positrons. Furthermore, the  
39 CEM is extremely sensitive to  $\gamma$ -rays so that background is high. The reason  
40 why they have failed to observe low energy positrons may be explained by

Replace with → (c) Electron multiplier, Pendyala et al [36] have  
successfully used a channel electron-multiplier to detect  
slow positrons even though the CEM is sensitive to  $\gamma$ -rays.  
The use of the CEM apparently increases the detection  
efficiency by a factor of 10 to 20 over the detection of  
annihilation  $\gamma$ -rays in coincidence.

the results of Cherry [31] who showed that the secondary emission for keV positrons is less than half that of an electron with equivalent energy. This is unfortunate since the use of the CEM would increase the detection efficiency by a factor of 10 to 20.

III. Background. The gamma-ray background is one of the most serious problems in positron beam experiments. For long-lived sources, there are the gammas which come from annihilation in the source or from cascade or other decay modes in the source. In some machine sources, where time-of-flight energy analysis is used, there is the problem of gamma flash [21,32]. Finally, there is the problem of the reflection of positrons in the vacuum system with subsequent annihilation near the detector. Large distance from the source, sufficient lead shielding, care that positrons do not reflect freely throughout the system, will minimize background. In pulsed high-energy electron systems which produce short-lived sources like  $^{11}\text{C}$ , one can carry on the experiment in the time between pulses, thus eliminating the gamma flash [37].

Only ( $e^+$ , He) total scattering through the energy intervals 1–40 eV and 17–26 eV has thus far been measured by beam techniques. For this experiment, first reported by Groce et al. [21] and Costello et al. [20], a high current 55 MeV LINAC was used in the pulsed mode (20 ns) to produce bremsstrahlung which subsequently was used to produce ( $e^+$ ,  $e^-$ ) pairs in a 0.04 inch tantalum target (cf. fig. 7). As mentioned ~~early~~ <sup>earlier</sup> in this report, several moderators were used (cf. table 2), but for the final results a mica slab, 0.005 inches thick, with a 200 Å gold coating, was used. The bulk of the positrons which come from the moderator-gold sandwich have an energy near 1 eV which could be changed by biasing the moderator with respect to the 3 m long time-of-flight spectrometer which was filled with gas and used as the collision chamber. Extreme care had to be taken to assure the purity of the helium gas.

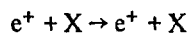
In the 17 to 16 eV energy interval, one obtains a spectrum simply and directly by measuring the attenuation of the positrons as a function of gas pressure. In the energy interval from 1 to 4 eV, a correction had to be made to allow for the trapping of particles in the axial magnetic field. As a result of the trapping, they reached the annihilation foil at longer times corresponding to lower energies. The ~~correction~~ <sup>(correction)</sup> was made by using the scattering phase shifts reported by Drachman [24]. With these phase shifts, Costello et al. [20,21] determined, as was suspected by Drachman, that the monopole term had to be completely suppressed. Further, it was demonstrated that Drachman's calculations of  $\sigma_{TS}$  at low energies are nearly correct, in agreement with the recent swarm measurements of  $\sigma_{TMT}$  reported by Leung and Paul [17]. The results are summarized in table 3 and fig. 5. At the positronium-

formation threshold, the Drachman calculations [23,24] are too low; however, when this p- and d partial waves are scaled to the known exact ( $e^+, H$ ) case, the agreement is excellent [38]. Above the positronium formation threshold at 17.8 eV, the cross section begins to rise and at 19.3 eV it is nearly a factor of two larger than that below 17.8 eV. At 26.1 eV it has increased by nearly a factor of four. This is generally in accord with the calculations of Kraidy [26] who has included the polarization of positronium by  $He^+$  as a primary factor in his model. The p-wave resonance predicted by Kraidy were not found perhaps because of the large energy intervals used in the experiment. The recent and as yet unpublished data of Jaduszliwer et al. [22] support these results. They are obtained with a mica-gold moderated  $^{22}Na$  source where the estimated low-energy positron yield was near  $3 \times 10^{-8}$  slow positrons per fast  $^{22}Na$  positron.

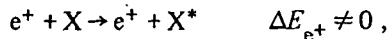
#### 4. Future of positron scattering

*Swarms.* The near future should bring a reduction of the background with an accompanying increase in the accuracy of low-energy measurements of  $\sigma_{TMT}$  and  $Z_{eff}$ . There should be an accompanying increase in the accuracy of o-Ps destruction measurements with a verification of the quenching of excited Ps. More sophisticated analytical and numerical techniques will also help. Better time resolution will allow studies of p-Ps formation and collisional destruction. Swarm experiments will make major contributions in Ps collision studies, a field which may not be studied by beams for many years.

*Beams.* Positron beam studies are in the era analogous to the nearly Ramsauer studies of total electron scattering, i.e., equivalent to the early thirties. One can predict that the next few years will herald the development of both short-lived artificial and long-lived natural sources, and a more ~~throughout~~ *through* understanding of positron energy moderation. With more efficient sources many atoms, X, and molecules, XY, will be studied. At first, total scattering measurements,



will be made through the onsets of inelastic thresholds. These, no doubt, will be accompanied by positron energy-loss studies,



1 differential scattering measurements,

2 X

3 X  $e^+ + X \rightarrow e^+(\theta) + X$ ,

4 X

5 ground state- and excited positronium formation studies,

6 X

7 X  $\rightarrow Ps^* + X^+$ ,

8 X

9 attachment processes analogous to dissociative electron attachment,

10 X

11 X  $e^+ + XY \rightarrow (e^+, X) + Y$ ,

12 X

13 annihilation,

14 X

15 X  $e^+ + X \rightarrow \text{gamma rays} + X^+$ ,

16 X

17 and so on.

18 X

19 All of the above beam- and swarm studies will give accurate information  
20 about target atoms and -molecules. In fact, with only a little imagination one  
21 can predict that  $e^+$  scattering will continue to develop as one of the basic  
22 atomic and molecular spectroscopies.

23 X

24 X

#### 25 Acknowledgements

26 X

27 This report and continuing studies at the University of Western Ontario ~~has~~ *have*  
28 been supported through the generosity of the University, NASA-Goddard  
29 grant NGR 42-029-006 and the National Research Council of Canada. My  
30 general appreciation goes out to the many people who have discussed prob-  
31 lems with me.

32 X

33 X

34 X

#### 35 References

- 36 [1] R.J.Drachman, *VII ICPEAC, Invited Talks and Progress Reports*, eds. T.R.Govers  
37 and F.J.de Heer (North-Holland Publ. Co., Amsterdam, 1972) p. 0  
38 [2] a) W.R.Falk, P.H.R.Orth and G.Jones, *Phys. Rev. Letters* 14 (1965) 447.  
39 b) D.A.L.Paul, *Proc. Phys. Soc.* 84 (1964) 563.  
40 c) S.J.Tao and J.Bell, *Positron Annihilation*, eds. A.T.Stewart and L.O.Roellig  
41 (Academic Press, New York, 1967) p. 393.  
42 d) P.H.R.Orth and G.Jones, *Phys. Rev.* 183 (1969) 7.

*North Holland  
to supply*

- e) S.J.Tao, Phys. Rev. A 1 (1970) 1257.  
 f) D.B.Miller, P.H.R.Orth and G.Jones, Phys. Letters 27 A (1968) 649.
- [3] H.S.W.Massey, J.Lawson and D.G.Thompson, *Quantum Theory of Atoms, Molecules and the Solid State*, ed. P.D.Lowdin (Academic Press, New York, 1966) p. 203.
- [4] S.Marder, V.W.Hughes, S.C.Wu and W.Bennett, Phys. Rev. 103 (1956) 1258.  
 [5] W.B.Teutsch and V.W.Hughes, Phys. Rev. 103 (1956) 1266.  
 [6] P.E.Osmon, Phys. Rev. 138 (1965) B216.  
 [7] P.E.Osmon, Phys. Rev. 140 (1965) A8.  
 [8] D.A.L.Paul and C.Y.Leung, Can. J. Phys. 46 (1968) 2779.  
 [9] S.J.Tao, Phys. Rev. A 2 (1970) 1669.  
 [10] J.L.Pack and A.V.Phelps, Phys. Rev. 121 (1961) 798.  
 [11] H.S.W.Massey, *Electronic and Ionic Impact Phenomena, Electron Collisions with Molecules and Photoionization*, Vol. 2, eds. H.S.W.Massey, E.H.S.Burhop and H.B.Gilbody (Oxford at the Clarendon Press, 1969).  
 [12] L.V.Spencer and U.Fano, Phys. Rev. 93 (1954) 1172.  
 [13] T.B.Daniel and R.Stump, Phys. Rev. 115 (1959) 1599.  
 [14] B.G.Duff and F.F.Heymann, Proc. Roy. Soc., Ser. A 270 (1962) 517.  
 [15] L.O.Roellig and T.M.Kelly, Phys. Rev. Letters 15 (1965) 746.  
 [16] V.I.Goldenskii and I.Levin, referred to in: B.G.Hogg, G.M.Laidlaw, V.I.Goldenskii and V.P.Shantarouich, Atomic Energy Review 6 (1968) 149.  
 [17] C.Y.Leung and D.A.L.Paul, J. Phys. B 2 (1969) 1278.  
 [18] S.J.Tao and T.M.Kelly, Phys. Rev. 185 (1969) 135.  
 [19] B.Albrecht and G.Jones, unpublished paper, presented at the *Second International Conference on Positron Annihilation*, Kingston, Canada, September 1971.  
 [20] D.G.Costello, D.E.Groce, D.F.Herring and J.Wm.McGowan, accepted for publication, Can. J. Phys. (1971).  
 [21] D.E.Groce, D.G.Costello, J.W.McGowan and D.F.Herring, Bull. Amer. Phys. Soc. 13 (1968) 1397; and *VIICPEAC, Abstracts of Papers*, ed. I.Amdur (MIT Press, Cambridge, Mass., 1969) p. 757.  
 [22] B.Y.Jaduszliwer, W.C.Keever and D.A.L.Paul, unpublished paper presented at the *Second International Conference on Positron Annihilation*, Kingston, Canada, September 1971.  
 [23] R.J.Drachman, Phys. Rev. 173 (1968) 190.  
 [24] R.J.Drachman, Phys. Rev. 144 (1966) 25.  
 [25] R.J.Drachman, private communication.  
 [26] M.Kraidy, Ph. D. Thesis, University of Western Ontario, London, Canada (1967).  
 [27] S.K.Houston and R.J.Drachman, Phys. Rev. A 3 (1971) 1335.  
 [28] G.F.Lee, P.H.R.Orth and G.Jones, Phys. Letters 28 A (1969) 674.  
 [29] P.A.Fraser, in: *Advances in Atomic and Molecular Physics*, eds. D.R.Bates and I.Estermann, Vol. 4 (Academic Press, New York, 1968) p. 63.  
 [30] In ref. [19], Albrecht and Jones reported the results of an experiment which duplicated that of Marder et al. [4], using the analysis of Teutsch and Hughes [5]. They find that the average value of  $\sigma_{TMT}$  up to the positronium-forbidden threshold is  $0.260 \pm 0.020 \pi a_0^2$  in excellent agreement with recent experiment and theory. They associate the earlier results with impurities in the helium gas.  
 [31] W.H.Cherry, Ph. D. Thesis, Princeton University, 1958.  
 [32] D.G.Costello, D.E.Groce, D.F.Herring and J.Wm.McGowan, ~~accepted for publication, Phys. Rev. (1971).~~ Phys. Rev. B 15 (1972) xxx

make  $\sigma$   
larger

1 [33] B.Y.Tong, ~~accepted for publication, Phys. Rev. (1971):~~ *Phys. Rev. B15 (1972) xxx*

2 [34] J.M.J.Madey, Phys. Rev. Letters 22 (1969) 784.

3 [35] J.H.Neiler and P.R.Bill, in: *Alpha-, Beta-, and Gamma-Ray Spectroscopy*, ed. K.

4 Siegbahn, Vol. 1 (North-Holland Publ. Co., Amsterdam, 1965) p. 262 (see es-

5 pecially section 3.2). Also a good summary is available in *Proceedings of the Total*

6 *Absorption Gamma-Ray Spectrometry Symposium*, Gatlinburg, Tennessee, May

7 10-11, 1960, U.S. AEC Office of Technical Information Report TID-7594.

8 [36] Pendyala, P.H.R.Orth, Zitzewitz and J.Wm.McGowan, unpublished.

9 [37] B.Y.Jaduszliwer, B.J.Bowden and D.A.L.Paul, Bull. Am. Phys. Soc. 15 (1970) 785.

10 [38] R.J.Drachman, submitted for publication. X

11 X X

12 X X

13 X X

14 X X

15 X X

16 X X

17 X X

18 X X

19 X X

20 X X

21 X X

22 X X

23 X X

24 X X

25 X X

26 X X

27 X X

28 X X

29 X X

30 X X

31 X X

32 X X

33 X X

34 X X

35 X X

36 X X

37 X X

38 X X

39 X X

40 X X

41 X X

42 X X

43 X X

44 X X

45 X X

46 X X

47 X X

48 X X

49 X X

50 X X

51 X X

52 X X

53 X X

54 X X

55 X X

56 X X

57 X X

58 X X

59 X X

60 X X

61 X X

62 X X

63 X X

64 X X

65 X X

66 X X

67 X X

68 X X

69 X X

70 X X

71 X X

72 X X

73 X X

74 X X

75 X X

76 X X

77 X X

78 X X

79 X X

80 X X

81 X X

82 X X

83 X X

84 X X

85 X X

86 X X

87 X X

88 X X

89 X X

90 X X

# APW Calculation for Band Structure of Cadmium<sup>1</sup>

SUBRAHMANYAM PENDYALA<sup>2</sup>, M. M. PANT, AND B. Y. TONG  
*Department of Physics, University of Western Ontario, London, Ontario*

Received June 7, 1971

An APW calculation of the band structure of cadmium is reported. The calculated band structure is similar to that obtained by others from pseudopotential calculations and explains some of the observed peaks in the optical absorption spectrum in terms of direct transitions.

On rapporte un calcul APW de la structure des bandes d'énergie du cadmium. La structure calculée est semblable à celle que d'autres auteurs ont obtenue en utilisant un pseudopotentiel et explique en termes de transitions directes certains des pics observés dans le spectre d'absorption optique.

Canadian Journal of Physics, 49, 2633 (1971)

The band structures of the hexagonal divalent metals, zinc and cadmium, have previously been calculated using pseudopotentials by Stark and Falicov (1967), Katsuki and Tsuji (1965). There has been a limited calculation by Mattheiss (1964) for zinc by the augmented plane wave method (APW), and it confirmed the free electron-like character of the band structure of zinc.

We report here the results of a nonrelativistic APW calculation of the band structure of cadmium. The APW method for energy band calculations has been described at length by Loucks (1966) and will therefore not be discussed here. The essential idea is to represent the solid as a periodic assembly of spherically symmetric potentials and represent the wave functions in terms of plane waves outside the spheres, and solutions of the radial equation inside. The expansion in spherical harmonics within the spheres was truncated at  $l = 12$ , and 31 reciprocal lattice vectors were used to construct the plane wave expansion. The potential at a given site was calculated by an overlap of charge densities from atoms at neighboring sites. The atomic charge densities were obtained from a Hartree-Fock-Slater calculation using the program of Herman and Skillman (1963). The overlap was carried out to fourteenth neighbors. To calculate the exchange contribution to the crystal potential, the Slater approximation was used (Slater 1951). The lattice parameters, the choice of reciprocal lattice vectors, and some other quantities pertinent to the calculation are given in Tables I and 2.

Energy values were calculated at the symmetry

<sup>1</sup>Partially supported by the National Research Council of Canada.

<sup>2</sup>On leave from Tata Institute of Fundamental Research, Bombay, India.

TABLE 1. Parameters used for cadmium

Lattice constant $a$	=	2.97889 Å
$c$	=	5.61765 Å
APW sphere radius $R$	=	1.489435 Å
Muffin tin zero	=	-1.0057 Ry
Fermi energy from our calculation	=	0.63 Ry

TABLE 2. Reciprocal lattice vectors for the hcp structure used in the APW expansion

(201)	(101)	(001)	(101)	(110)	(110)	(111)	(101)
(101)	(111)	(110)	(100)	(110)	(121)	(111)	(101)
(001)	(011)	(010)	(000)	(010)	(021)	(011)	(001)
(101)	(111)	(110)	(100)	(110)	(121)	(111)	(101)
		(210)				(211)	
		(300)	(200)				

points  $\Gamma$ , A, L, H, K, and M, and along the symmetry axes  $\Gamma A$ , AL, LM,  $\Gamma K$ , KH, HA, HL, LK, and KM, thus covering 1/24th of the Brillouin zone of the hexagonal close packed lattice shown in Fig. 1. With such a limited calculation it is not possible to have a good calculation of the density of states. The metallic character

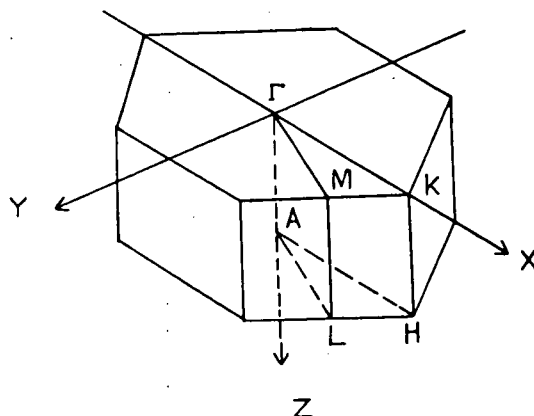


FIG. 1. Brillouin zone for the hexagonal close packed structure showing the symmetry points and lines.



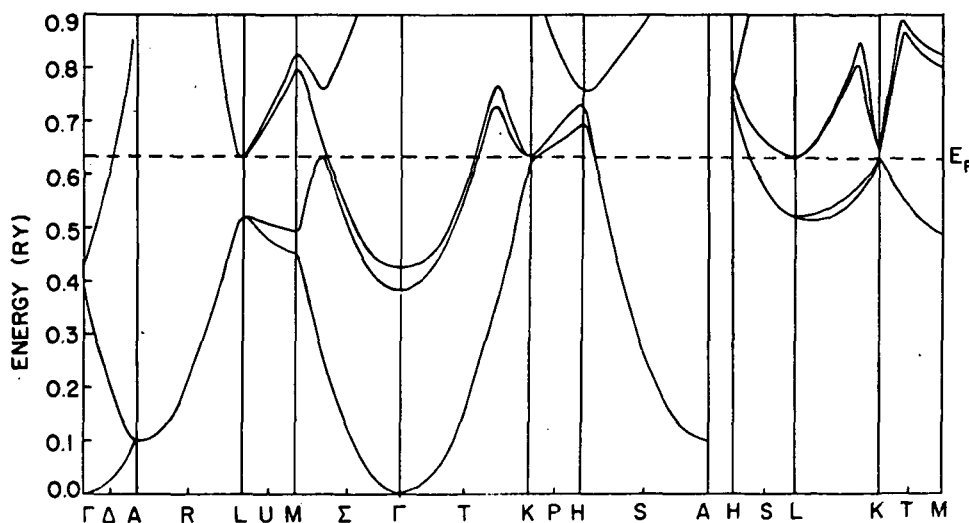


FIG. 2. Energy bands for cadmium calculated by the APW method.

of the divalent metals, like cadmium, arise due to the overlap of the energy bands along different directions. We therefore determined the Fermi energy, by the requirement of equal hole and electron volumes in  $k$  space and using the parabolic shape of the energy bands near the region of overlap. The energy bands together with the Fermi level are shown in Fig. 2. Not shown in the figure are a set of  $d$  bands of width about 0.06 Ry and located 0.23 Ry below the bottom of the  $s$  band. A similar structure was revealed in the APW calculations of Mattheiss (1964) for zinc, who found  $d$  bands of width 0.1 Ry lying 0.5 Ry below the  $s$ -like bands. It is true that the relative positions of the  $s$  and  $d$  bands will depend on the choice of the crystal potential (possibly through the use of different coefficients in the local density approximation for exchange), and it is conceivable that for some choice of the potential the  $d$  bands may overlap with the  $s$  bands, as observed by Juras *et al.* (1971), in a Kohn-Rostoker type calculation for zinc. In the absence of any soft X-ray data for cadmium to locate the  $d$  bands below the Fermi level, we made no further attempt to investigate the dependence of the energy bands on the choice of crystal potential. Without experimental data to corroborate, it would not be clear whether the position and the shape of the  $d$  bands is due to arbitrariness in the potential or a reflection of reality.

These energy bands calculated from first principles are quite similar to those of Stark and

Falicov (1967), confirming the success of their pseudopotential. Our results partially explain the optical spectrum for cadmium. The optical properties of single crystals of cadmium have been measured by Lenham and Treherne (1964). The absorption curves obtained by them show structures with peaks around 1.05, 1.23, 1.50, and 1.90 eV.

We attempt to correlate these peaks with direct transitions only and note that for the case of polyvalent metals, the critical points may occur away from as well as at the symmetry points (Ehrenreich *et al.* 1963; Harrison 1966). The effects away from the symmetry points are largest where the bands are parallel. In the present case, we see that the second and third bands are nearly parallel along  $\Gamma$ M,  $\Gamma$ K, and LH. The energy corresponding to these transitions along  $\Gamma$ M and  $\Gamma$ K is, however, very small and is not covered in the range of experimental observation of Lenham and Treherne (1964). On the other hand, the bands along LH are nearly parallel in two regions where the energy separations are 1.24 eV and 0.9 eV. These transitions, together with those associated with the symmetry points L and M, corresponding to gaps of 1.51 eV and 1.88 eV respectively, seem to account reasonably for the observed experimental structure.

#### Acknowledgments

The authors would like to thank Prof. J.

William McGowan for his interest. One of us (MMP) wishes to acknowledge useful discussions with Dr. G. E. Juras, regarding his calculations.

- EHRENREICH, H., PHILLIP, H. R., and SEGALL, B. 1963. Phys. Rev. **132**, 1918.
- HARRISON, W. A. 1966. Phys. Rev. **147**, 467.
- HERMAN, F. and SKILLMAN, S. 1963. Atomic structure calculations (Prentice Hall, Englewood Cliffs, New Jersey).
- JURAS, G. E., SOMMERS, C. B., and SEGALL, B. 1971. Bull. Am. Phys. Soc. **16**, 313.
- KATSUKI, S. I. and TSUJI, M. 1965. J. Phys. Soc. Jap. **20**, 1136.
- LENHAM, A. P. and TREHERNE, D. M. 1964. Proc. Phys. Soc. **83**, 1059.
- LOUCKS, T. L. 1966. Augmented plane wave method (Benjamin, New York).
- MATTHEISS, L. F. 1964. Phys. Rev. A, **134**, 192.
- SLATER, J. C. 1951. Phys. Rev. **81**, 385.
- STARK, R. W. and FALICOV, L. M. 1967. Phys. Rev. Lett. **19**, 795.

## APPENDIX 2

Within the Physics Department at the University of Western Ontario, there are five experimentalists carrying out atomic collision studies (T.D. Gaily, H.I.S. Ferguson, R.P. Lowe, J. Wm. McGowan, S.D. Rosner) and two theoreticians who are carrying out theoretical studies (D.F. Gallaher and J. Nuttall). These people are complemented by P.A. Fraser and T.M. Luke in the Applied Mathematics Department, and J.W. Meath in Chemistry, all of whom are interested in simple atomic systems.

Considerable work is focussed upon two, three and four-body systems from the point of view of understanding fundamental processes, and, in particular, the application of detailed theories to experimental results. The program is further complemented by theoretical work of B.Y. Tong and his associates who are studying the nature of the negative work function, the process whereby low energy positrons are thrown from moderating surfaces.